Improvements of thermoforming of thermoplastic composites using a collection of rubber particles as a soft mould half

Experiments and modelling

Proefschrift

ter verkrijging van de graad van doctor
aan de Technische Universiteit Delft;
op gezag van de Rector Magnificus prof. ir. K.C.A.M. Luyben;
voorzitter van het College voor Promoties
in het openbaar te verdedigen op maandag 7 april 2014 om 10:00 uur

door

Valeria ANTONELLI

Ingegnere Aeronautico, Università degli studi di Roma "La Sapienza"
geboren te Rome, Italië

Dit proefschrift is goedgekeurd door de promotoren:

Prof. dr. ir. R. Marissen
Prof. ir. A. Beukers

Samenstelling promotiecommissie:

Rector Magnificus,	voorzitter
Prof. dr. ir. R. Marissen,	Technische Universiteit Delft, promotor
Prof. ir. A. Beukers,	Technische Universiteit Delft, promotor
Prof. dr. ir. R. Benedictus,	Technische Universiteit Delft
Dr. ir. O.K. Bergsma,	Technische Universiteit Delft
Prof. dr. ir. R Akkerman,	Universiteit Twente
Prof. dr. ing. K. Schulte,	Technische Universität Hamburg-Harburg
Prof. ing. I. Crivelli Visconti,	Università degli Studi di Napoli Federico II
Prof. dr. R. Curran,	Technische Universiteit Delft, reservelid

ISBN: 978-90-8891-847-6

Cover design: V. Antonelli
Photography: M. Wedekind

Published by: Uitgeverij BOXPress, ´s-Hertogenbosch

a Eleonora

Summary

Compression moulding is the ideal candidate for large series production of thermoplastic composite parts. Improvements in this production technique will make it more appealing for those markets that are reluctant to use composites because of their development costs. Unlike other composites processing systems, the compression moulding press is capable of producing fibre-reinforced plastic parts in significant volumes, with the accuracy, repeatability and speed to which, for example, the automotive industry has been accustomed in the stamping of metal parts.

This thesis aims at a better understanding of the behaviour of the rubber mould during compression moulding of thermoplastics and consequently at the reduction of the development costs and improving the design of the rubber mould.

The classical problems that need to be addressed when designing a rubber mould are the correct dimensions to accommodate the laminate and the positions of the details. The standard process, though, does not take into account the temperature changes in the mould during production and in particular the effect of the coefficient of thermal expansion of the rubber. In this thesis, an envisioned method to reduce this problem is to add a certain amount of aramide in the rubber mould, in order to restrict the expansion due to increased temperature. The second issue that has to be considered is the friction between the melted thermoplastic and the rubber mould. The use of lubricant is extremely effective, but can be used only in a prototyping phase, as the lubricant affects the mechanical properties of the thermoplastic composite. Proper modelling of the rubber forming process, considering the correct rubber parameters, allows identification of the problems that might occur during manufacturing. The way to eliminate those problems numerically, though, is computationally challenging as well as uncertain and time consuming.

With those results in mind, an improved method was developed which substitutes the flexible rubber mould with a collection of rubber particles. The collection of rubber particles acts in a way similar to that of a fluid and has the advantage of filling the mould completely so that there is always contact between the rigid and the flexible mould. The new method allows the manufacturing of a wider range of products and allows the reduction of development costs related to the definition of the proper rubber mould shape.

To be able to describe the collection of rubber particles as a homogeneus material, a series of tests has been designed for the determination of some of their physical parameters. The obtained material has a very variable stiffness, from a very low modulus when the particles are not compressed, to two orders of magnitude higher values when compaction is almost complete. Bulk and shear modulus are related to the Poisson's ratio that does not vary much during the entire process, having a value always slightly below 0.5. This value is consistent with the fluid-like behavior in the beginning of the process and with the, almost incompressible, solid rubber block at the end of the process.

Finally, the parameters found have been used to model the compression moulding process with a collection of rubber particles. Modeling is not strictly necessary because most of the existing problems in the conventional production method have been eliminated. However it might become useful when the limitations of the new production technique will be explored and in particular for those geometries that are not possible with the conventional method.

Samenvatting

Compressievormen is de ideale kandidaat voor serieproductie van thermoplastische composiet onderdelen. Verbetering van deze productietechniek maakt het aantrekkelijker voor die markten die terughoudend zijn om composieten te gebruiken vanwege hun ontwikkelingskosten. In tegenstelling tot andere composiet productieprocessen, is de compressievormpers geschikt voor het fabriceren van significante volumes van vezelversterkte kunststofonderdelen, met de nauwkeurigheid, herhaalbaarheid en snelheid die, bijvoorbeeld, de auto-industrie met het stampen van metaalonderdelen gewend is.

Het doel van deze thesis is een verbeterd inzicht van het rubbermalgedrag tijdens het compressievormen van thermoplasten en bijgevolg het verminderen van ontwikkelingskosten en het verbeteren van het rubbermalontwerp.

Het klassieke probleem dat aan de orde gesteld moet worden tijdens het ontwerpen van een rubbermal is de juiste maatvoering zodanig dat het laminaat en de locaties van de details er goed in passen. Het standaard proces houdt echter geen rekening met de temperatuurverandering in de mal en het effect van de thermische uitzettingscoëfficiënt van de rubber. De beoogde methode in deze thesis is dit probleem te verkleinen door aramide als versterking voor de rubbermal te gebruiken om de uitzetting door de verhoogde temperatuur te beperken. De tweede kwestie die beschouwd moet worden is de wrijving tussen de gesmolten thermoplast en de rubbermal. Het gebruik van een smeermiddel is zeer effectief, maar kan alleen gebruikt worden tijdens prototyping omdat het smeermiddel de mechanische eigenschappen van het thermoplastische composiet beïnvloedt. Passende modellering van het rubbervormproces met de juiste rubberparameters zorgt voor identificatie van het probleem dat kan ontstaan tijdens de productie. Het elimineren van deze problemen met numerieke oplossingen is echter rekenkundig uitdagend, onzeker en tijdrovend.

Met deze resultaten in het achterhoofd is een verbeterde methode ontwikkeld die de flexibele rubbermal vervangt door een verzameling van rubberdeeltjes. De verzameling van rubberdeeltjes gedraagt zich vergelijkbaar met een vloeistof en heeft het voordeel dat de mal volledig gevuld kan worden zodat er altijd contact is tussen de stijve en flexibele mal. De nieuwe methode betekent dat een grotere variëteit aan producten gefabriceerd kan worden en

zorgt voor een vermindering van de ontwikkelingskosten die gerelateerd zijn aan de definitie van de juiste rubbermalvorm.

Om de verzameling van rubberdeeltjes als een homogeen materiaal te kunnen beschrijven is een serie van testen ontwikkeld om een aantal van hun fysische parameters vast te stellen. Het verkregen materiaal heeft een grote variabele stijfheid, van een zeer lage modulus wanneer de deeltjes niet gecomprimeerd zijn, tot twee ordes van grootte hogere modulus wanneer de persing bijna afgerond is. De compressie- en glijdingsmodulus die gerelateerd zijn aan de dwarscontractie varieren weinig tijdens het gehele proces, met een Poisson's modulus die altijd iets onder 0,5 is. De modulus is consistent met het vloeibare gedrag in het begin van het proces en met de nauwelijks samendrukbare massieve rubberblokken op het einde van het proces.

De gevonden parameters zijn tenslotte gebruikt om het compressievormproces te modelleren met een verzameling van rubberdeeltjes. Modelleren is niet strikt noodzakelijk dankzij het feit dat de meeste bestaande problemen van de conventionele productiemethode geëlimineerd zijn. Het kan echter bruikbaar zijn wanneer de grenzen van de nieuwe productietechniek onderzocht worden, vooral voor die geometrieën die met de conventionele methode niet maakbaar zijn.

Table of Contents

Chapter 1
Introduction

The use of continuous fibre reinforced polymers in large civil aircraft has been slowly developing in the last decades. Up to ten years ago, their use was limited to the control surfaces and the empennage [1], whereas for large structural parts metal was preferred. When Airbus decided to start the production of the A380, things have started to change. Of the 25% of the composite material used for the entire aircraft, also highly loaded structural parts have been built of composite material. For the first time an aircraft has a composite centre wing-box and the composite rear fuselage section behind the rear pressure bulkhead made of carbon fibre reinforced plastics [2].

Only with the advent of the Boeing 787 (Figure 1.1), composites have taken a predominant role in aircraft industry.

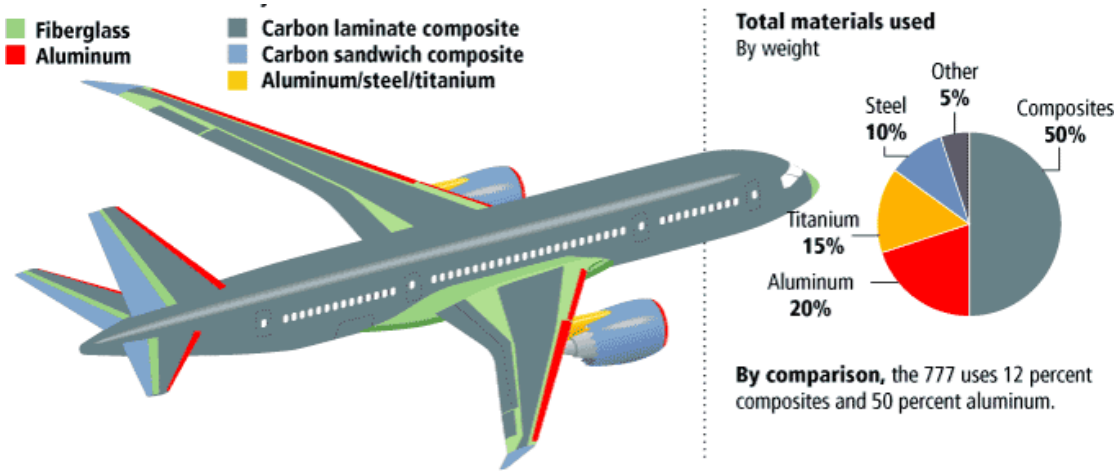

Figure 1.1 Materials used in the 787 body [3].

This last generation of aircraft in fact is the first passenger carrier to have a total of 50 % structural parts made of composite material. This number includes the whole fuselage, whose barrel sections are made in one piece joined end to end to form the fuselage, thereby eliminating the need for the fifty thousand fasteners required to build a conventional aluminium fuselage, making it an authentic masterpiece of composite technology.

As an answer to the Boeing's Dreamliner, Airbus came up with the decision of increasing the amount of composites in their new aircraft, the A350 (Figure 1.2).

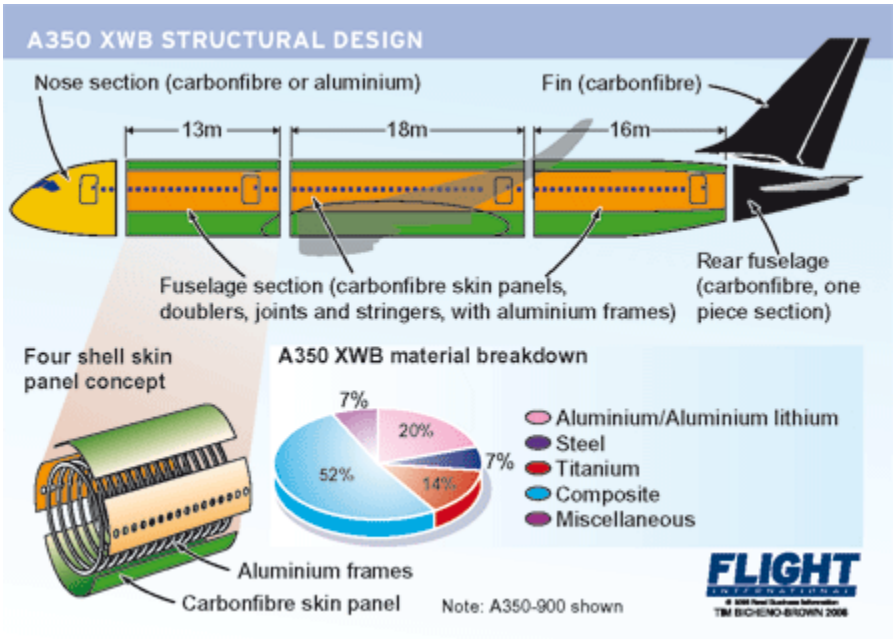

Figure 1.2 A350 XWB Structural Design [4].

The technology of the A350 is different from the one used for the Dreamliner. In the fuselage sections, in fact both composites and aluminium are used, eliminating the advantage of the integrated structural concept with the elimination of joints. This is, in principle, a step back compared to the Boeing 787 and suggests that composite materials have proven to bring many advantages in aircraft design, but still need more care in design and certification than metals, making companies reluctant to undertake many changes at once. This is also justified by the fact that the entry into service of the Dreamliner, still planned for 2010 in 2008 [5], took place in October 2011 and still suffered from several early in-service problems which culminated in grounding the aircraft in January 2013 for several months.

In the last ten years, however, a great effort has been made to make industrial, reproducible production techniques for composite structures available [7]. First to be mentioned is Automated Fibre Placement [8], which was first used in the A380 for the unpressurised rear fuselage, and it is the current production technique for the fuselage sections of the B787 and thus more and more widely used.

One production technique that is still in a more or less experimental stage is thermoforming of thermoplastic composites. The potential advantages come from the high efficiency of the

forming process in converting a sheet to a three dimensional part, plus the fact that a long curing cycle is not required for thermoplastics.

In particular, rubber forming allows the series production of composite parts with high mechanical properties. Its limited implementation in aircraft industry is caused by the lack of knowledge and the lack of proper design and process tools and manufacturing techniques for thermoplastic composites. In particular, the large amount of time spent in the definition of the suitable rubber mould, normally made based on the craftsmanship of the manufacturing engineer and material supplier, leads to the decision of producing very simple parts, mainly flat plates or single curved panels to avoid long development periods.

One of the known exceptions in aircraft industry is the fixed wing leading edge of the Airbus A380, Figure 1.3, the so-called J-nose, for which all ribs and stiffeners, more than two hundred different pieces, are rubber pressure formed.

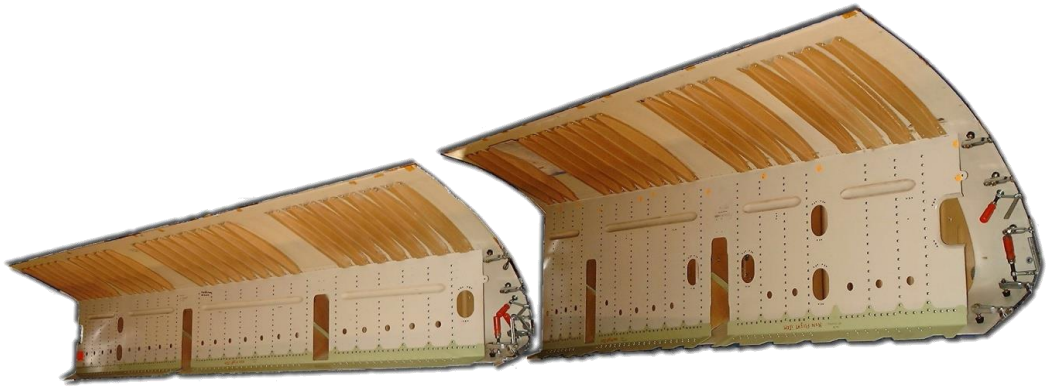

Figure 1.3 J-nose of the Airbus A380 [9].

For the J-nose, produced in the Netherlands by Stork Fokker, preconsolidated Cetex is used. Pre-cut blanks are loaded into the press to produce three to four ribs in a single press cycle, which lasts about one minute only. The stiffeners are used using the same process parameters as the ribs, though more stiffeners are produced from each mould due to their smaller size. On the contrary, each rib needs its own mould.

A growing sector for thermoplastic material is the automotive industry. As automotive engineers continue to search for ways to make lighter, less-costly components, the compression moulding of composites has taken centre stage in composites-for-metal substitution. Unlike other composites processing systems, the compression moulding press is capable of reproducing fibre-reinforced plastic parts in significant volumes, with the accuracy, repeatability and speed to which the automotive industry has been accustomed in the stamping of metal parts. Examples of structural car parts that have been recently designed to be pressure formed are the front and rear bumper of the BMW M3 each produced from 2003 in 20,000 units per year [10]. Lotus launched the project Ecolite, aiming at the development of thermoplastic composite crash systems that are economical for higher volume production. The demonstrator consisted in the replacement of the thermoset (RTM) bumpers present in both Lotus Elise and AML Vanquish with a thermoplastic one increasing their performances.

Compared to the BMW M3 bumper, the Lotus one would allow for both low and high-speed crash management. From the study, it emerged that it was possible to obtain a competitive piece cost allowing realistic business cases at 30,000 units per year.

In the beginning of 2010, large contracts have been signed between cars manufacturers and carbon fibre suppliers ([11], [13], [14]). In particular, Daimler and Toray signed a Joint Development Agreement for the development of components made from fibre-reinforced plastics of which the first results will be seen in series production at Mercedes-Benz within the next three years [15]. Even if thermoplastics do not necessarily mean rubber pressure forming, this production technique is the ideal candidate for large series production and improvements in this production technique will only make it more appealing for the automotive market, not only high for performance and expensive sports car. Another market that will benefit from the improvements of pressure forming is the wind turbine one [18] whose need for longer blades makes it necessary to move forward the currently produced RTM turbines. Other small but not unimportant markets are protection goods (helmets, safety shoes) and the leisure market [19].

An explicative picture of the different problems that could occur during pressure forming is shown in Figure 1.4.

Figure 1.4 Product development of a rubber formed part produced at the Structures and Material Laboratory.

The figure shows two pictures of the same product at different development phases. The first picture shows all the typical problems that can be encountered while pressing for the first time a new thermoplastic product: the edges are not well pressed; in the corners, the fabric presents many wrinkles. There are many voids showing a bad consolidated product with consequently poor material characteristics. With a series of trials, the product on the right is obtained. Here most of the problems are solved, though some of the edges are not yet perfectly pressed. It is evident that, in order for this production technique to be more used in a wider range of applications, it is necessary to cut the development cost by reducing the amount of trials and increasing the knowledge on the various elements that play an important role.

1.1 Thesis objectives

In the beginning of this thesis, two main goals were formulated:

- *To understand the behaviour of the rubber mould during pressure forming of thermoplastics*
- *To reduce the development costs of the thermoplastic products produced by thermoforming improving the design of the rubber mould*

The two goals are closely related. Currently, the design of the proper rubber mould for a certain product is made based on the single manufacturer experience. This means both rubber hardness and brand are chosen because of the single experience and the shape of the more complicated rubber moulds is defined by trials and errors. This method works only when the number of pieces to be produced is limited and also when the technique is so new and advanced that cost and time become a secondary issue.

In the long run, though, in order to make this process competitive for large series productions and also accessible to any manufacturer, independently from the capabilities of the workshop, it is necessary to establish production rules and methods that make rubber pressure forming as automated and reliable as possible.

The manufacturing issues related to rubber forming mainly involve two parameters [22]: the uniformity of the pressure distribution during the consolidation phase, which is particularly important to have a perfectly consolidated product, including details and corners, and the capability of the thermoplastic laminate to be perfectly draped into the desired shape during the forming phase. The latter problem mainly involves intraply and interply shear of the fibres. In this thesis, only the first topic has been tackled, leaving the second one to other, dedicated, researches, as, for example, in [23], [24] and [25].

1.2 Thesis overview

In Chapter 2 a brief introduction on rubber forming of thermoplastics is made, while in Chapter 3 the manufacturing problems related to the use of a rubber mould as mould half during pressure forming have been described. Some typical rubber grades and types are also tested at different temperatures in order to understand their behaviour better. In Chapter 4, the pressure distribution as influenced by the deformation of a rubber mould is studied in depth and some possible methods to improve it are shown and analysed. Chapter 5 focuses on the definition of an appropriate rubber model, which can be used to analyse numerically the production method and predict the quality of the product during production, as well as possible problems that can be encountered when choosing a particular mould. Chapter 6 describes the envisioned improvement in the rubber pressure forming of thermoplastics which consists of substituting the solid rubber with a collection of rubber particles. The method is explained, the advantages and disadvantages are explained and some preliminary products are shown as well as some considerations on the choice of rubber particles shape, dimensions and hardness. In order to be able to make a proper numerical analysis of the production process with rubber particles, the rubber particles are characterised as a continuum material. Several test methods are presented in order to obtain values to be translated in mechanical characteristics to be used in a Finite

Element Analysis in Chapter 7. In Chapter 8, the characterisation of a material made of rubber particles is presented and compared to the test results. Conclusions and future research recommendations are presented in Chapter 9.

1.3 Bibliography

[1]. Middleton, DH, "Composite Materials in Aircraft Structures", Longman Scientific & Technical 1990, Essex, England

[2]. http://www.netcomposites.com/newspic.asp?2704, Internet Publication accessed 16/03/2010

[3]. http://www.seattlepi.com/dayart/20070629/787materials.gif, accessed 18/03/2010

[4]. http://www.aviationnews.eu/blog/wp-content/uploads/2009/12/A350_Layout.gif, accessed 18/03/2010

[5]. http://www.reinforcedplastics.com/view/1106/airbus-takes-on-boeing-with-composite-a350-xwb-/ ,accessed 18/03/2010

[6]. http://www.telegraph.co.uk/finance/newsbysector/transport/farnborough-airshow/7897812/Farnborough-Airshow-2010-Boeing-787-Dreamliner-in-focus.html accessed 26/07/2010

[7]. Hinrichsen J, Bautista C, "The Challenge of Reducing both Airframe Weight and Manufacturing Cost", Air & Space Europe, vol. 3, No3/1- 2001

[8]. Bannister M, "Challenges for composites in the next millennium - a reinforcement perspective", Composites: Part A 32 (2001) 901-910

[9]. http://www.compositesworld.com/articles/thermoplastic-composites-gain-leading-edge-on-the-a380, accessed 24/03/2010

[10]. http://www.compositesworld.com/articles/glass-reinforced-thermoplastic-succeeds-in-car-crash-structure, accessed 27/07/2010

[11]. http://www.arb.ca.gov/cc/ccms/meetings/042108/4_21_current_techn_3_sills.pdf, accessed 28/07/2010

[12]. http://www.emercedesbenz.com/autos/mercedes-benz/corporate-news/daimler-signs-carbon-fiber-deal-with-toray-for-mercedes-benz-models/, accessed 27/07/2010

[13]. http://www.boerse-online.de/aktie/empfehlung/deutschland/:BMW--Joint-Venture-mit-SGL-Carbon/518465.html, accessed 27/07/2010

[14]. http://www.compositesworld.com/news/carbon-fiber-suppliers-set-foundations-for-production-auto-supply-chains, accessed 26/07/2010

[15]. http://www.daimler.com/dccom/0-5-7153-1-1291729-1-0-0-0-0-0-12080-0-0-0-0-0-0-0-0.html, accessed 27/07/2010

[16]. http://www.4wheelsnews.com/lamborghini-unveils-new-advanced-composite-structure-laboratory/ accessed 12/08/2010

[17]. http://www.arb.ca.gov/cc/ccms/meetings/042108/4_21_current_techn_3_sills.pdf, accessed 28/07/2010

[18]. Joncas S, "Thermoplastic wind turbine blades – an integrated design approach", PhD Thesis, 2010 Delft

[19]. http://www.bond-laminates.de/en/index.php?nav=4.01, accessed 28/07/2010

[20]. Okine RK, "Analysis of Forming Parts from Advanced Thermoplastic Composite Sheet Material" Journal of Thermoplastic Composite Materials, Vol 2- January 1989

[21]. http://www.airbus.com/en/presscentre/pressreleases/pressreleases_items/10_06_05_A350_Launch.html, accessed 18/03/2010

[22]. L.M.J. Robroek, "The development of Rubber Forming as a Rapid Thermoforming Technique for Continuous Fibre Reinforced Thermoplastic Composites", PhD Thesis, 1994 Delft University Press
[23]. E.A.D. Lamers, "Shape distortions in fabric reinforced composite products due to processing induced fibre orientation", PhD Thesis, Twente University, 2004
[24]. S.Wijskamp, "Shape distortions in composite forming", PhD Thesis, Twente University, 2005
[25]. R. ten Tije, "Finite Element Simulations of Laminated Composite Forming Process", PhD Thesis, Twente University, 2007

Chapter 2
Overview of the rubber pressure forming process

2.1 Introduction

The present chapter aims at summarising the current state of the art for the rubber forming process. The aim is to give an overview of all the parameters involved in the process and explain how these parameters are influencing the result of a well press formed product.

A typical rubber forming setup consists of set of infrared panels, a rigid mould, a flexible (rubber) mould, a clamping or sliding frame and a hydraulic press. A schematic of the process is shown in Figure 2.1.

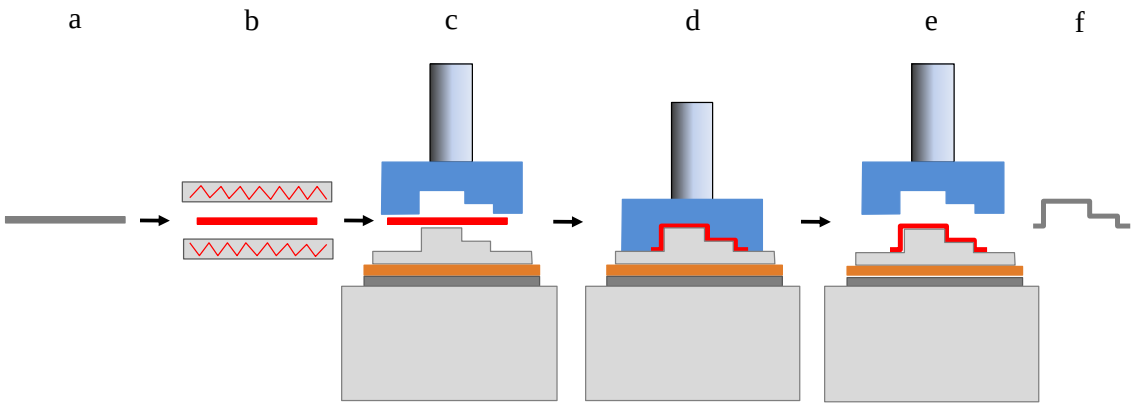

Figure 2.1 Schematic representation of the rubber forming process.

The pre-consolidated thermoplastic laminate (a) is placed close to infrared panels (b) where, when the thermoplastic laminate is at the necessary processing temperature, it is quickly transferred to the forming press (c). This can be done by a clamping frame, which transfers the hot laminate to the forming system. When the hot laminate is positioned between the two moulds (one elastomeric and one metal tool, which can be female or male depending on the application), the press is closed and the product is formed (e). After cooling down, the product can be taken out of the mould (f).

The forming time is generally a few (1-5) seconds. When the shape is formed and final (re)consolidation is assured, the product must be cooled down under pressure to below the glass transition temperature T_g. Depending on the preform used, the part has to be trimmed to yield the final shape.

2.2 Press

The characteristics of the press to be chosen for series production, mainly depend on the dimensions of the part that has to be produced.

A small-scale press, capable of producing parts of maximum 700 x 1000 mm is the one shown in Figure 2.2. In this press, all the product-independent equipment is contained in the press.

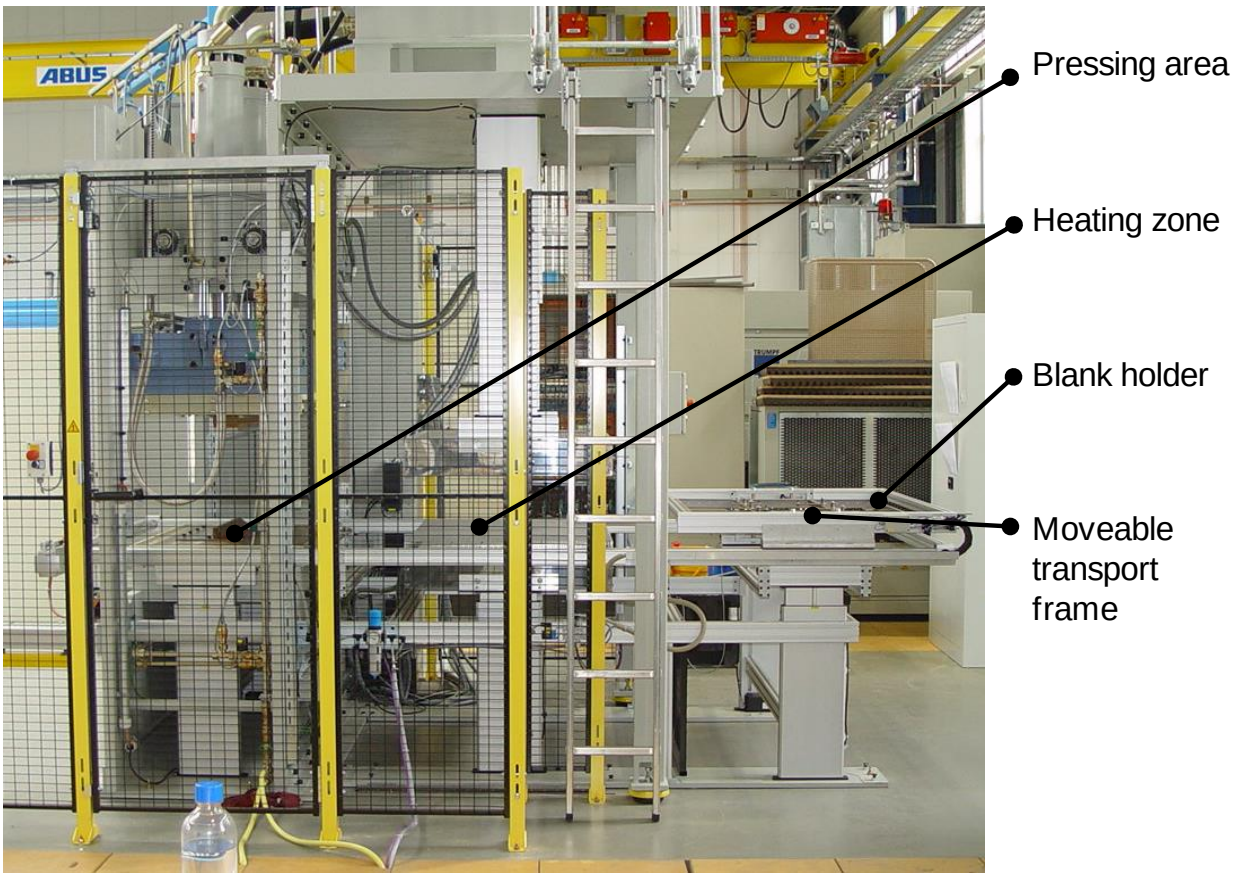

Figure 2.2 Overview of a small pressure forming equipment.

A similar press is in use at the Faculty of Aerospace Engineering of the Delft University of Technology. This type of press allows the fabrication of series production of products and is used, in similar dimensions or slightly larger, in small and medium enterprises (as, for example [4]) involved in the production of press formed thermoplastic products.

A basic experimental system, as used at the Faculty of Aerospace Engineering of the Delft University of Technology is shown in Figure 2.3. Here two Infra-Red (IR) plates and a simple transport mechanism to the pneumatic press substitute the infrared oven, which is able to apply a maximum moulding pressure of 40 bar. The dimensions of the products that can be pressed depend on the force that can be applied. The press in question can press parts whose maximal dimension is 500 cm^2.

Figure 2.3 The experimental test set-up at the Structure and Material Laboratory of the TUDelft.

2.3 Process parameters

Rubber forming cycle times are very short and are usually measured in terms of seconds rather than minutes. A typical temperature profile of the laminate's surface during a forming cycle is shown in Figure 2.4. The heating time of the thermoplastic is often the longest part of the process time. The ramp rate depends on the fibre type, colour, thickness of the laminate, the IR capacity and the processing temperature of the thermoplastic matrix (typically 300 °C – 400 °C for PPS and PEI). The figure shows also a temperature drop of 10 °C in the three seconds the thermoplastic hot laminate is moved from the infrared panels to the forming press. This time therefore has to be minimised as every second implies a temperature drop and therefore a decrease in formability of the plate.

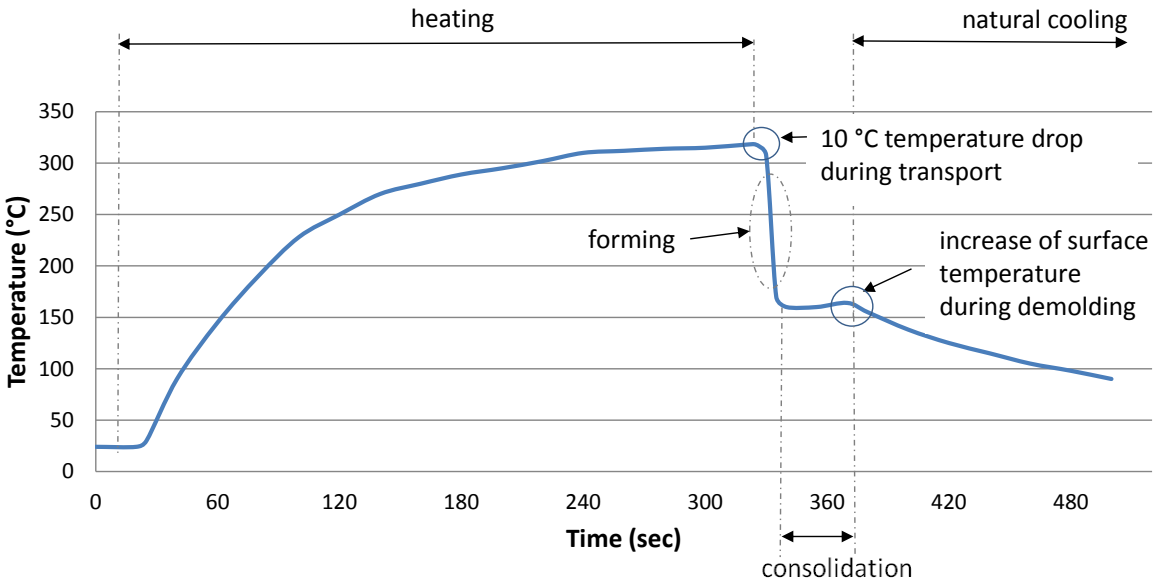

Figure 2.4 Surface temperature profile during the rubber forming process [5].

After forming, the pressure on the product is increased for consolidation. This typically takes one to three minutes, depending on part thickness, mould heat transfer, etc. If the tool is opened too soon, the surface temperature of the part increases due to the heat content of the inner part of the laminate (see Figure 2.4). During consolidation, the temperature of the product's surface is constant and equal to the temperature of the metal mould. In order to achieve optimal crystallinity with PPS, the tool temperature should be 170 °C, whereas PEI can be formed using a room temperature tool, which, if desired can be anyhow heated up to 170 °C. The rubber tool, on the other hand, is not heated. It is common practice, though, closing the press before starting production to allow the rubber to be warmed up by the metal mould. After rubber moulding a number of parts, the rubber tool maintains the elevated temperature.

2.4 Blank holder

In case of rubber forming of complex products, the maximum shearing angle of the fabric might be exceeded causing the creation of wrinkles that are not acceptable in case of structural components. The common practice in rubber forming is the use of a so-called blank holder. The blank holder holds the hot thermoplastic plate during the forming phase, creating a tension force that has the function of preventing those wrinkles.

Figure 2.5 shows various types of clamping methods for the thermoplastic laminate. In (a) the thermoplastic laminate is held via heated clamps, allowing the fibres to follow the contour of the mould.

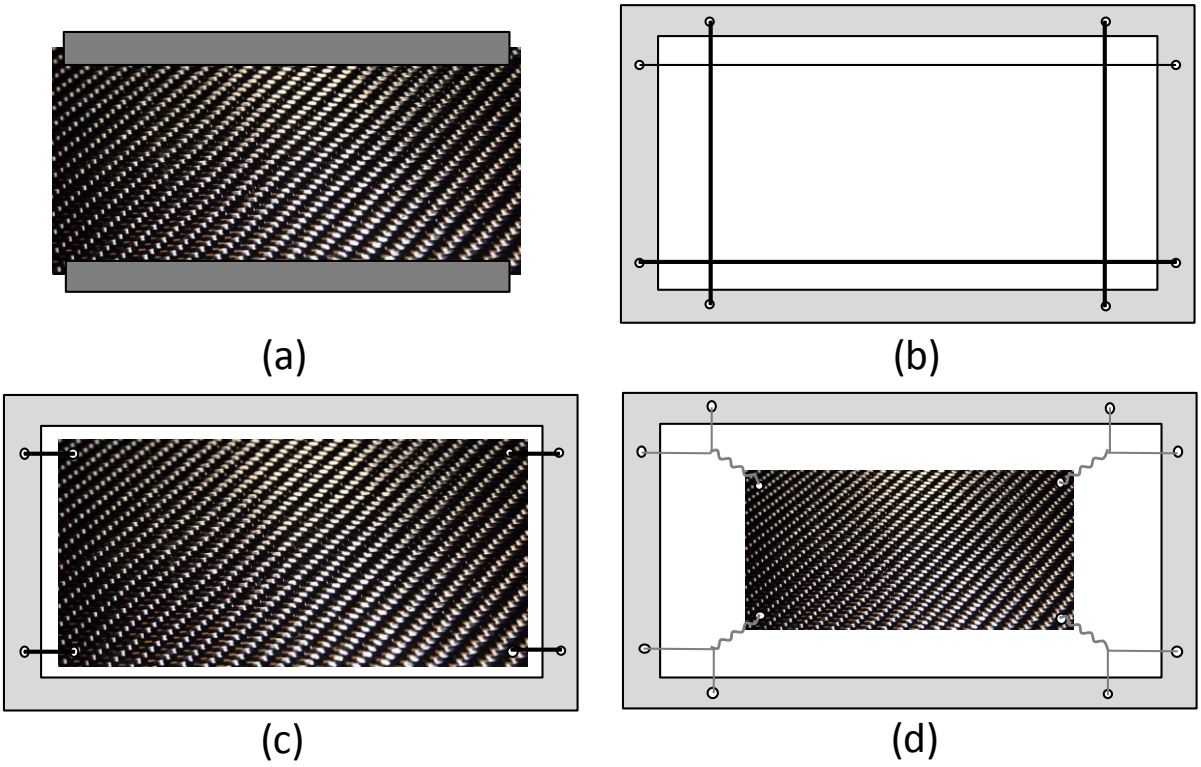

Figure 2.5 Schematic representation of various types of blank holder.

In the case of relatively rectangular shapes, it is sufficient to support the laminate with four steel wires (b). It must be checked in advance that the dimensions of the mould are such that the mould is contained within the wires frame. Another possibility is to use metal pins that could be eventually straightened under load (c). The optimal position of the pins can be chosen using the results obtained by a DRAPE [3] analysis which gives the final shape of a formed product given a flat plate of certain dimensions. The last solution, shown in (d) is the use of springs. This system allows a larger material displacement without losing control. The dimensions of product that can be formed, though, will be smaller.

The blank holder is clamped in the transport system of the press and its function is therefore the one of a material handling device. During heating of the laminate, the flexural stiffness reduces significantly due to the melting of the resin, which in turn results in a large deflection of the laminate due to gravity. Due to the large deflections, the distance between the laminate and the heating elements will not be constant, causing large temperature gradients in the laminate. For the products currently being rubber formed, such as ribs for non-primary structures, and brackets, the gradient is still acceptable. When larger, structural parts, need to be formed, this temperature gradient has to be taken into account and a more efficient clamping mechanism should be considered.

2.5 Thermoplastics

Thermoplastic composites are available with various types of glass, carbon and aramid reinforcements, in both fabric and tape form. The typical matrix systems that are used in aircraft

structures are high performance, high temperature systems. A distinction can be made among the following ([4], [5] and [6]):

Polyetheretherketone (PEEK): it has high thermal and mechanical performance. Excellent environmental resistance, very high fire and smoke resistance, high toughness and fatigue resistance, low wear. Applications include aircraft primary structures, space components and wear resistant applications. Due to the crystallinity of the polymer, PEEK can be used at temperatures above glass transition temperature (Tg): 121ºC for aerospace and 260ºC for non-aerospace applications.

Polyetherketoneketone (PEKK): it presents high toughness and an excellent chemical resistance. The material has a very low flammability, smoke and toxicity. Used in aircraft interiors, aerospace structure and industrial applications. Its service temperature is 121ºC.

Polyetherimide (PEI): the material is inherently flame resistant with low smoke emission. It exceeds 35/35 OSU and is qualified at Airbus and Boeing for both structural and interior applications. It presents high toughness. The standard grade is not recommended for use in hot hydraulic fluids. The service temperature gets up to 200ºC.

Polyphenylene sulfide (PPS): it has an excellent chemical resistance. it may be used at temperatures above Tg due to the crystallinity of the polymer: 100ºC for aerospace and 204ºC for non-aerospace. The material is inherently flame resistant with low smoke emission. It exceeds 35/35 OSU and is qualified at Airbus and Boeing for multiple structural applications

For various industrial applications it is possible to work with low cost fibre reinforced thermoplastic materials based on PA, ABS, PC, PET, TPU, and PP, with both carbon and glass fabric reinforcements. For example, for anti-ballistic applications PA, PP and PE offer a cheaper solutions with respect to aerospace grade matrices, while PA, PC, TPU are successfully used for automotive components, helmets, bicycle parts and many more not heavily loaded parts. It is also possible to pressure form parts from self-reinforced polypropylene and polyethylene such as PURE® and Dyneema®.

2.6 Moulds

In rubber forming, one of the moulds is made of hard, often steel, material and the other one of an elastomeric one.

The method to produce the elastomeric tool is to coat the steel tool with tooling wax to simulate the thickness of the product that has to be produced. When a male elastomeric mould is produced, the liquid rubber solution is poured in the (coated with wax) female mould followed by curing according to the processing specifications. In the case a female mould is produced, the male (coated with wax) steel mould is placed in the liquid rubber solution.

As mentioned above, it is very important for the thermoplastic sheet to be kept at the highest temperature for the longest time possible. The material selection for the hard mould is therefore influenced by the thermal conductivity. Being aluminium an excellent thermal conductor, it is preferred to steel. In those cases in which a very stiff mould is preferred, steel is used.

Apart from the single preferences of the manufacturer, there are two main factors for which a male or female elastomeric mould is chosen, these are the surface quality of the product and the thickness of the product.

When the product to be manufactured needs to be joined to another piece, the two surfaces to be joined have to be produced with a high accuracy for the proper tolerance; therefore, those two surfaces need to be in contact with the metal mould.

An example of a part produced using metal female moulds are the ribs of the Dornier 328 landing flap, Figure 2.6. The ribs are connected to the surrounding structure, therefore the outer surface of the ribs needs to be smooth and precise. Due to the shearing of the fabric during forming of a doubly curved product, the thickness of the flange is not perfectly constant after forming. In this case, the best way to control the outside surface is the use of a metallic negative/female tool combined with an elastomeric positive/male tool.

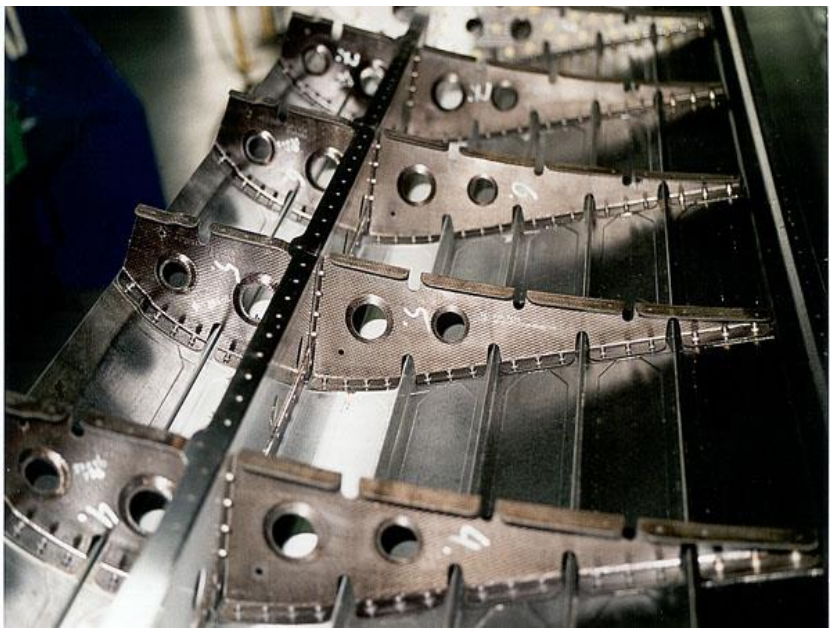

Figure 2.6 Example of part produced using a male elastomeric mould.

Another case in which a female rubber mould is preferred is the case of the production of the ribs for a full thermoplastic rudder [8], Figure 2.7 which was produced at the Structure and Material Laboratory and whose problems during manufacturing will be also illustrated in this thesis. In particular, the rubber mould was severely damaged by the male steel mould after the production of only a few components.

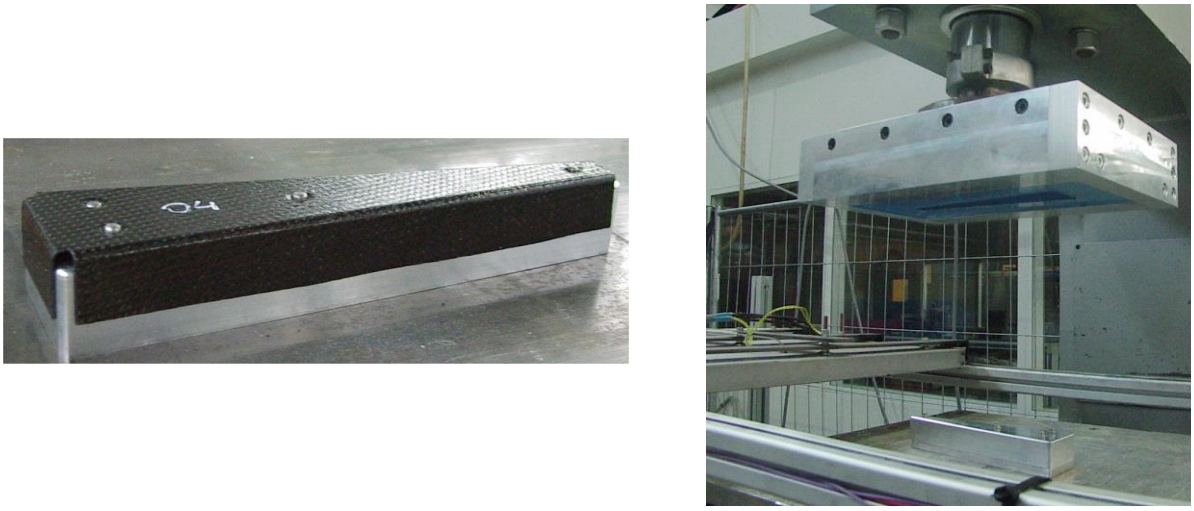

Figure 2.7 One of the press formed thermoplastic ribs belonging to a two-seater aircraft and its production tooling.

Another factor that leads to the decision of using a female elastomeric mould is the thickness of the product. As soon as the hot laminate touches the tool, this starts to cool down; even when the tool is heated, it is cold compared to the laminate at its forming temperature. Cooling down means a reduction of the formability of the laminate, that in order to be managed, requires a thorough investigation of the forming process.

In the case of the rib, when the hot laminate is transferred in-between the two moulds, it enters in contact with the skin of the rib which starts cooling. The flange area, though, is not in physical contact with the tooling and stays hot much longer. There is, therefore, more time to form the flanges compared to a negative/female metal tool.

2.7 Outlook

The present chapter shows an overview of the parameters that play a role and have to be taken into account when a thermoplastic product is manufactured via press forming. As most of the manufacturers rely on their own experience and preference, this list is not exhaustive and can vary depending on the single experiences and expertise of the company producing press formed products. It is evident, though, that so far the choice of the rubber and its composition is a matter of singular experience and habit, more than the ability to predict its behaviour during forming, also due to the little knowledge of its behaviour in general, which is mostly limited to tire behaviour, and during the press forming process in particular.

2.8 Bibliography

[1]. Robroek LMJ, “The development of Rubber Forming as a Rapid Thermoforming Technique for Continuous Fibre Reinforced Thermoplastic Composites”, PhD Thesis, 1994 Delft University Press

[2]. Bersee HEN, “Diaphragm Forming of Continuous Fibre Reinforced Thermoplastics – process Analysis and Development”, PhD Thesis, 1996 Delft University Press

[3]. Bergsma O.K., "Three Dimensional Simulation of Fabric Draping", PhD Thesis, Delft University press, 1996
[4]. http://www.composites.nl, accessed 20/06/2011
[5]. http://www.tencate.com/TenCate/Aerospace_composites/documents/TCAC%20USA%20docs/TCAC%20USA%20Handling%20Guide/Compression%20Molding%20Guidelines.pdf, accessed 12/05/2010
[6]. Offringa AR, "Thermoplastic composites – rapid processing applications" Composites: Part A 27A (1996) 329-336
[7]. Okine RK, "Analysis of Forming Parts from Advanced Thermoplastic Composite Sheet Material" Journal of Thermoplastic Composite Materials, Vol. 2- January 1989
[8]. H.E.N. Bersee, B. Weteringe, M. Van Dongen, A. Beukers, Manufacturing of a thermoplastic composite rudder", SAMPE 2006 - Long Beach, CA April 30 - May 4, 2006
[9]. K. 0. Walls, R. J. Crawford "The 'design for manufacture' of continuous fibre-reinforced thermoplastic products in primary aircraft structure", Composites Manufacturing 6 (1995) 245-254
[10]. M. Hou, L. Ye and Y. W. Mai "Manufacturing Process and Mechanical Properties of Thermoplastic Composite Components", Journal of Materials Processing Technology 63 (1997) 334-338

Chapter 3
Rubber parameters relevant to the pressure forming of thermoplastics

The typical rubber used during press forming of thermoplastic material is a silicon based rubber due to its better thermal and mechanical properties, especially with respect to fracture toughness, compared to polyurethane based ones. The different rubber types can vary in hardness and maximum working temperature. Generally, every producer of thermoplastic products uses only one type because he is used to its behaviour and can design every new mould more easily then when he is not accustomed to the type of rubber. Nevertheless, in case of single or doubly curved products, many trials are needed before the product with the desired accuracy of details is obtained.

Three main characteristics are analysed in this chapter. The mechanical properties of rubber in tension and compression, the friction between rubber and steel and at last the coefficient of thermal expansion.

The rubber used to manufacture the mould is a two-component material consisting of a base and a curing agent which are mixed in different ratios as described in the producer data sheet. Curing occurs by an addition reaction at room temperature. In order not to have voids in the cured rubber, the entrapped air in the fluid product is removed in a vacuum chamber, where the mix completely expands and then collapses leaving it free from air bubbles. The mix is then gently poured into the mould avoiding new air entrapment. The catalysed material will cure at room temperature in the time defined in the datasheet of the used rubber after which the mould can be removed and the rubber product is ready for use.

3.1 Rubber characterisation

The known characteristics of the rubber used are often limited to those values contained in the datasheets of the rubber producer, which normally defines the hardness, strength and elongation at break at room temperature. For a better understanding of the parameters that could influence the pressure forming process and a thorough numerical simulation of the process itself, however, more data are needed.

To be able to determine some mechanical properties, the most common and available rubbers have been tested in tension and compression at different temperatures. The purpose of those tests is twofold: on one side, those tests evidently allow the definition of the mechanical properties of the rubber in tension and compression, data that are not available in the producer fact sheets. In order to have a better view on the behaviour of the rubber during production, the characterization is done, when possible, up to 250 °C, though in general the maximum temperature of the rubber mould during the rubber pressing process is measured to be around the 160 °C.

The second reason to perform those tests is to gather data for the modeling of the rubber behaviour to be implemented in a Finite Element code, enabling simulations of the rubber forming process.

The main characteristics given by the producer of the five rubber types that have been tested are reported in Table 3.1. Tests on four types of silicon rubber have been carried out, together with a urethane rubber, normally used for rubber press forming of metal, for comparison.

Rubber	Producer	Chemical base	Hardness	Tensile Strength	Elongation at break	Tear Strength
			Shore A	MPa	%	kN/m
UR 3450	Axon	urethane	75	10	650	40
Silastic S	Dow Corning	silicone	20	6.3	600	23
Silastic J	Dow Corning	silicone	59	4.5	250	16
KE-1604	Shin-Etsu	silicone	60	n.a.	n.a.	n.a.
KE-113	Shin-Etsu	silicone	70	5.5	120	3

Table 3.1 Technical data of the tested rubber types reported in the producer datasheet.

The considered rubbers are tested up to failure in a Zwick-Roell tension machine with an oven to allow for tests at elevated temperatures.

3.1.1 Compression tests

Compression have been carried out according to the ASTM standard D 575 [1]

The compression tests were carried out on cylindrical specimens as shown in Figure 3.1.

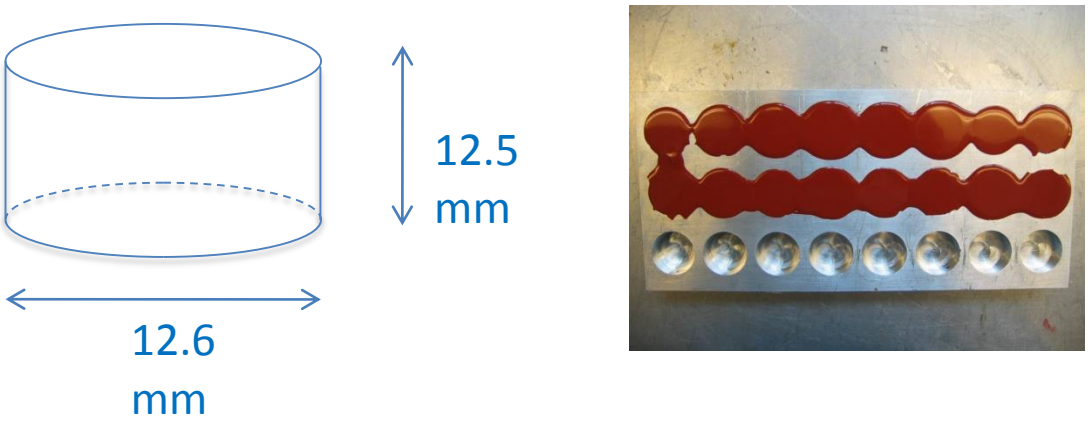

Figure 3.1 Compression test specimen and the mould to produce the specimens.

The specimens had to be produced following as much as possible the guidelines mentioned in [1], in which, though, it was stated that they had to be extracted from a large piece of rubber by means of a suitable rotating hollow cutting tool. This method works well with hard rubbers, while the softer the rubber, the more evident is the hourglass shape of the specimen. For this reason, an ad hoc mould is fabricated which allows the production of 24 specimens at once. This way the environmental condition at which the specimens are made are the same, as well as the amount of time needed for mixing and degassing of the components and the composition, intended as percentage of the two components, of the rubber specimens. In this specific case, only the desired height of the specimen is obtained by sanding after having removed the specimens from the mould.

According to the ASTM specifications, the force and displacement data used to define the mechanical characteristics have to be recorded after being tested twice. In order to have a better view of what is happening with the material properties of the specimens, the rubber specimens were tested at least three times and often up to seven times, where force and displacement data were recorded each time. An example of the series of tests and the stress strain curves is described in Figure 3.2.

In this picture, it is visible that the stress-strain behaviour of the rubber has a different shape from the first test to the following ones, implying a modification of the rubber composition when tested the first time. In the following compression, the rubber tends to slightly reduce its stiffness. This phenomenon is not very significant in the linear area, but an evident reduction in stiffness is evident in the non-linear area.

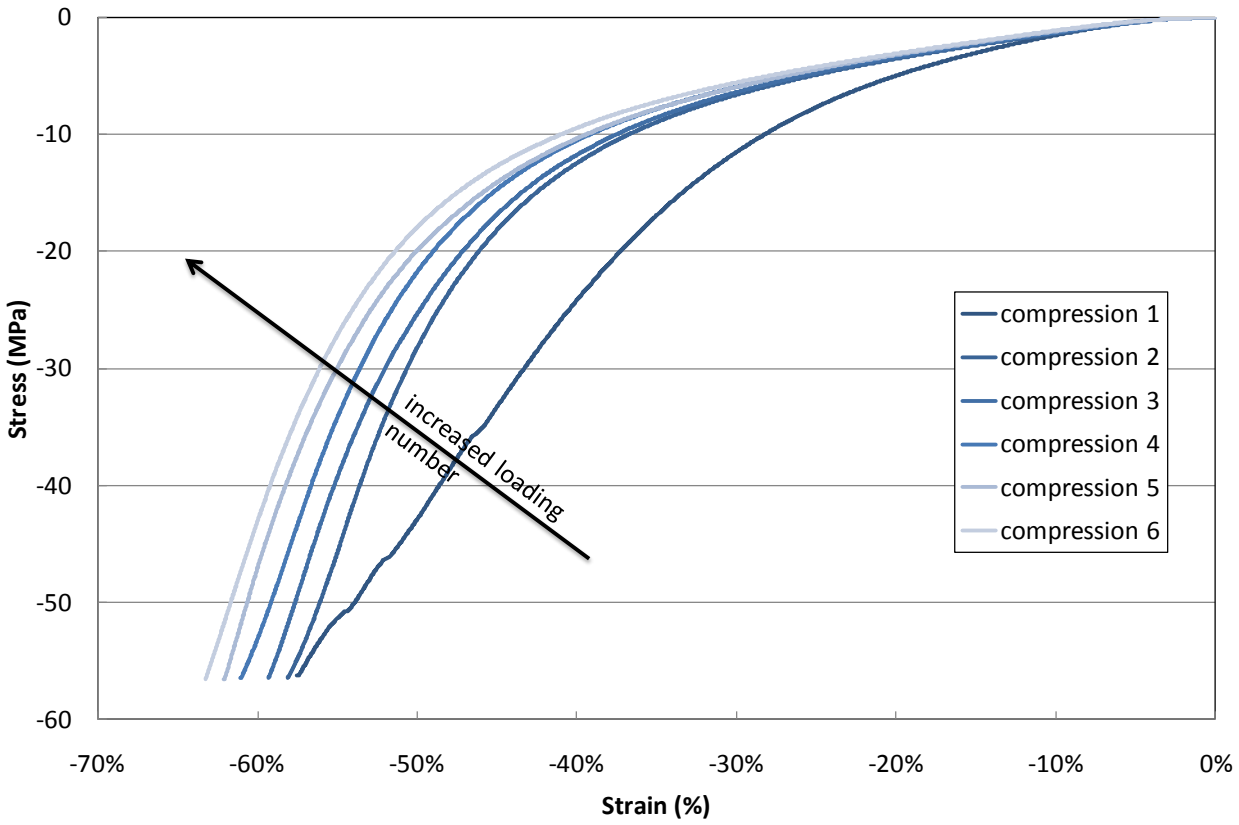

Figure 3.2 Stress-strain curves of a rubber block tested several times.

A major difference between the specimens tested is the failure behaviour of the tested rubbers. The urethane rubber presents a brittle behaviour, which is visible in Figure 3.3, in contrast with the silicon rubbers that do not break in compression.

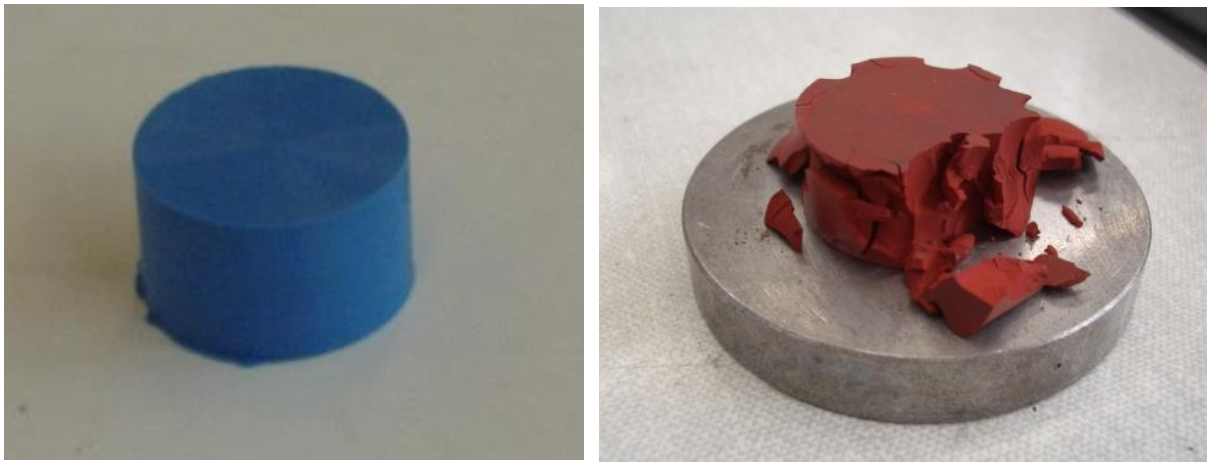

Figure 3.3 Difference in behaviour between silicon, Silastic J, (left) and urethane, UR 3450, (right) rubbers loaded in compression.

3.1.2 Tension tests

Tension tests were carried out on dumbbell specimens as shown in Figure 3.4 according to ASTM standard 412-98a [2].

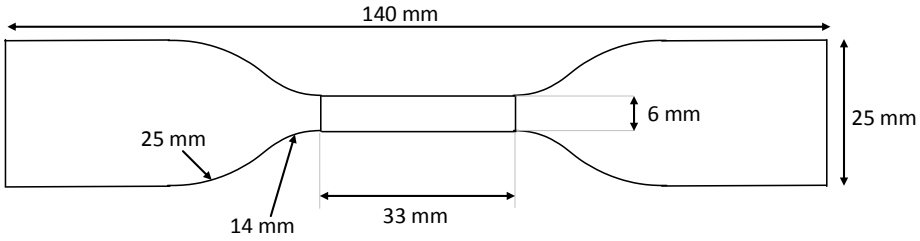

Figure 3.4 Dimensions of the dumbbell specimens as used for tension tests.

The specimens were cut from a sheet of rubber produced in a large closed mould and consolidated in a press at room temperature and at a pressure of 20N, in order to maintain a constant thickness of the sheet. According to the ASTM standard, the thickness of the specimens should be 3mm.

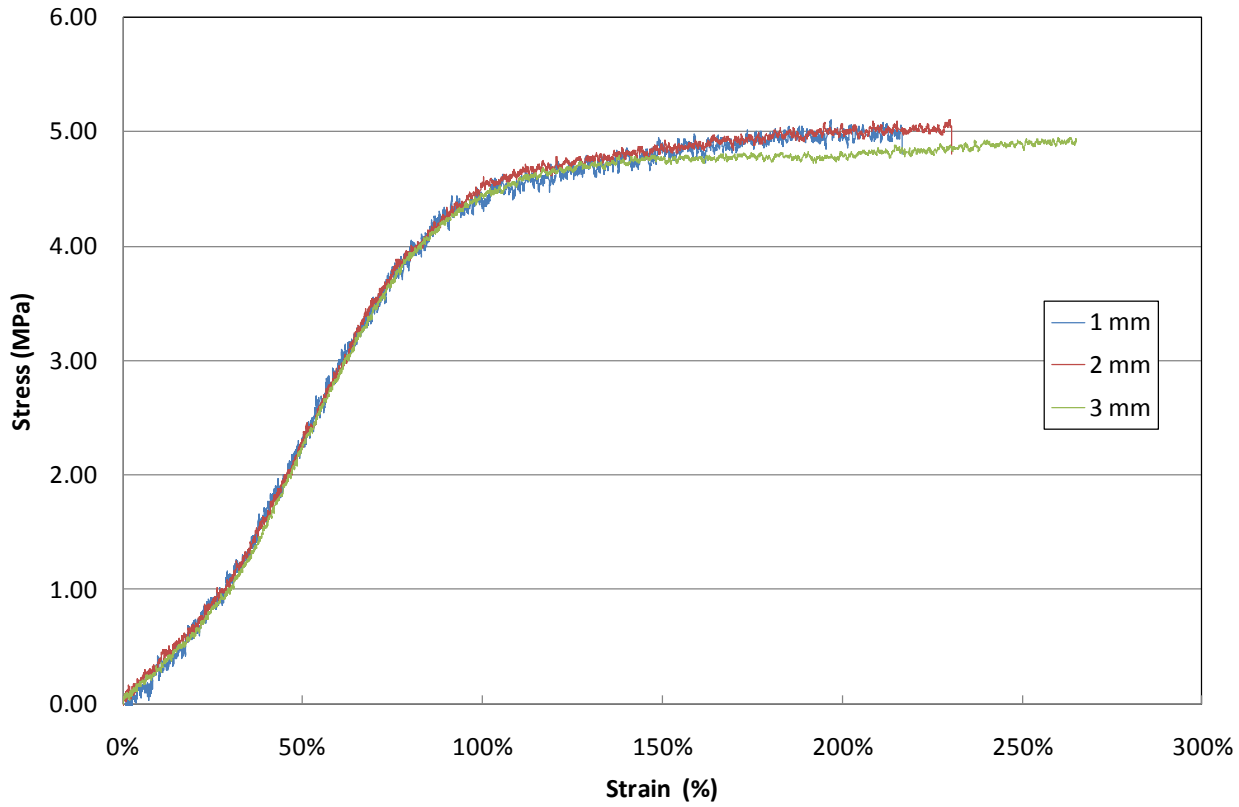

Figure 3.5 Effect of specimen thickness on for Silastic J specimens loaded in tension.

To be able to verify whether the thickness has an influence on the mechanical properties, Silastic J rubber was tested in tension at three different values of thickness from 1mm up to 3 mm.

Figure 3.5 shows that the effect of thickness is not influencing the behaviour of the rubber specimen, as long as the thickness of the specimens is constant. In fact, especially for thin specimens, a variation of the thickness of 10% has a large influence on the overall graph. The only noticeable difference in the three graphs is that the elongation at break increases with the thickness, but as for this work the rubber is mostly loaded in compression, the strength of the rubber is not an important factor.

The rubber sheets from which the specimens are cut are measured in several places and iso-thickness lines have been drawn in order to obtain specimens of an almost constant thickness. Each specimen is then measured in three places and the average thickness is taken for further calculations. The specimens with a thickness variation of more than 5% are excluded.

3.1.3 Discussion of the results

Typical stress-strain curve of the tested rubbers are shown in Figure 3.6 to Figure 3.10.

Results common to all silicon rubbers are that ductility is reduced while stiffness increases up to 20% in the linear area with the increase of the temperature. This behaviour agrees with the behaviour of the rubber during production, in which cracks easily occur in correspondence to sharp edges as it will be shown in the following chapters.

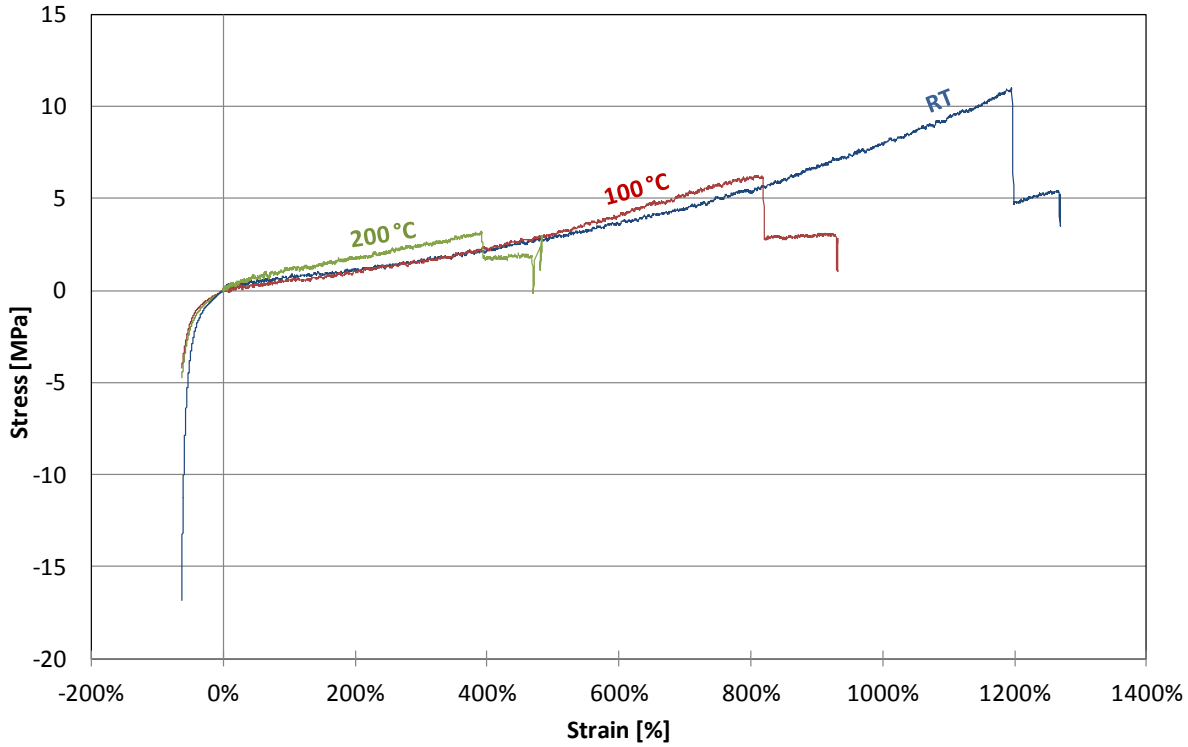

Figure 3.6 Typical stress strain curves for Silastic S (20 Sh A) silicon rubber for various temperatures.

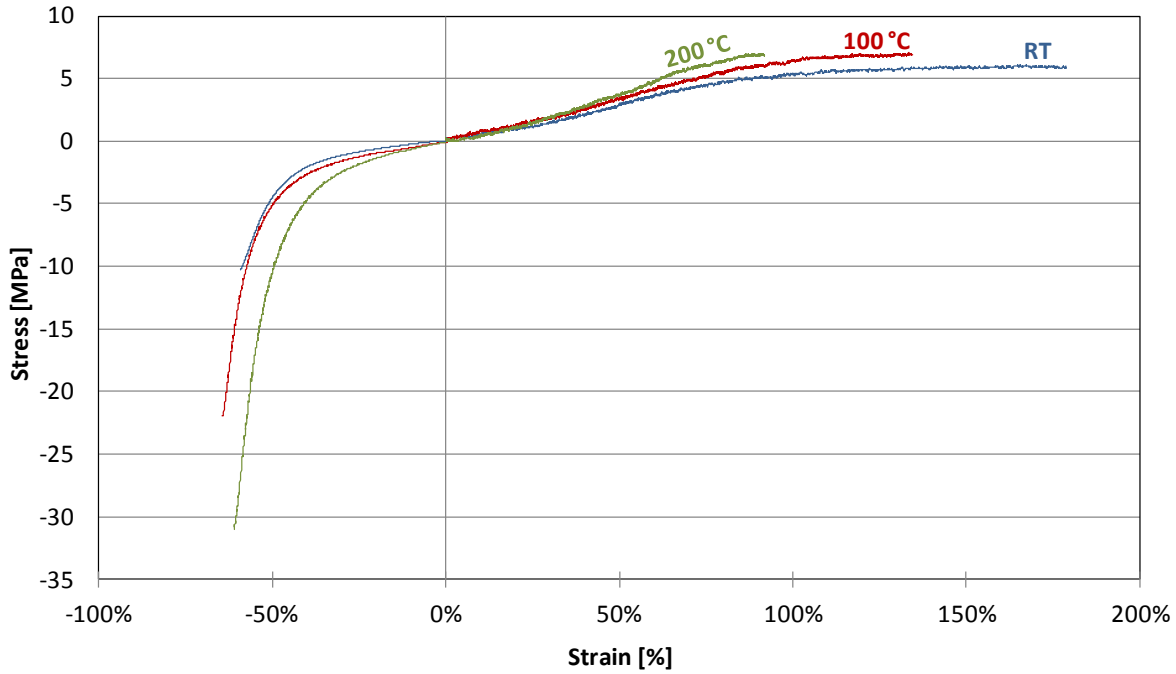

Figure 3.7 Typical stress strain curves for Silastic J (59 Sh A) silicon rubber at for various temperatures.

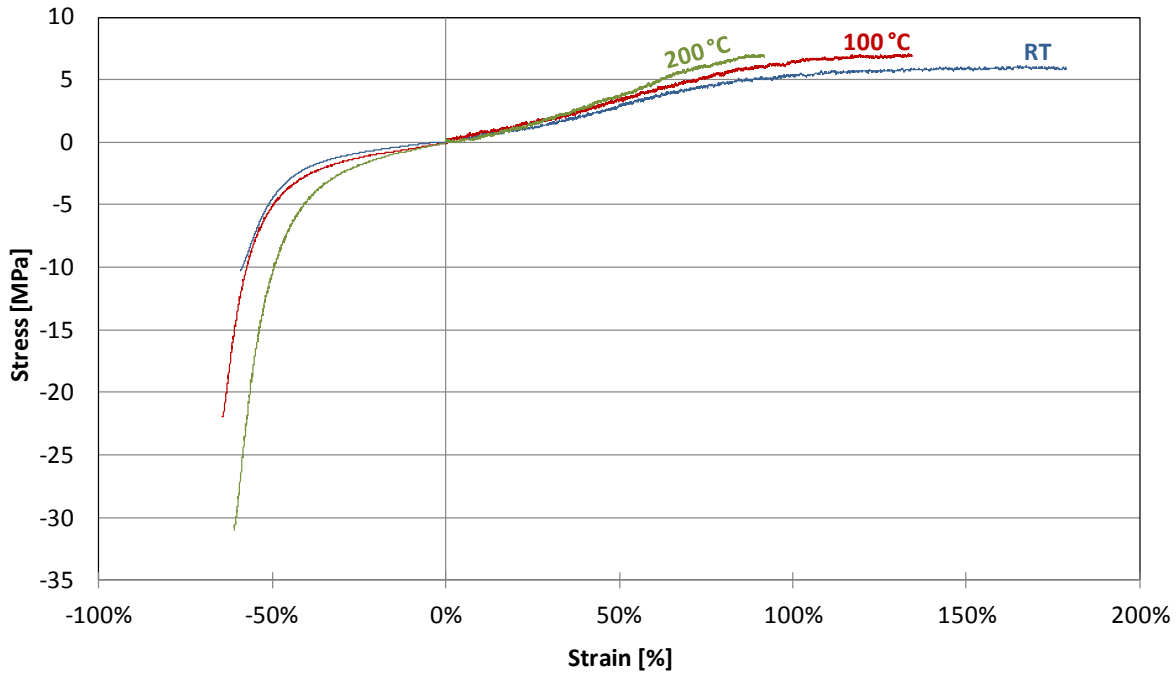

Figure 3.8 Typical stress strain curves for KE1604 (60 Sh A) silicon rubber for various temperatures.

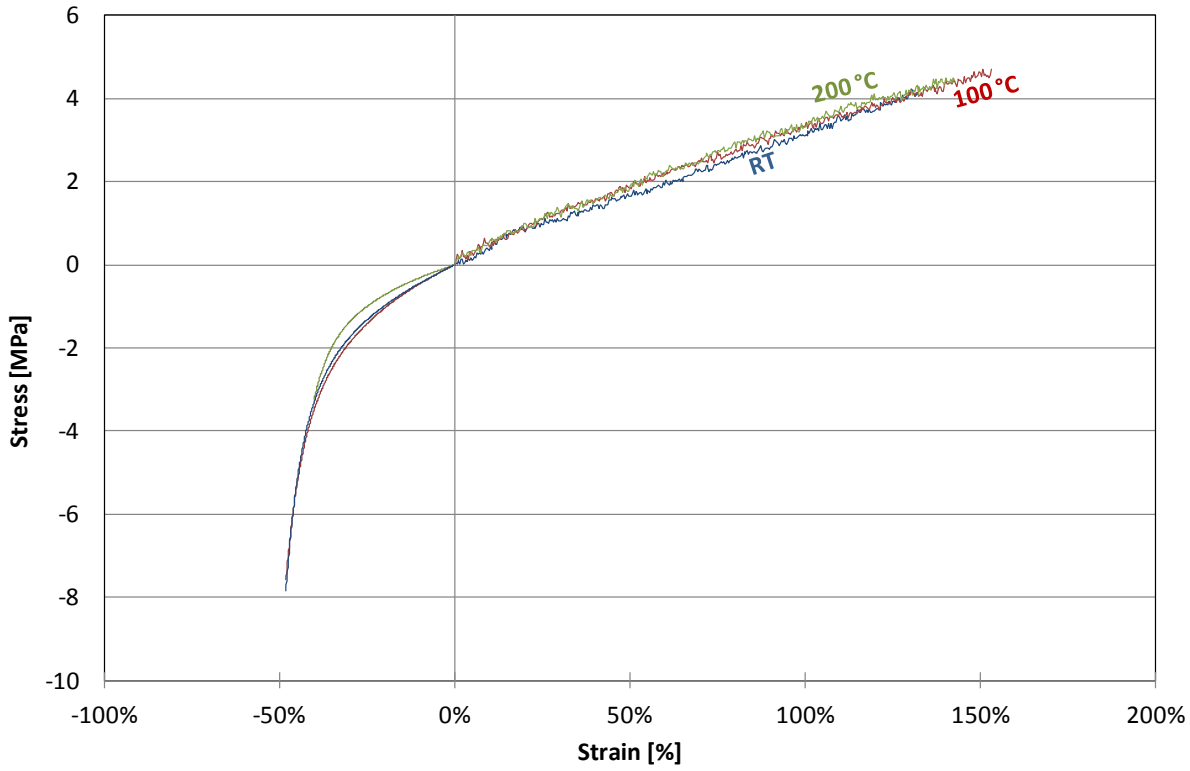

Figure 3.9 Typical stress strain curves for KE113 (70 Sh A) silicon rubber for various temperatures.

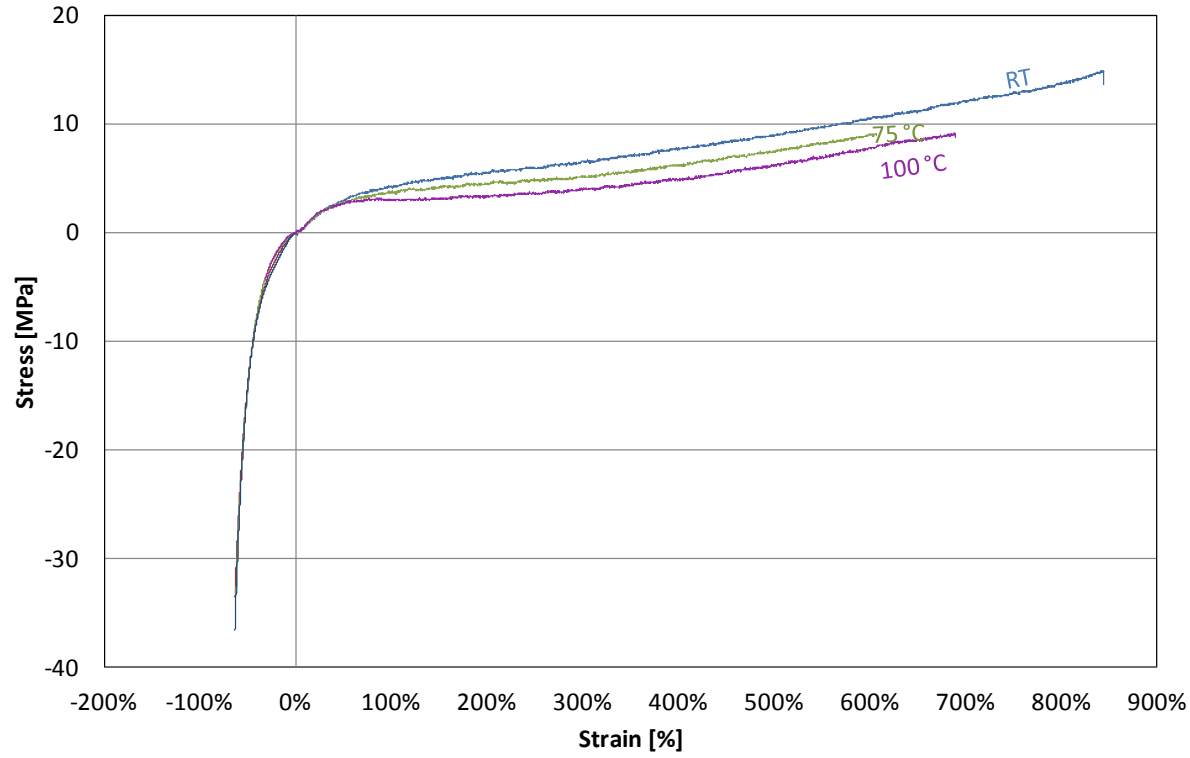

Figure 3.10 Typical stress strain curves for UR-3450 (75 Sh A) urethane rubber for various temperatures.

It should be particularly noted that the hardness of the rubber is responsible for the overall stress-strain curve behaviour of the rubber, as shown in Figure 3.7 and Figure 3.8, where, independently from the manufacturer, the mechanical characteristics are the same.

Though the stiffness of the rubber in the linear area is related to its hardness, it is not possible to predict, through scaling a rubber behaviour of a particular hardness, the stress-strain curve of another one. In order to have the correct stress-strain curves at various temperatures, it is necessary to carry out material tests, unless material data of the used rubber are already available.

Overall, the behaviour of polyurethane rubber in compression is not influenced by temperature, but the maximum working temperature is limiting its use to press forming of metals where heat is not part of the process. In tension, though, the stiffness of the rubber is decreasing with the increase of temperature, in contrast to the silicon rubber, which gets stiffer at higher temperatures. The elongation at break of polyurethane rubber is moreover much higher than the one of silicone, especially considering the hardness of the two types. Yet, as illustrated in Figure 3.3, the Polyurethane rubber is more susceptible to fracture.

3.2 Coefficient of friction

During press forming, contact occurs between the rubber tool and the thermoplastic and between the melted thermoplastic and the steel mould.

The friction between rubber and a hard surface is a topic of practical importance especially for the construction of tires and a great deal of literature is found on this topic ([4], [5], [6]). For this particular topic, the effect of friction between the mould and the melted thermoplastic plate is considered, combined with the friction between the melted thermoplastic and steel. As the thermoplastic stays in its melted form only for a very short period and the measurements could not be carried out in an oven, the melted thermoplastic was substituted by polyurethane rubber. The same rubber is also used as matrix for a substitute laminate in the experimental set-up shown in Chapter 4.

The static coefficient of friction (CoF) between either steel or urethane rubber and silicon rubber has been measured making use of a simple measuring system [3], whose components are shown in Figure 3.11.

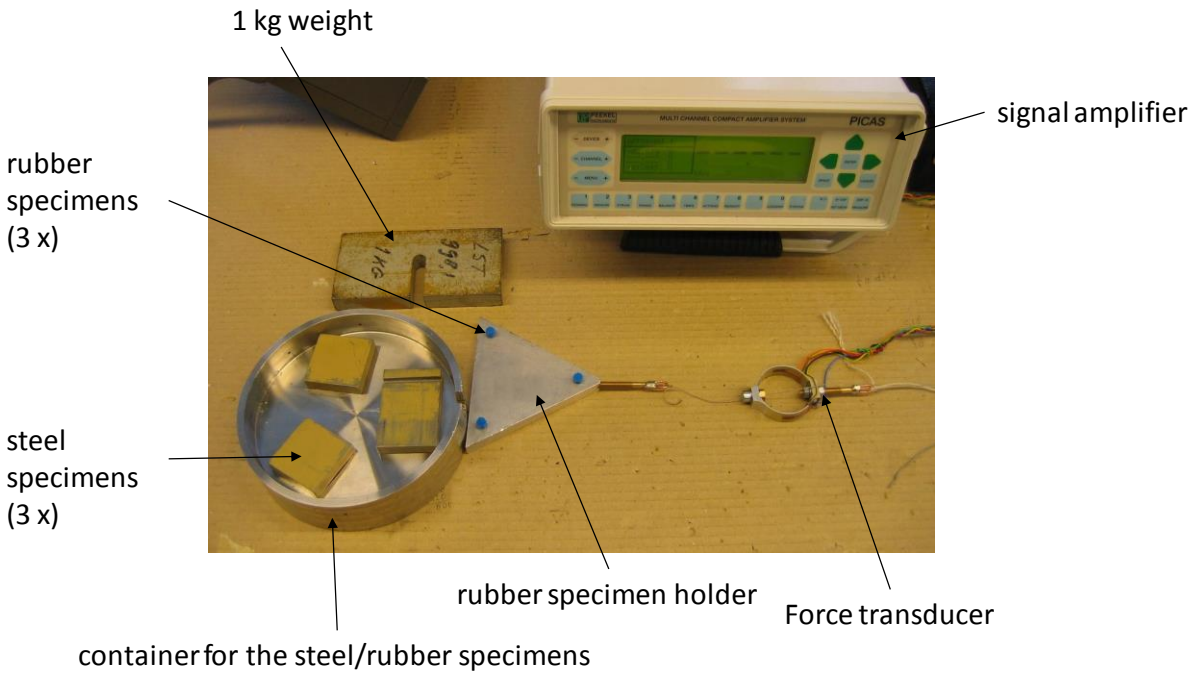

Figure 3.11 Overview of the components of the experimental test set-up to measure the static coefficient of friction.

Three steel (or rubber) specimens are placed in the container, while three elastomeric specimens are fixed in the triangular holder. The triangular holder is then placed above the container for the steel specimens in such a way that each steel specimen is in contact with one rubber specimen. A weight of 1 kg is then placed on top of the triangular holder (Figure 3.12) which is connected to a force transducer, connected to the amplifier on the other side. A schematic representation of the test is shown in Figure 3.13 for simplification.

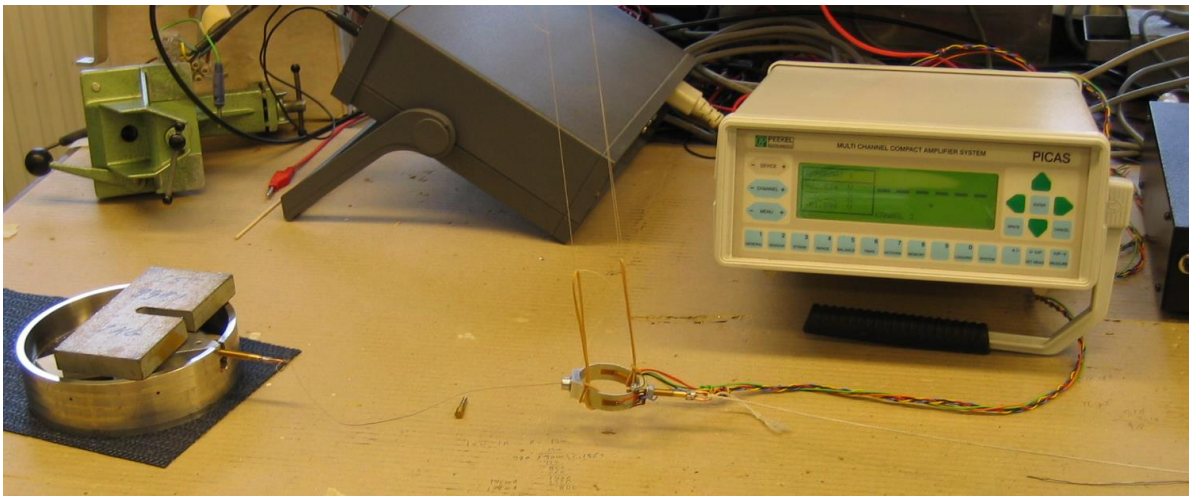

Figure 3.12 Assembled set-up for the measurement of the CoF.

The force sensor that transmits the electrical signal to the amplifier measures the pulling force F. At that moment, the force is shown and recorded. The static friction is measured when the triangular holder starts to move.

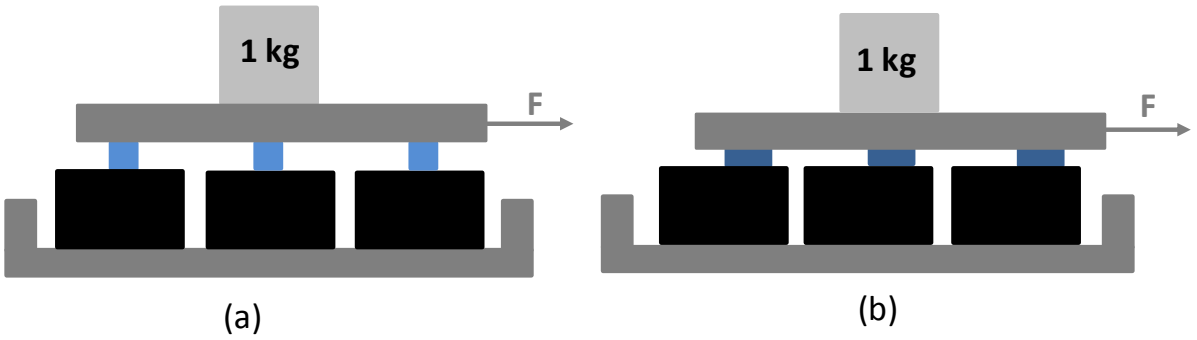

Figure 3.13 Schematic representation of the friction measurement test.

The tests were carried out at room temperature and elevated temperature in a range from 50°C up to 200°C as shown in Table 3.2.

T	RT	50°C	75°C	100°C	150°C	200°C
rubber-metal	0.829	0.816	0.790	0.737	0.715	0.634
rubber-rubber	0.914	0.902	0.814	0.801	-	-

Table 3.2 CoF between Silastic J rubber and metal and between Silastic J rubber and urethane rubber at different temperatures.

In both cases, the coefficient of friction is decreasing with the increase of temperature, which is consistent with the results found in literature. As the trend is the same with both rubber and metal, the results seem to be consistent.

3.2.1 Effect of lubrication on the CoF

According to the Dow Corning, the coefficient of friction can be lowered by surface treatment or incorporation of molybdenum disulphide into the rubber. The use of molybdenum disulphide means that the property becomes a feature of the rubber, while surface treatments are subjected to wear. If case molybdenum disulphide is used, the rubber needs to be characterised again in order to verify the change in mechanical characteristics. The surface treatment, on the other hand, must be investigated as well, to control whether the treatment influences the characteristics of the thermoplastic during forming. In practice, the use of lubricants is already in use in a preliminary production phase, when the production parameters are not identified yet. In order to be able to quantify the effect of different lubricants, the same experiment described before, is carried out with three different types of lubricants: pure water, vaseline and a release agent (Shell Morlina® Oil).

	No lubrication	Water	Oil	Vaseline
rubber-metal	0.829	0.671	0.079	0.071
rubber-rubber	0.914	0.390	0.089	0.055

Table 3.3 Effect of lubrication on the CoF at room temperature.

In the case of water, the CoF is reduced of 20% with respect to the non-lubricated one, while for both Vaseline and release agent the reduction is much more drastic, arriving at more than 90% reduction. The reduction of the CoF seems therefore an important topic for further investigations once it is demonstrated that it plays an important role during pressure forming.

3.3 Coefficient of thermal expansion

A characteristic of the silicon rubber used is the high coefficient of thermal expansion (CTE). The coefficient of thermal expansion of silicon rubber is in the order of 10^{-3} K^{-1}, which is an order of magnitude higher than metals. With this coefficient, a rubber expands about 15% of its original length while heated up from room temperature to 160 °C, which is a typical working temperature during rubber forming. This is quite a large value, which means that even when the product to be manufactured is small, the increase in volume of the mould is significant, especially when small details are changing the shape of the final product, in particular during series production.

The CTE has been measured in the case of Silastic J. The value provided by Dow Corning Co. Ltd of this rubber is 8.7 x 10^{-4} K^{-1} (between 25~125°C). Because the allowed operation temperature of the rubber mould is higher than 200°C and the temperature inside the mould for series production reaches 160°C, tests are carried out to be able to measure the coefficient of thermal expansion of the rubber in this range of temperatures.

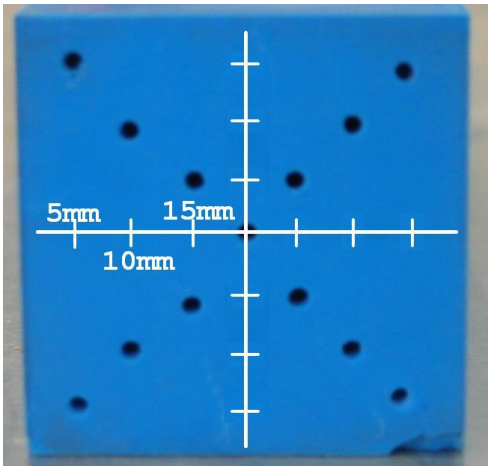

Figure 3.14 measurements of the CTE

The tests are simply done by measuring the dimensions of a rubber die, as shown in Figure 3.14, at room teperature and higher temperatures. The measured thermal expansion coefficient is 1.605 x 10^{-3} K^{-1}**,** which not only is twice as large as the value given by the manufacturer, but also is a very high value, which considerably influences the shape of the rubber during the process and has to be taken into account when designing the rubber mould.

3.4 Conclusion

In this chapter, the most important characteristics of some of the rubbers used to manufacture the moulds for pressure forming have been investigated. It is shown that the three parameters considered, namely hardness, coefficient of friction and coefficient of thermal expansion, have to be taken into account when designing a proper mould. In particular, the hardness of the rubber has to be considered, because it is influencing the stiffness of the mould and its ability to deform, especially at corners. The coefficient of friction between the rubber mould and the steel mould is also very high. This, combined with the coefficient of friction of the melted thermoplastic, is a factor that negatively influences the forming process but cannot be avoided in an easy way, as lubricants might negatively influence the mechanical performances of the thermoplastic material and therefore of the product. The coefficient of thermal expansion is also a parameter of great importance as, especially for large products, the shape of the mould changes at high temperatures and that might influence the pressure distribution exactly in the places it is needed more. The material characterisation can be used for a thorough finite element analysis of the process as usually the rubber type and mechanical properties are not taken as important parameters during simulations.

3.5 Bibliography

[1]. ASTM standard D 575 “Standard Test Methods for Rubber Properties in Compression”
[2]. ASTM standard 412-98a “Standard test methods for vulcanized rubber and thermoplastic elastomers-tension”
[3]. R. Oosterom “Design Considerations for the Glenohumeral Prosthesis” PhD Thesis, Delft University of Technology 2005
[4]. Grosch K.A. “The Relation between Friction and Visco-Elastic Properties of Rubber” Proceedings of the Royal Society of London. Series A, Mathematical and Physical Science, Vol. 274, No1356, pp21-39
[5]. Schallamach A. “Friction and Abrasion of Rubber” Wear, Elsevier 1057/58
[6]. Persson, B.N. “Theory of Rubber Friction and Contact mechanics” Journal of Chemical Physics, volume 115, number 8, 2011

Chapter 4
Pressure distribution during forming

4.1 Introduction

As shown in Chapter 3, the behaviour of each silicon rubber is different and depending on hardness and brand. Generally, every producer of thermoplastic composite products uses only one or two types because he is used to their behaviour, can design the moulds more easily, and does not want to experiment on new types. On the other hand, many trials are still needed to obtain a good product, even if the rubber is known. To be able to reduce and ideally eliminate the trials to find the ideal shape of the rubber mould, it is necessary to understand the behaviour of the mould during the forming process, therefore the pressure distribution on a steel mould exerted by the rubber mould during pressing is measured. The tests are carried out at room temperature and at elevated temperatures, in order to verify the effect of the thermal expansion on the pressure distribution. The effect of the thermoplastic laminate is simulated as well.

4.2 Method

The test set up consists of a steel mould for press forming of U-beams. This shape is very useful because it allows carrying out tests in which the only parameter that has to be taken into account is the rubber mould, while the in plane shearing of the fibres is not present. The mould allows the production of beams of different heights and widths. The results that are presented in this chapter though are for beams 40 mm wide and 40 mm high. The length of the mould is 180 mm.

A series of pressure sensors is placed in the centre section of the mould, as shown in Figure 4.1. This way the pressure distribution on the three sides of the mould is measured, so that it is possible to verify whether the distribution is constant, as desired.

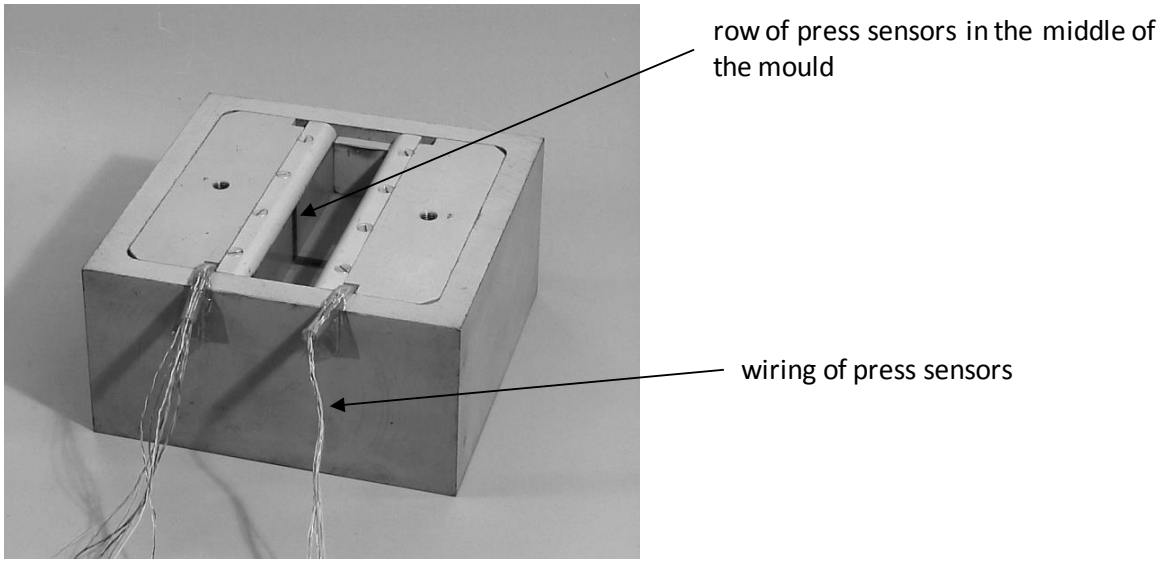

Figure 4.1 Metal mould and pressure sensors.

To be able to acquire data on the pressure distribution during pressing of thermoplastics, a test set up has been built as shown in Figure 4.2.

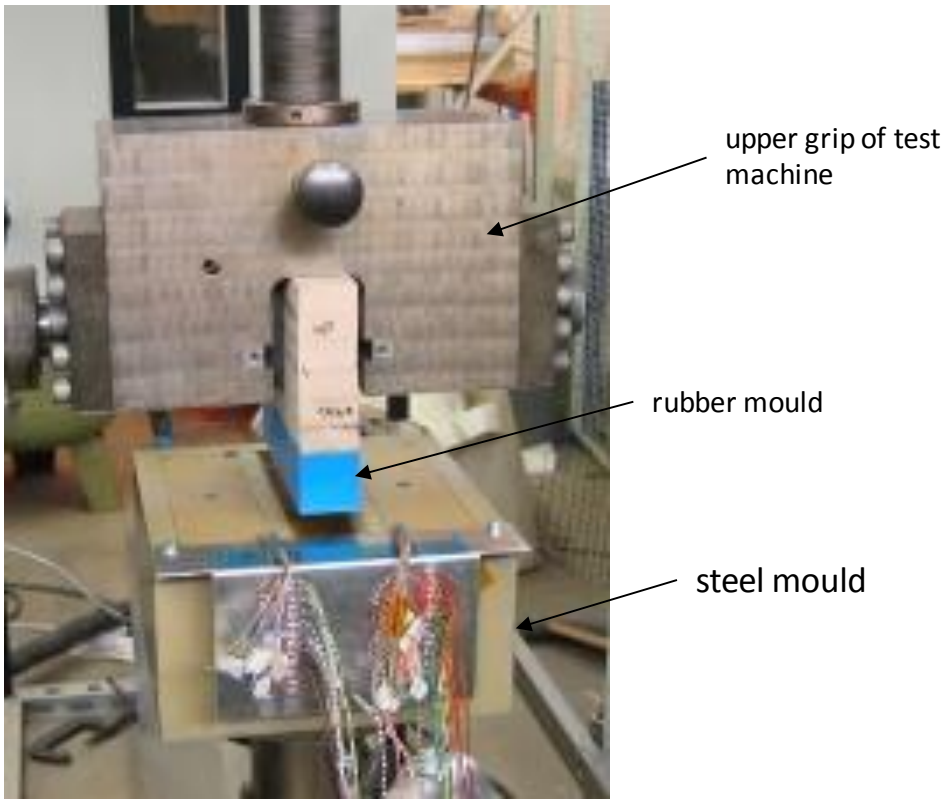

Figure 4.2 Test set-up.

The tests have been carried out on a 25 Tons static Zwick Roell testing machine that, with the addition of an oven, allows carrying out tests at higher temperatures.

4.2.1 Pressure sensors

The pressure sensors consist of a steel plate supported at both edges by a 1mm ridge made in the mould. A strain gauge is placed in the middle of the backside of the plate. The pressure exerted on the upper surface of the steel plate makes it bend, creating a strain, which is measured by the strain gauge (either 10 x 10 mm, 2 mm thick or 10 mm length, 5 mm width and 2 mm thickness).

The pressure sensors are incorporated in the mould by machining two superimposed slots of respectively 8 and 10 mm wide and 4 and 2 mm deep. This way, the pressure sensors are supported at both sides by 1mm ridge in the mould.

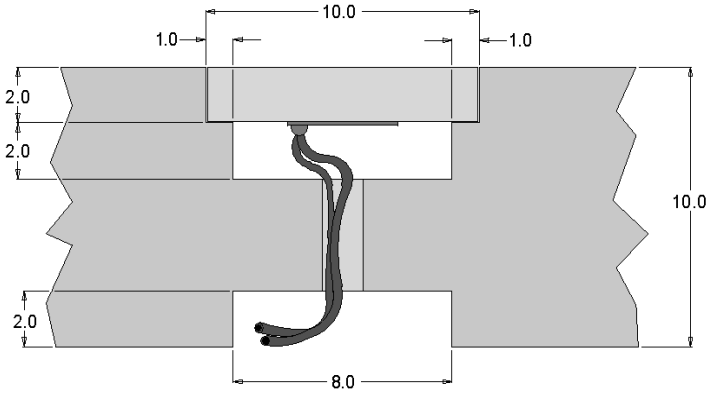

Figure 4.3 Schematics of the pressure sensors in the steel mould.

The sensor can be regarded as a beam, supported at both ends and loaded by a distributed load. It is unknown how the ridge exactly supports the steel plate, and a point load halfway the support is assumed, as shown in Figure 4.4 .

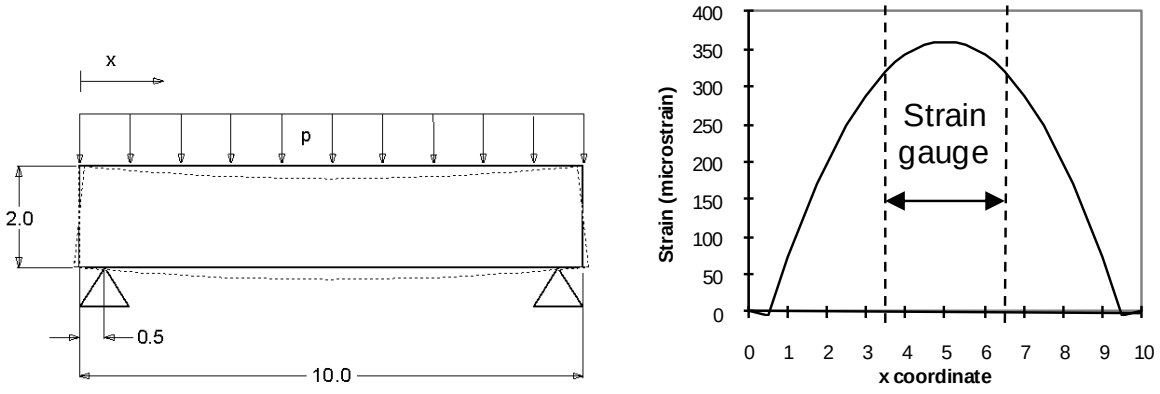

Figure 4.4 Schematisation of the pressure sensor and its strain distribution in case of a 5 MPa applied pressure.

The bending moment in the beam is (left side):

$$
\begin{aligned}
0 \le x \le 0.5: \quad & V = -pbx \\
& M = -\tfrac{1}{2}\, pbx^2 \\
0.5 < x \le 5: \quad & V = -pbx + 5pb \\
& M = -\tfrac{1}{2}\, pbx^2 + 5pb(x - 0.5) \\
& \quad = pb(-\tfrac{1}{2}\, x^2 + 5x - 2.5)
\end{aligned}
$$

The strain at the lower side of the steel plate (of width b) then is:

$$\varepsilon(x) = -\frac{My}{EI} = \frac{M\,\frac{1}{2}h}{E\,\frac{1}{12}h^3 b} = \frac{6M}{Ebh^2} = \frac{6p}{Eh^2}(-\tfrac{1}{2}\, x^2 + 5x - 2.5)$$

A 3 mm strain gauge records the average strain in the middle of the steel plate:

$$\varepsilon_{sg} = \frac{1}{6.5 - 3.5}\frac{6p}{Eh^2}\int_{3.5}^{6.5}(-\tfrac{1}{2}\, x^2 + 5x - 2.5)dx = \frac{2p}{Eh^2}\left[-\tfrac{1}{6}\, x^3 + 2.5x\right]_{3.5}^{6.5} = 57.75\frac{p}{Eh^2}$$

Two different types of strain gauges were used. Initially, only measurements at room temperature were made. In that case resistance type strain gauges (micro measurements© EA-06-060LZ-120) were used. Later, tests at higher temperature were carried out, for which high temperature strain gauges (BLH S6) were used.

4.2.2 Laminate

There are several reasons why it is not possible to use a hot thermoplastic laminate during static tests. The most important reason is that the laminate would solidify during testing. Moreover, the strain gauges are influenced by the sudden change in temperature and will not be able to properly measure the change of pressure. In order to simulate the effect of the laminate in the pressure distribution during pressing, a cold laminate made of carbon fibre fabric with a flexible elastomeric matrix was used. It approximately simulates the important characteristics of a real thermoplastic laminate: flexibility, strength, stiffness and the friction with the rubber mould during the process. The advantages of this laminate are that the experiments are not influenced by the variables that are introduced by real laminates such as the laminate thickness variation, the quick temperature drop in the laminate, the matrix viscosity and fibre orientation. This reduces the number of variables and makes the results more clear and consistent.

Two types of laminate were used. The first one consists of one layer of UD carbon fibres was used with a polyurethane rubber (UR 5801/5825) from AXON with a 58 ShA hardness. The thickness of the laminate was 0.5 mm. The results are presented in section 4.3.

For the high temperature tests, a second laminate was made, consisting of one layer of carbon fabric and the silicon based rubber, namely Zermack ZA 22 Mould with a nominal hardness of 22 ShA. The thickness of the laminate was 0.5 mm.

In order to simulate a blank holder, a frame to be attached to the test mould was built, as shown in Figure 4.5. By varying the weights attached to the cable system, the blank holder forces could be varied. This arrangement allows the laminate to translate in only one direction, i.e. inside the mould.

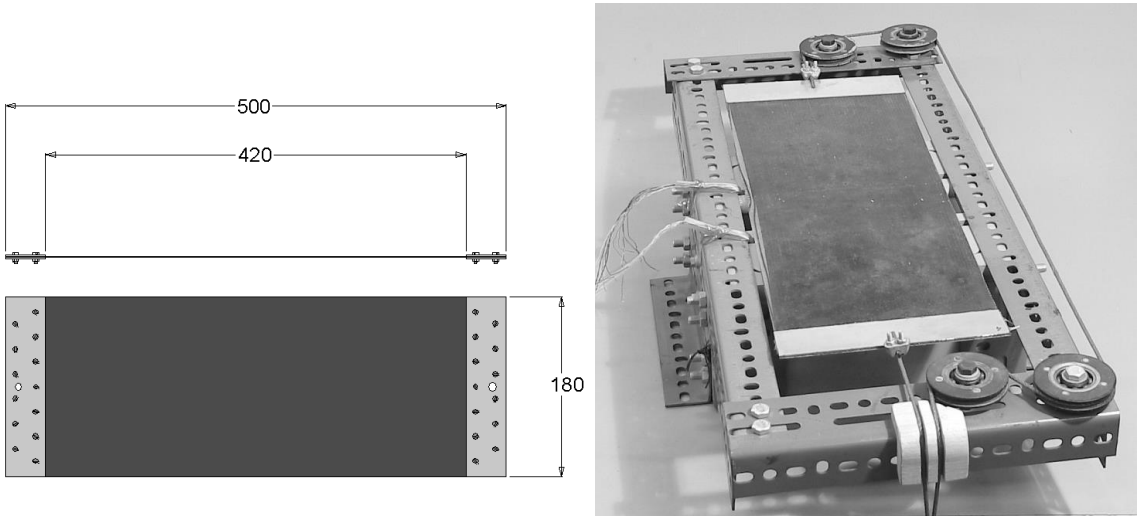

Figure 4.5 Dimension of the laminate used for the static tests and blank holder frame.

The blank holder frame could not be used in the tests at higher temperature, due to the fact that the frame could not fit in the oven. In those cases, the laminate was just placed over the mould, simulating the absence of the blank holder, which is a normal case when the first trials are made.

4.3 Possible mould designs

In general the process conditions need to be taken into account during the design of an elastomeric mould. The easiest way to manufacture the mould is casting it into the negative steel mould, assuming that the elastomer will exert a constant pressure distribution.

In this specific case, the shape of the rubber mould will be the one shown in Figure 4.6 (a). In practice, the rubber mould is attached to the press, thus the top side of the rubber mould will be limited in deformation. The bottom side is limited in deformation as well, as high friction occurrs between the steel mould and the thermoplastic composite and between the thermoplastic composite and the rubber mould. The deformation of the rubber will be therefore similar to what shown in Figure 4.6 (b).

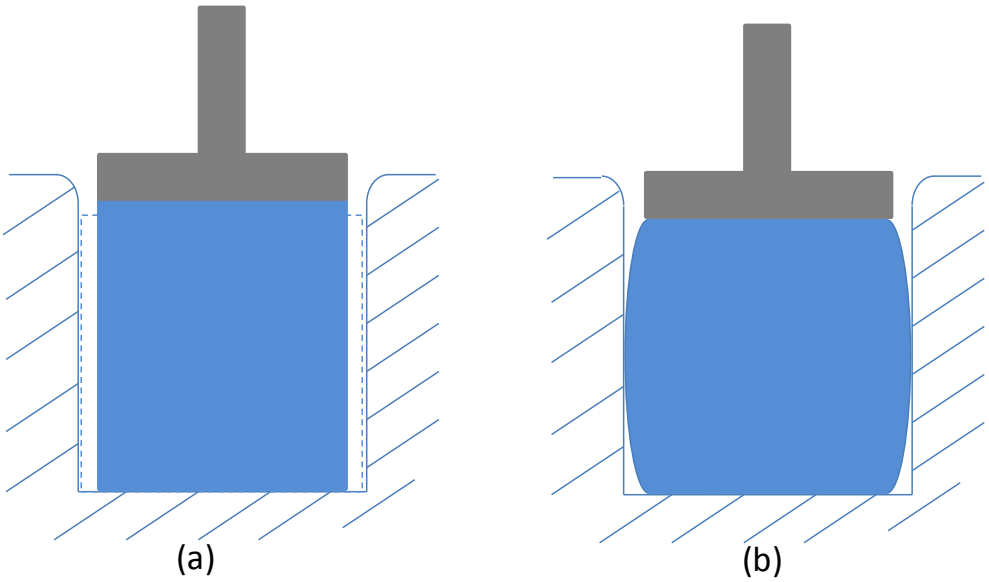

Figure 4.6 Expected deformation of a rectangular cross-section before (a) and during (b) pressing.

For this reason, several options have been considered and are shown in Figure 4.7 [4].

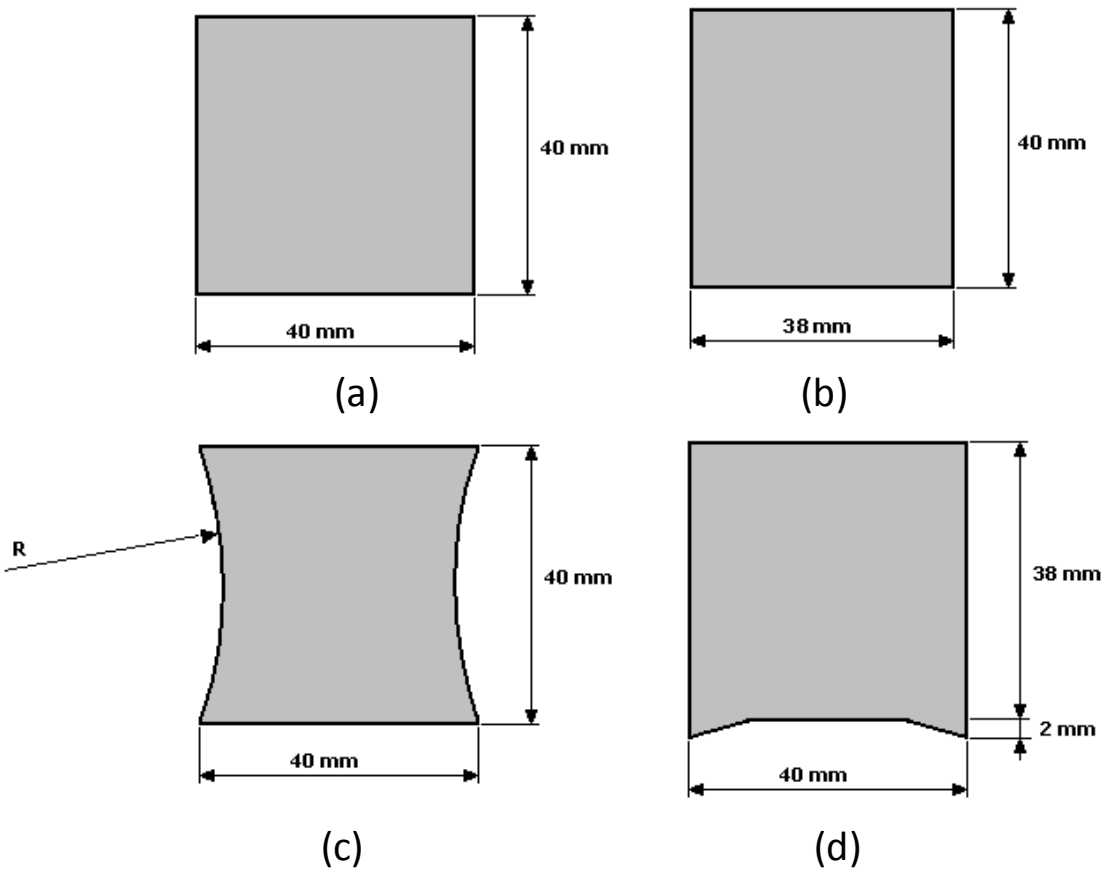

Figure 4.7 Mould designs for the production of a U-beam: classical shape (a), classical shape with additional clearance (b), hourglass shape (c), dents at the bottom to allow more pressure at the corners (d).

The first one (a) is the classical shape, with almost no clearance between the two moulds. In the second, (b) an additional clearance of 1 mm on each side is left, to account for the laminate thickness. Option (c) has an hourglass shape, to counteract the natural barrel shape deformation due to pressing. The two dents in option (d) are made to be sure that the corners of the beam are pressed correctly. In this case, the thermoplastic laminate will get in contact with the mould at the corners, reducing the temperature in that point and allowing for a better consolidation at the corners.

Option (c) and (d) are typical "trials and errors" shapes. In fact, the ideal radius of the hourglass is not known as well as the shape of the dents. Also in this simple case the trials necessary to achieve the correct shape, could be many.

4.3.1 Experimental details

Tests have been carried out, when possible for all four types of mould, at both room temperature and at 75 °C with and without laminate. The maximum applied load is 5 MPa pressure.

4.3.2 Discussion of the results

All the results are presented in plots where the x-axis represents the expanded view of the cross section of the mould where the pressure sensors are placed. In Figure 4.8 the position of the pressure sensors as schematised in the plots is shown. In the y-axis the pressure distribution in the mould is shown.

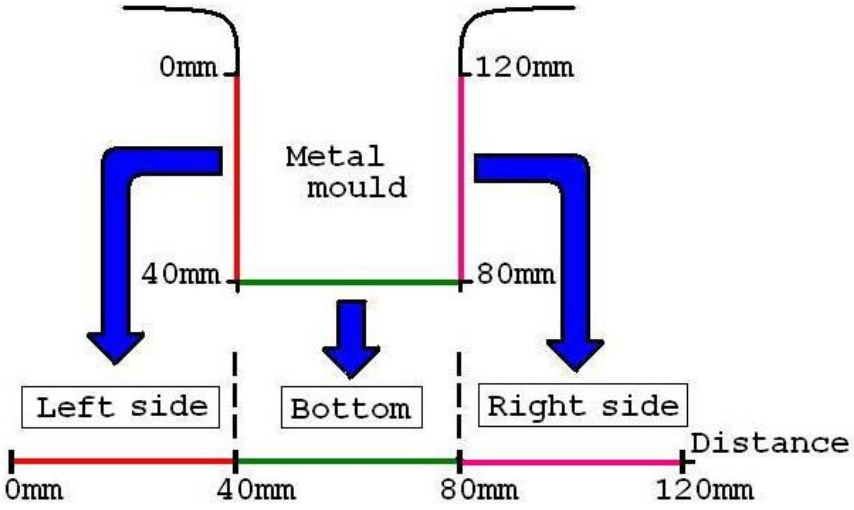

Figure 4.8 Graphical representation of the test results

In Figure 4.9 the four moulds are tested at room temperature without the presence of the laminate. In this case, the perfectly fitting mould, type (a) has the best performance, giving a more uniform pressure distribution, as expected. The second best is type (d), with the dents on the bottom side of the rubber mould. Both moulds, though, cannot be used in the presence of a 5 mm thick laminate, as shown in Figure 4.10, as they could not fit in the mould. In this case the hourglass-shaped mould (c) performs better than the mould with a constant clearance, being

the loss of pressure at the corners less, but the pressure distribution at the sides is not optimal, as the pressure distribution is lower than the one with constant clearance.

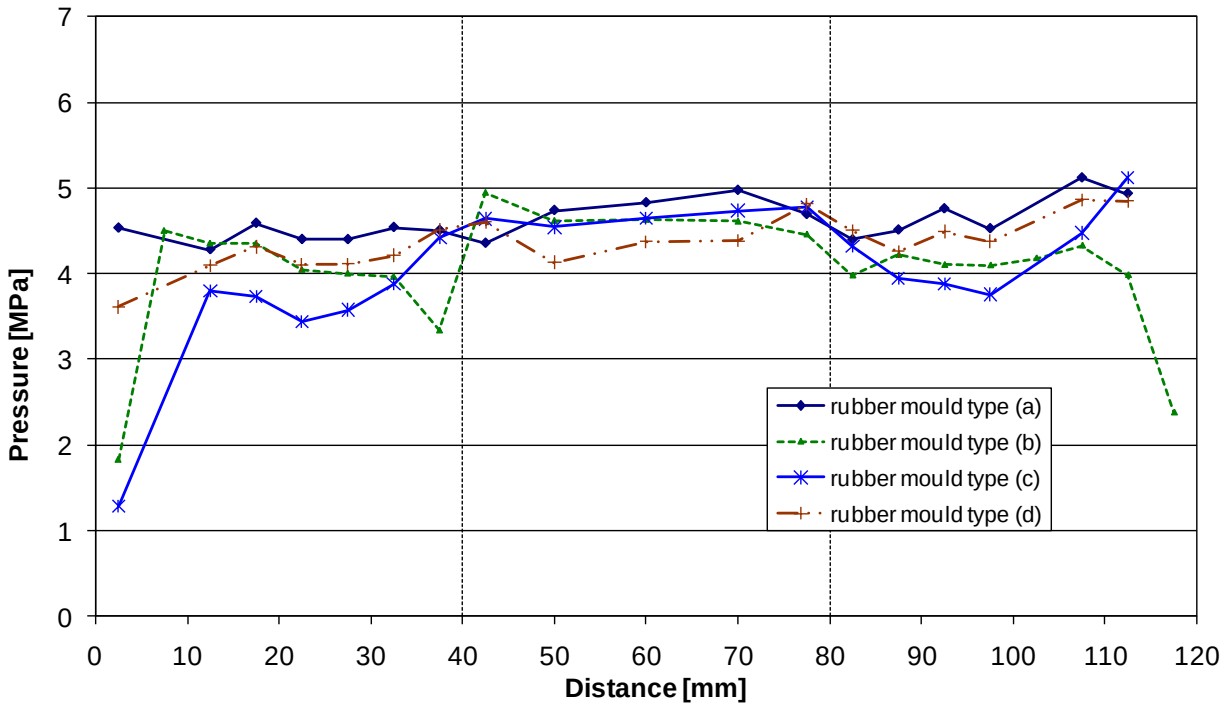

Figure 4.9 Pressure distribution at room temperature without laminate.

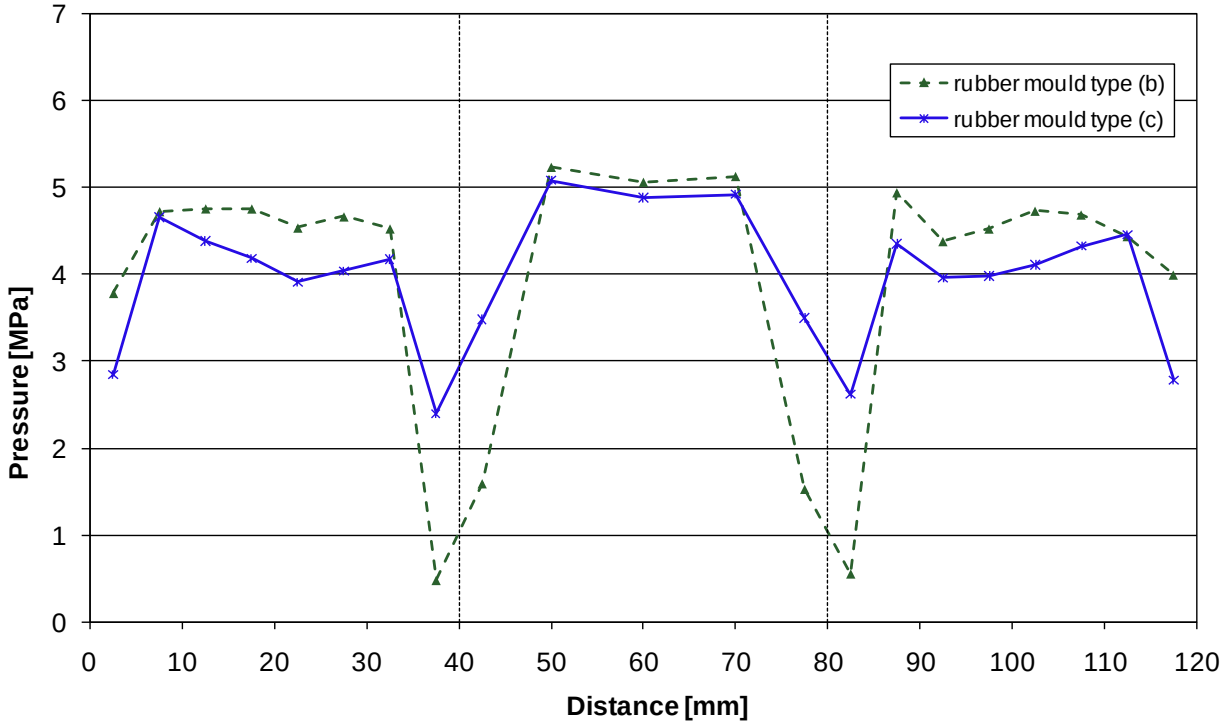

Figure 4.10 Pressure distribution at room temperature with laminate.

The effect of the presence of the laminate, even at room temperature, is also very interesting. Both usable moulds, in fact, present a worst pressure distribution with the laminate. The explanation is that due to the relatively low stiffness of the silicon, the laminate makes the mould deform in such a way that there is less rubber at the corners than without the laminate.

A representation of what happens in the case a laminate is rubber pressed in the mould is shown in Figure 4.11. Here, the blank holder with a certain force holds the laminate while the rubber mould presses it into the steel one. The laminate, still held by the blank holder, exerts also a certain force into the rubber mould, deforming it even more in the corners, reducing the amount of pressure in the corners.

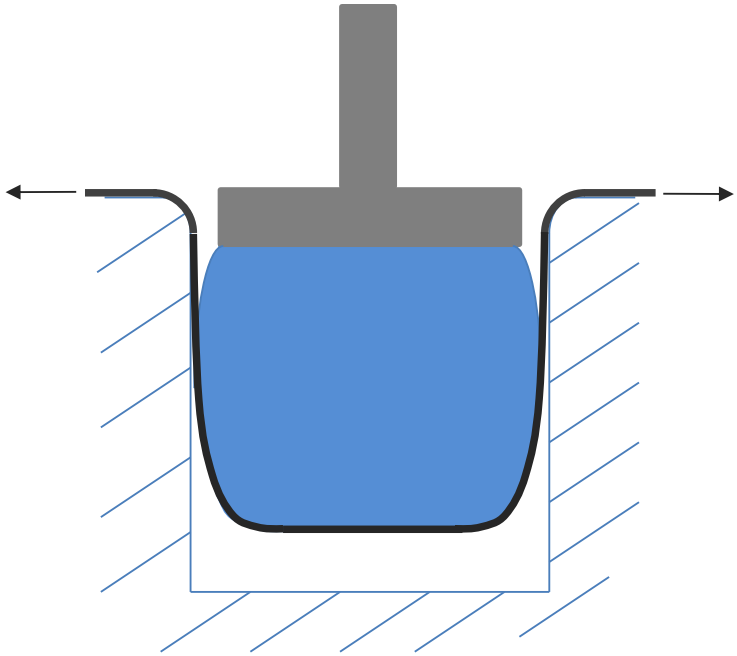

Figure 4.11 Schematic view of the barrelling effect of the rubber die during rubber forming.

Only two moulds could be pressed with the laminate, namely the mould with the constant spare (b) and the one with an hourglass shape (c). The width of the other two rubber moulds is too large to allow the introduction of a laminate to be pressed.

A variation of about 50 °C can bring a substantial variation of pressure distribution, as shown in Figure 4.12 and Figure 4.13. The use of a mould with an optimised shape at room temperature, in fact, has a different behaviour when using a laminate and at elevated temperatures. The effort to optimise a mould, therefore, is still high and only valid for large series production, where the mould temperature has become stable or taking care that the mould is always at the same temperature, for example keeping it warm during the entire process.

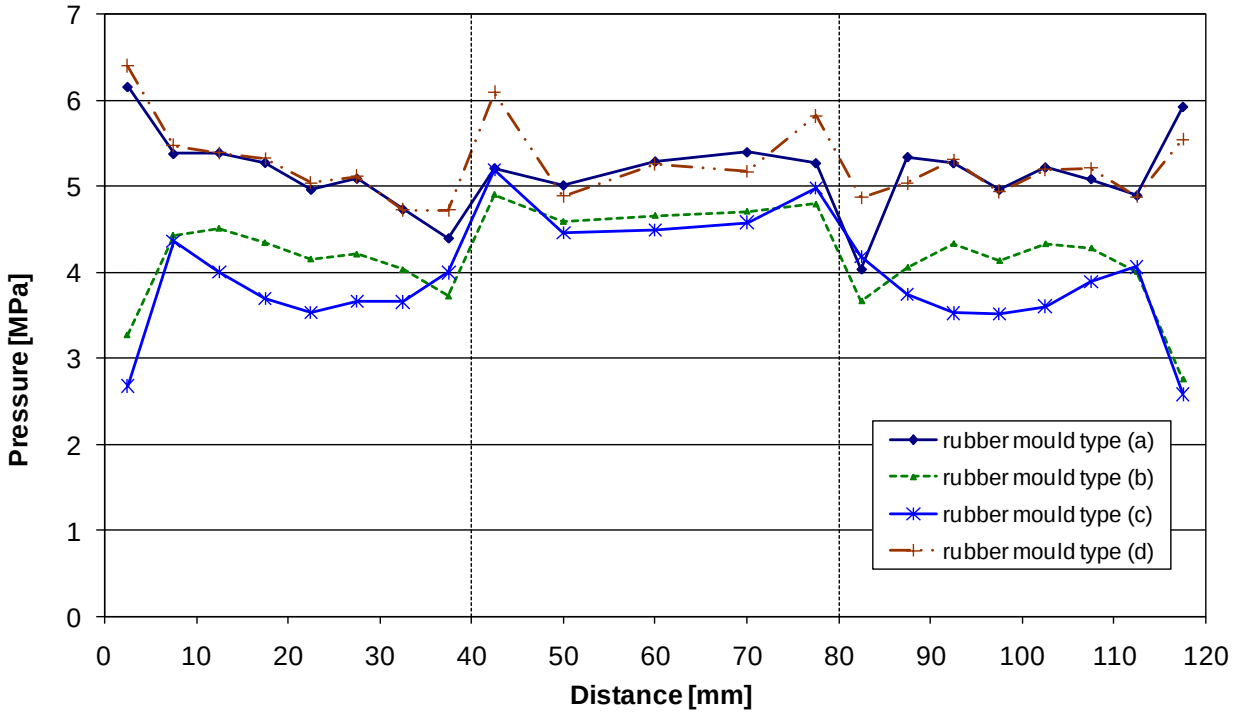

Figure 4.12 Pressure distribution at 75 °C without laminate.

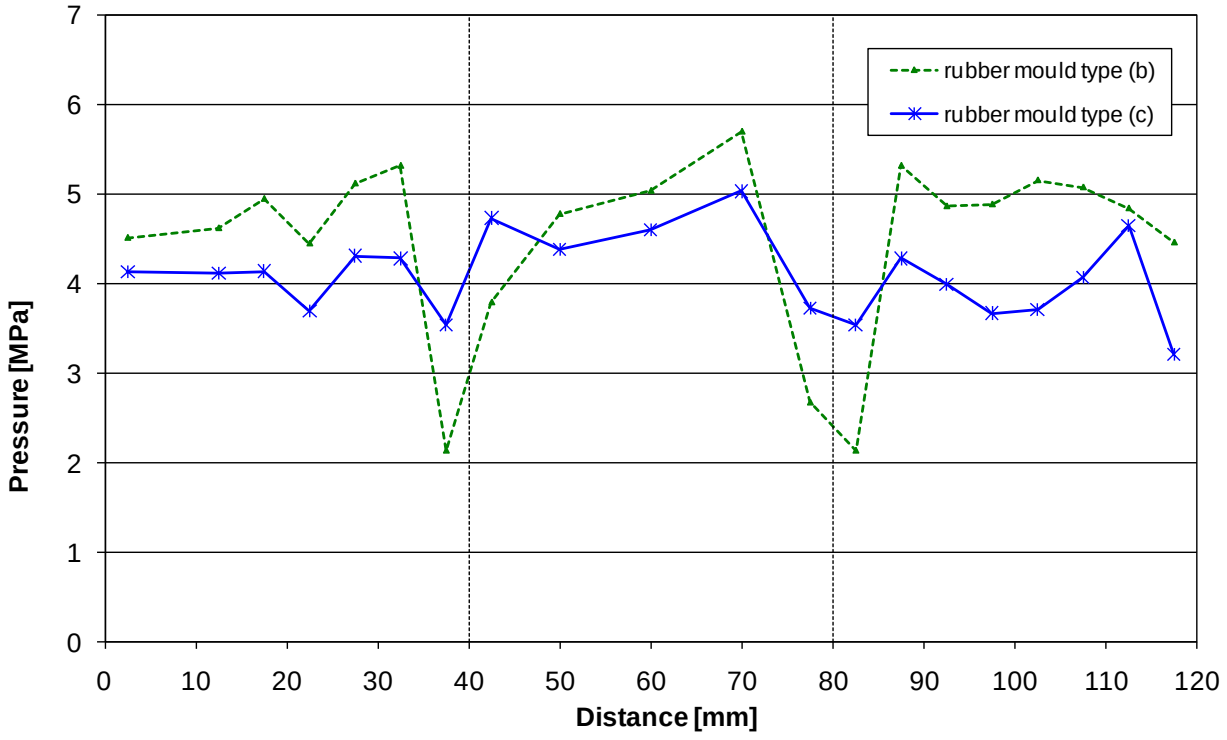

Figure 4.13 Pressure distribution at 75 °C with laminate.

From those results, it appears that the temperature has quite an important effect on the pressure distribution, even with a small increase of temperature. Though the best shape is the hourglass one, still more trials are needed in order to define the best radius of curvature at the sides to reach a constant pressure distribution.

Another important aspect is the fact that the temperature and the consequent expansion of the mould, is influencing the pressure distribution at the corners of the simple mould with clearance. It suggests that at higher temperatures the pressure distribution might be more constant, as the pressure drop at the corners is reduced at higher temperature. This consideration will be verified later in this chapter. This result means in general that, in a series production, the pressure distribution can vary depending on the temperatures of the moulds.

4.4 Methods to improve the pressure distribution

Two major attempts have been carried out to improve the pressure distribution on the mould surfaces: the reduction of the coefficient of thermal expansion of the mould and the reduction of the coefficient of friction between mould and thermoplastic sheet.

4.4.1 Silicone reinforced aramide mould

To be able to reduce the coefficient of thermal expansion, it is possible to add fillers to the silicon, in order to prevent the silicon to expand. Fillers, such as nano-clay, are commonly used in silicone to alter the mechanical properties of the silicone alone. The addition of fillers also increases the viscosity of the silicone during preparation and therefore only small amounts can be used.

It is expected that the use of fillers with a very low coefficient of thermal expansion might decrease the expansion of the rubber mould at high temperatures. The most suitable filler for this purpose are chopped aramid fibres, as aramid is a material with a negative coefficient of thermal expansion [6], in particular, Twaron pulp, as shown in Figure 4.14, is considered. It has the advantage of the aramid fibres at a low price; in particular, the strength, toughness and flexibility of Twaron protect the fibre from suffering any damage during the mixing process [7]. Twaron is also used for products that need a high wear resistance, which would be an additional advantage for the rubber moulds.

Figure 4.14 Aramid pulp [6].

The pulp that was used was Twaron 1095, which is a standard dry pulp of the 1st generation with a low degree of fibrillation and has an expansion coefficient of -3.5×10^{-4} K^{-1}. The production of a rubber mould with pulp has its own disadvantages. The volume content that is possible to include in the rubber compound is limited to a few percent, due to the increase of viscosity, as visible in Figure 4.15, in the rubber compound and the consequent difficulty of properly degassing the rubber before casting.

Figure 4.15 Rubber compound with 1% of Twaron pulp.

It was therefore chosen to add 1% of Twaron pulp, though an addition up to 5% was found possible. The measured coefficient of thermal expansion of the rubber with 1% Twaron pulp was 9.612 x 10^{-4} K^{-1}, about 60% of the CTE of the original rubber die. The addition of Twaron pulp also had an effect on the hardness of the rubber that slightly increased from 59 ShA up to 62 ShA. The surface of the mould resulted moreover rougher than a standard one, running the risk of a non-uniform pressure distribution due to the surface quality. The surface, though, could be machined to get the desired surface quality.

In order to verify the pressure distribution on a mould containing Twaron pulp, a mould of the type (b) of Figure 4.7 was manufactured. The tests were carried out at different temperatures with a laminate. The results are summarised in Figure 4.16 where the plots of the pressure distribution for two moulds of the same shape and rubber type, with (straight lines) and without (dashed lines) Twaron pulp, at increasing temperature values, are presented.

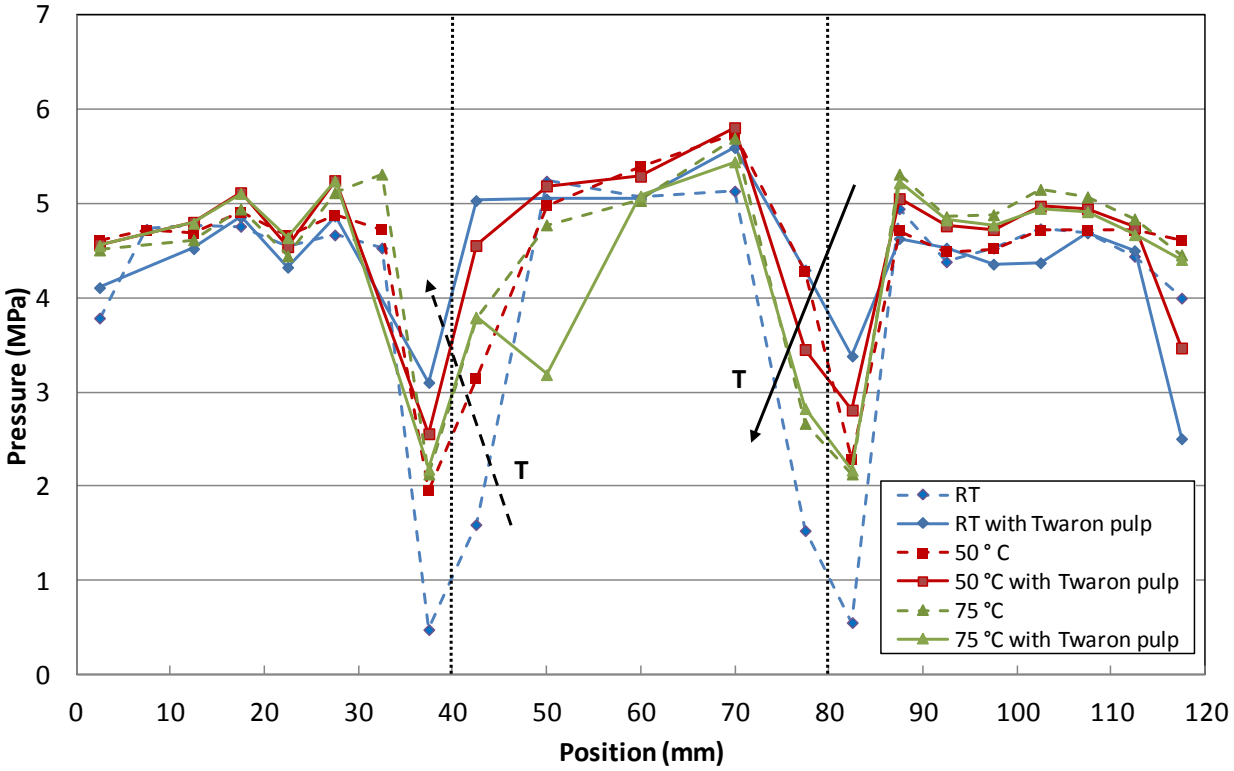

Figure 4.16 Effect of temperature on a normal die and a Twaron reinforced aramid die with a laminate.

In the case of a standard rubber mould, there is a drop in pressure at the corner of the mould, which decreases once the temperature increases due to the expansion of the rubber that tends to fit better in the mould, as shown in the previous section. In the case of the mould containing Twaron pulp, the pressure drop at the corners decreases with the increase of temperature. As the coefficient of thermal expansion is lower in the case of Twaron pulp, but still positive, this cannot be due only to the difference CTE, but it might be due to the difference in hardness and the increase in the coefficient of friction that does not allow the mould to fill in the corners.

In general, the effect of the Twaron pulp is positive as the difference in pressure drop is much less than in the case of pure rubber, therefore this effect could be verified with tests at higher

temperature and tuned with different Twaron content. From the tests presented above, it looks like that the amount of Twaron is too much as it works better at room temperature than at higher temperatures. Different percentages of Twaron should be added in order to verify this statement.

4.4.2 Effect of lubrication

Another option that could help the reduction of the coefficient of friction is the use of lubricants. In the preliminary design phase of a product, when the mould is not yet optimised, lubricants are often used to facilitate the production of the first prototypes. In Figure 4.17 the effect of lubrication is shown on a standard mould, type (b) of Figure 4.7, of Silastic J and one with the addition of 1% volume of Twaron pulp at 75 °C. The results of the different mould materials are very similar. On the other hand, the lubricant reduces the friction and allows a more uniform pressure distribution with a reduction of pressure loss at the corners of more than 30%.

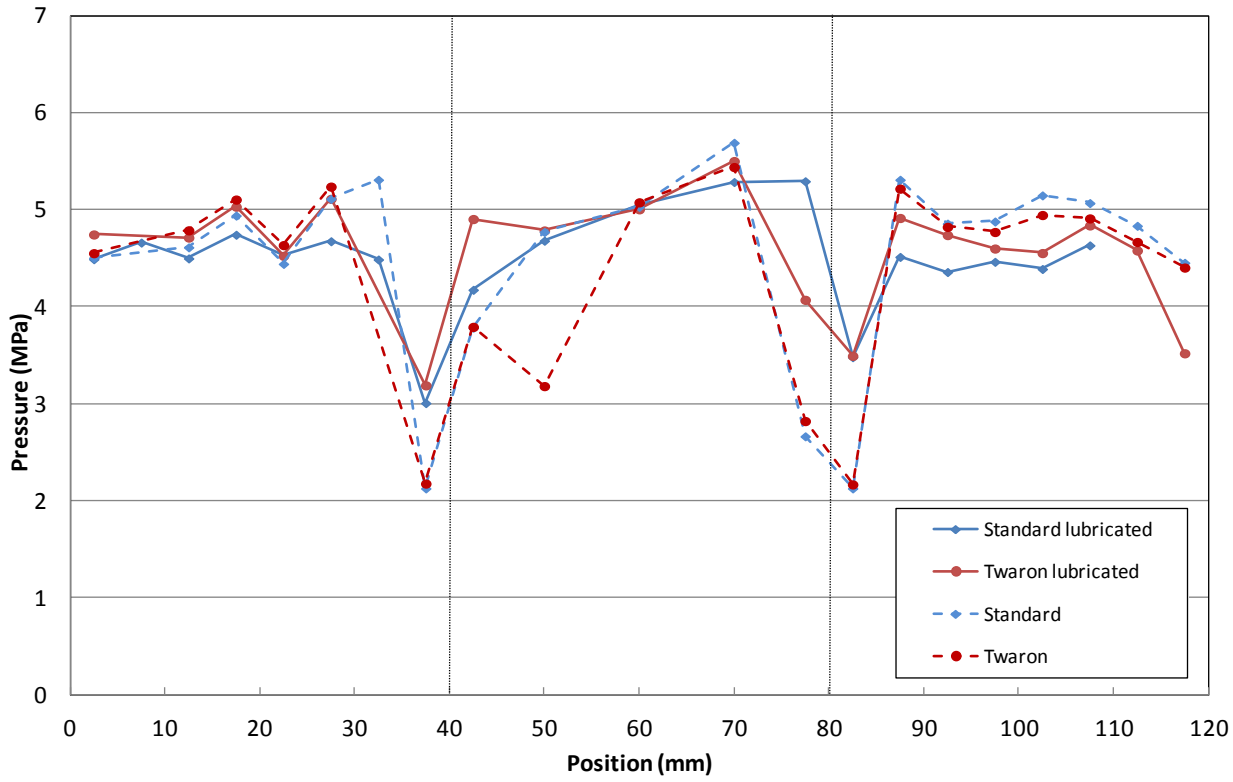

Figure 4.17 Effect lubrication on a normal die and a Twaron reinforced aramid die with a laminate at 75 °C.

At present the use of lubricants is generally allowed only in the prototyping phase, due to the fact that the lubricant might reduce the mechanical properties of the thermoplastic product; therefore its influence on the mechanical properties of the thermoplastic should be tested.

4.5 Conclusions

Using silicon rubber to press thermoplastic composites assures a more uniform pressure distribution compared to metals as it assures an almost uniform pressure distribution on all sides of the products at low pressing forces.

Nevertheless, the pressure is not uniformingly distributed when using a rubber mould, which is made as an exact negative of the metal mould; therefore, trials are needed to obtain a more uniform pressure distribution. In order to assure the same pressure distribution during the entire process, the expansion of rubber during series production has to be taken into account. In this case it is necessary to keep in mind that the mould is designed to be functional at higher temperatures and not at room temperature.

Both presented methods to improve the pressure distribution on the mould during rubber pressing have shown that some improvements are possible. The inclusion of Twaron pulp in the rubber has shown that the pressure distribution is changing less at different temperatures, though an optimisation of the amount of Twaron to be applied and its influence in different types of silicon should be investigated in more detail. In addition, the use of lubricants shows that some improvements are possible to reduce the very high coefficient of friction. The use of a proper lubricant that is not influencing the mechanical properties of the thermoplastic laminate should be investigated. The use of the lubricant though, does not eliminate the problem of the thermal expansion of the mould; therefore, attention should be paid in the design of a proper mould that is optimised for functionality at the process temperature.

4.6 Bibliography

[1]. L.M.J. Robroek, “The development of Rubber Forming as a Rapid Thermoforming Technique for Continuous Fibre Reinforced Thermoplastic Composites”, PhD Thesis, 1994 Delft University Press
[2]. de Bie R., Tooling Design for Rubber Forming of thermoplastic Composites, Master Thesis, Delft University of technology 2004
[3]. de Bruijn G., Pressure Distribution During Rubber Forming of TPC’s, Delft University of Technology 2003
[4]. Buis E., Mould Pressure Distribution Analysis in the Press Forming of Thermoplastic Composites”, Delft University of Technology 2005
[5]. Huang C.Y., “A Fundamental Investigation of the Friction Effect Upon Rubber Forming of Thermoplastic Composites”, Delft University of Technology 2005
[6]. http://www.teijinaramid.com/, accessed 18 November, 2011
[7]. Twaron – Pulp and chopped fibres datasheet.

Chapter 5
Solid rubber model

Physical tuning of an initial mould, which is often called a “trial and error aproach”, or computer simulations allow designing the final rubber mould. Computer simulations hold the promise to reduce the initial development costs and improve the final solution. Therefore, it is important to be able to simulate the rubber forming process.

Once the material properties of the rubber are defined, a further step is to define a rubber model, which is able to predict the behaviour of the rubber during pressure forming, and be able to quantify in a correct way the pressure applied to the metal mould and consequently the thermoplastic sheet.

5.1 Review of existing rubber models

Most of the available hyperelastic material models are phenomenologically based; they have been mathematically justified and correlated with the experimental data to determine the material parameters as in [1] and [4].

In order to characterise the mechanical behaviour of hyperelastic materials it is common practice to represent the constitutive equation through a strain energy density function. An elastic material for which a strain energy density exists is known as a hyperelastic material. The strain energy density function must be expressed such that it can describe the high deformability, recoverability after deformation, and highly non-linear load-deformation behaviour for this class of materials.

Assuming the complete recoverability after deformation, the strain energy density depends only on the final state of strain and not at all on the loading history. The final state of strain is characterised by the principal strains or equivalently by the strain invariants.

5.1.1 Rivlin model

Various material models have been introduced to describe hyperelasticity. Rivlin [2], [3] developed a mathematical theory which describes the deformation, under the action of applied forces, of bodies of ideal highly elastic materials which are incompressible and isotropic in their undeformed state. The relevant physical properties of the material are specified in terms of a stored energy function W that must be a function of two strain invariants I_1 and I_2. These invariants are expressed in terms of the principal extension ratios λ_1, λ_2 and λ_3 at the point of the deformed body considered, by the formulae:

$$I_1 = \lambda_1^2 + \lambda_2^2 + \lambda_3^2 \qquad and \qquad I_2 = \frac{1}{\lambda_1^2} + \frac{1}{\lambda_2^2} + \frac{1}{\lambda_3^2}$$

In which, since the material of the body is assumed incompressible, $\lambda_1\lambda_2\lambda_3 = 1$.

When the material is undeformed $\lambda_1 = \lambda_2 = \lambda_3 = 1$, so that $I_1 = I_2 = 3$. It is therefore convenient to consider the stored-energy function to have the form of a doubly infinite series in (I_1-3) and (I_2-3) thus:

$$W = \sum_{i=0,j=0}^{\infty} C_{ij}\,(I_1 - 3)^i (I_2 - 3)^j, \qquad C_{00} = 0$$

5.1.2 Mooney-Rivlin model

In the case, the deformations are sufficiently small, (I_1-3) and (I_2-3) are in general small quantities of the same order, so, for any form of W:

$$W = C_{10}(I_1 - 3) + C_{01}(I_2 - 3)$$

represents a good approximation in case of sufficiently small deformations.

Mooney [5] demonstrated that this form is the most general form that can be valid even for large deformations for an ideally incompressible, highly elastic material, isotropic in its undeformed state. All this, provided the relationship between the shearing force and the amount of simple shear is linear when the material is subjected to a simple shear superposed on a constant simple extension and therefore this form on the stored-energy function is known as the Mooney form.

5.2 ABAQUS material model

For the Finite Element Analysis, the computer program ABAQUS has been used. The choice was based on the intrinsic non-linear characteristics of the program, together with the possibility of defining a material with hyperelastic behaviour through tests results.

When defining a hyperelastic material in ABAQUS it is possible to choose a material model, already defined in the code, which represents the tested values. The values of the tested material are inputted in the code as a table and compared with the several material models already present in ABAQUS.

The hyperelastic material model that defines more accurately the stress strain curves obtained by material tests is a strain energy potential polynomial of second degree [3]:

$$W = \sum_{i+j=1}^{N} C_{ij}\,(I_1 - 3)^i (I_2 - 3)^j + \sum_{i=1}^{N} \frac{1}{D_i}(J_{el} - 1)^{2i}$$

Although the parameter N can take up to 6, values N greater than 2 are rarely used when both first and second invariants are taken into account. The elastic volume strain J_{el} follows from the total volume strain J and the thermal volume strain J_{th} with the relation:

$$J_{el} = \frac{J}{J_{th}}$$

and J_{th} follows from the linear thermal expansion ε_{th} with

$$J_{th} = (1 + \varepsilon_{th})^3$$

where ε_{th} follows from the temperature and the isotropic thermal expansion coefficient defined by the user.

The D_i values determine the compressibility of the material: if D_i are all zero, the material is taken as fully incompressible. If D_1=0, all D_i must be zero.

Regardless of the value of N, the initial shear modulus, μ_0 and the bulk modulus k_0 depend only on the polynomial coefficients of order N=1:

$$\mu_0 = 2(C_{10} + C_{01}), \qquad k_0 = \frac{2}{D_1}$$

The rubber model used is applied to the Silastic J rubber, to be able to compare the experimental results with the numerical ones. The comparison between the test data at room temperature and the polynomial function are shown in Figure 5.1. They accurately represent the material behaviour, particularly in compression.

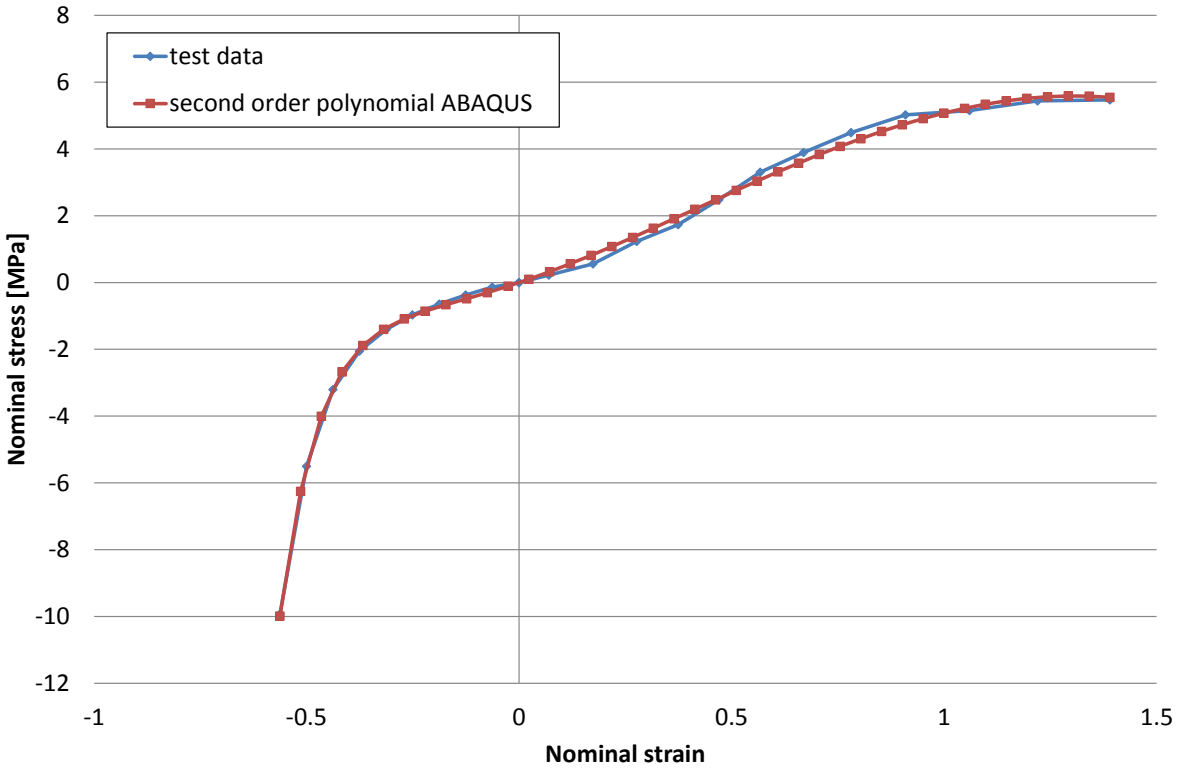

Figure 5.1 Comparison between test data and the polynomial form of the strain energy potential of second order as calculated and used in ABAQUS.

The coefficients used for the strain energy potential are reported in Table 5.1.

C_{01}	C_{02}	C_{10}	C_{20}	C_{11}	D_1	D_2
-1.2499	-2.2289	1.9648	-0.4284	0.9376	0.1447	0

Table 5.1 Coefficient of the polynomial form of the strain energy potential for Silastic J.

5.3 Verification of the material model

The tests carried out to determine the pressure distribution on the mould for the production of a U beam, as described in Chapter 4, have been modelled in ABAQUS to judge how accurate the material model is and to be able to tune the different parameters that are not included in the material's stress-strain curve (like Poisson's ratio and coefficient of friction between steel and rubber).

5.3.1 2D solid model

The FE-model is shown in Figure 5.2. A steel female mould has been modelled, together with the male rubber mould. A gap of 1 mm along the side walls is considered in accordance with the experiments. The initial calculations have been carried out on a 2D model with solid elements, in order to save computational time. This assumption is expected to give sufficiently

accurate results, as the length of the beam is much higher than the cross section and the test results are obtained from the mid-section of the beam.

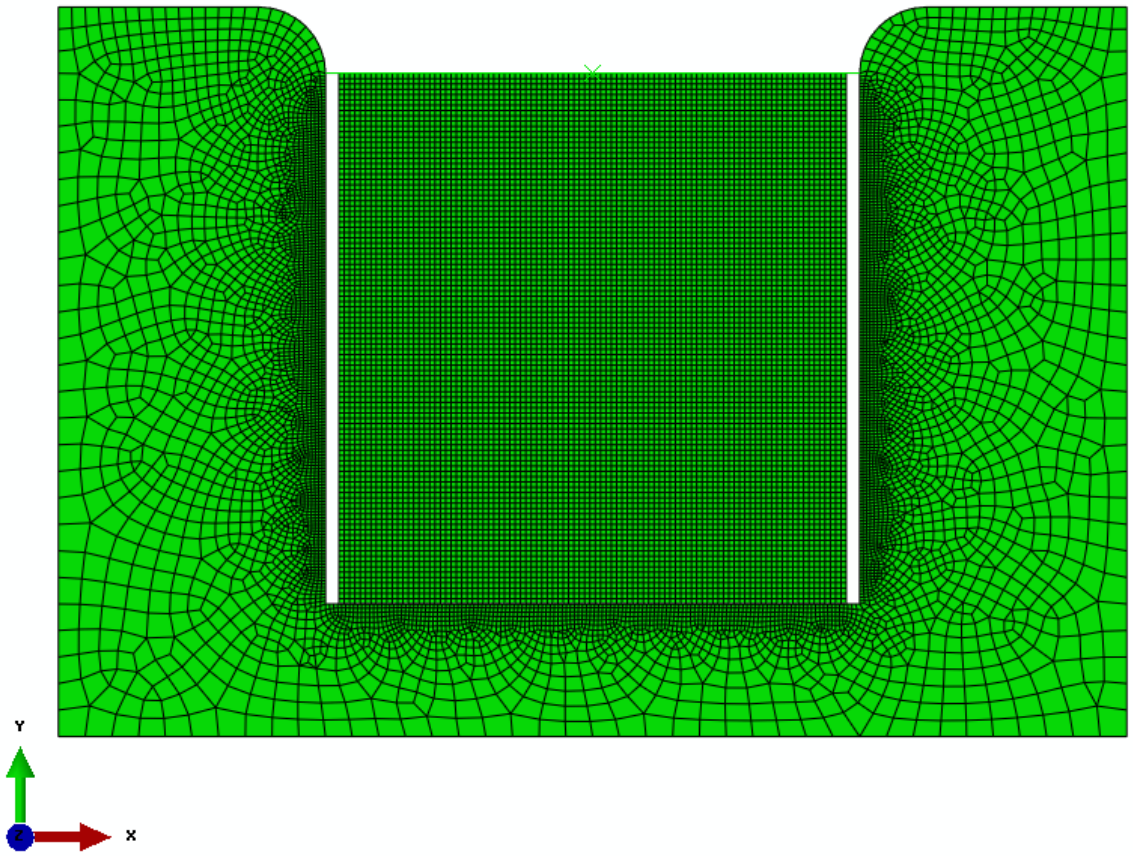

Figure 5.2 2D-Finite Element model.

The rubber mould is pushed into the metal mould via a geometrical line representing the press to which either a displacement or a force is applied. In this case, a geometric element with infinite stiffness is used as the press exerting the force can be considered infinitely stiff and the pressure on the top surface of the mould is equally distributed.

The press and the rubber are tied together, whereas between the metal mould and the rubber mould a contact is applied. The contact has a normal part and a tangential part, representing the friction. In Chapter 3, the coefficient of friction between rubber and steel had been found to lie between 0.9 at room temperature and 0.6 at 200 °C.

Another parameter of interest is the Poisson's ratio. As rubber is an almost incompressible material, a Poisson's ratio of almost 0.5 is expected. The exact value, though, has not been measured with experiments and its influence will be verified through the FE calculations.

In order to verify the effect of both Poisson's ratio and coefficient of friction and to define their best fitting values, the following procedure has been adopted. Both values are tuned so that the load-displacement diagram of the test results and the FEM analysis are similar. When the

correct values of friction and Poisson's ratio are found, the stress distribution on the sides of the mould is verified.

The comparison of the load-displacement diagrams between the various FEM models and the experimental results is shown in Figure 5.3.

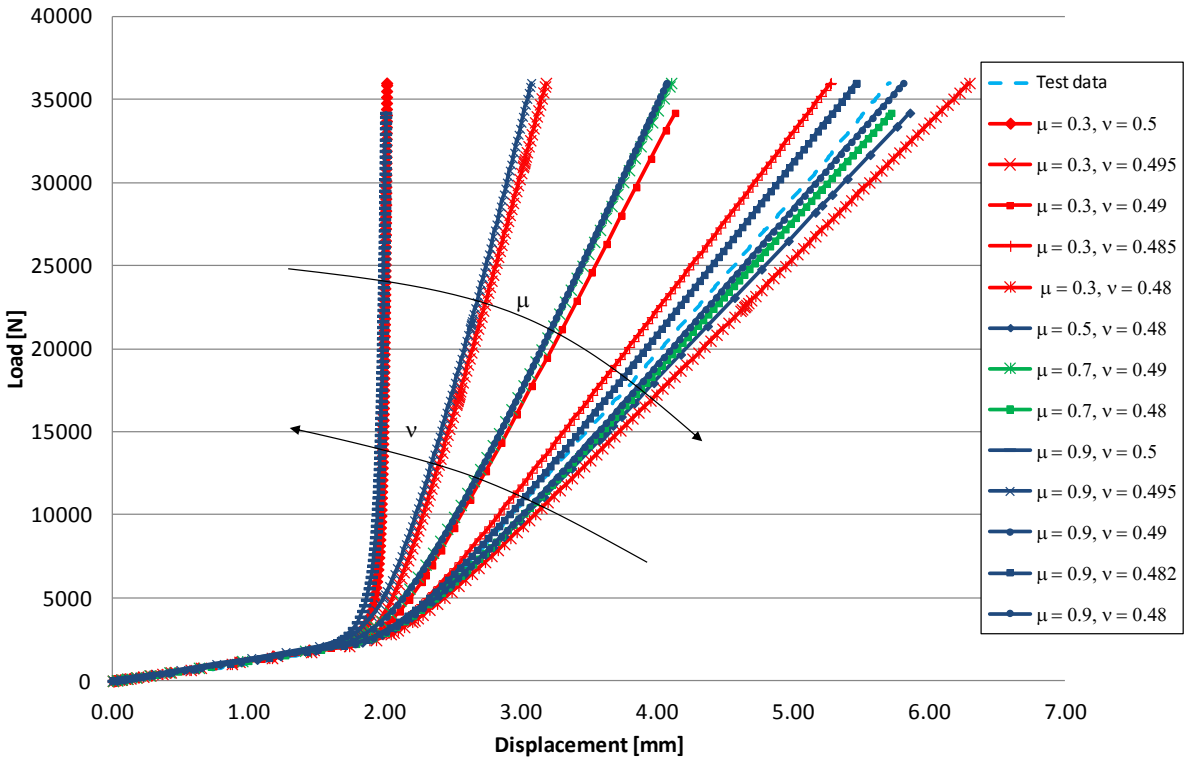

Figure 5.3 Comparisons between the load displacement plots of various FEM models and experimental results.

All the diagrams depict quite well the bilinear behaviour of the load displacement diagram. The vertical displacement of the rubber mould is higher when the friction is lower so that the bottom and the top of the mould show more relative displacement. The vertical displacement decreases when the rubber mould can contract much less due to its incompressibility.

Figure 5.2 shows also that up to the moment the mould is filled, the coefficient of friction is not influencing the load displacement diagram, showing that there is very little sliding of the bottom and top side of the mould along the sides. This is shown more in detail in Figure 5.4. Moreover, the influence of the coefficient of friction (μ) is less important than the Poisson's ratio (ν). In the case of an almost incompressible rubber, there is no difference between a low and high coefficient of friction.

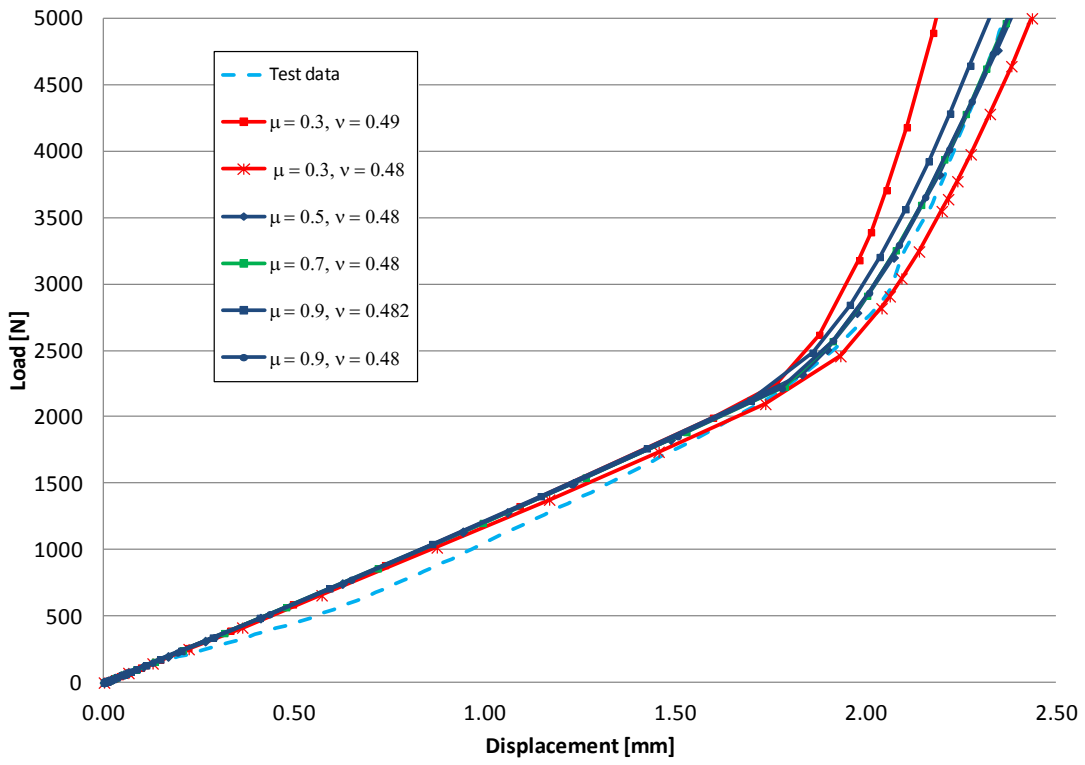

Figure 5.4 Detail of Figure 5.3.

From the load displacement diagram it appears that many combinations of friction and Poisson's ratio are possible to fit the test results. When the friction is quite high as measured in the experiments, though, there is no appropriate value of the coefficient of friction, which could match the load-displacement diagram completely.

When the pressure distribution is taken into account, however, it is observed that high values of Poisson's ratio give a better result, compared to the tests, as shown in Figure 5.5 and Figure 5.6, whereas the coefficient of friction plays a marginal role.

When comparing pressure distribution, the best results appear to be with a Poisson's ratio of 0.498 and a coefficient of friction of 0.9, but looking at the load displacement diagram using the same coefficients, this is far from resembling the test results as in the second part of the load-displacement curve, the rubber seems to be more rigid.

A possible reason for that might be that in a 2D solid model, the rubber is seen as infinite in the length direction, while in reality not only the rubber mould has a finite length, but also there is a gap between the rubber and the steel mould allowing for a further displacement of the rubber mould before it touches the steel one. In order to verify this assumption, a 3D solid model has been created.

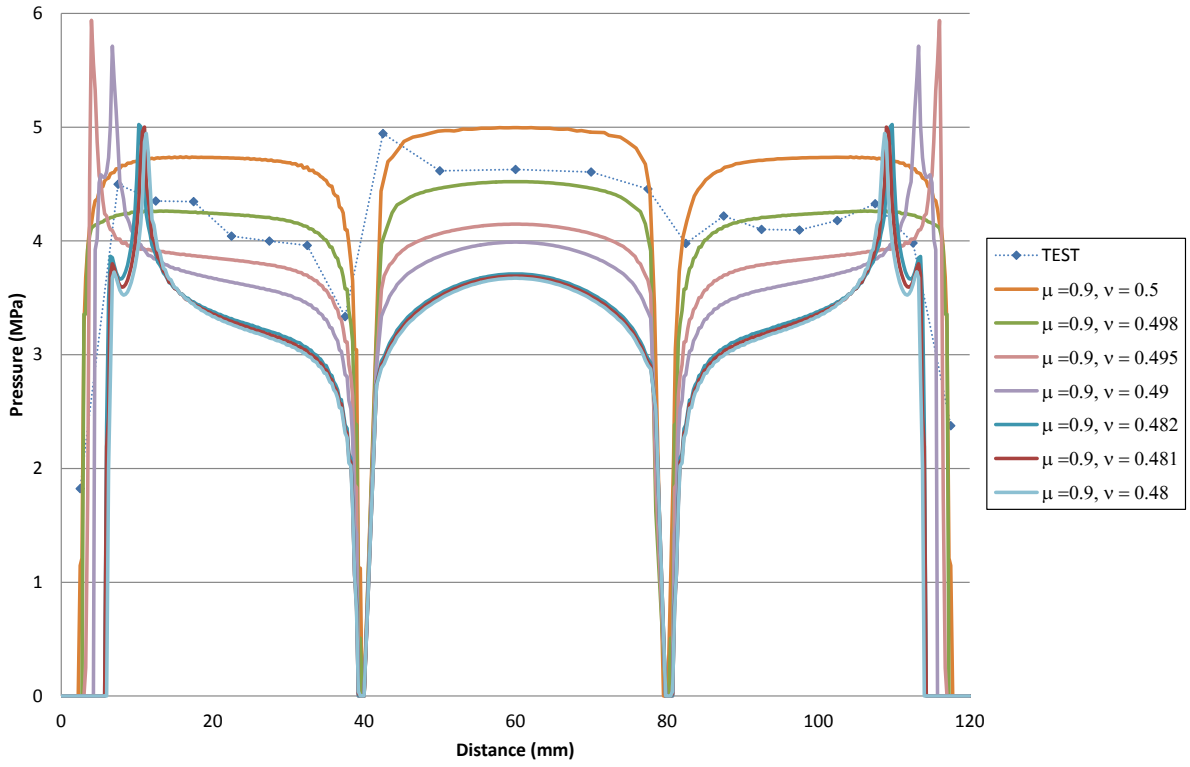

Figure 5.5 Pressure distribution for a coefficient of friction of 0.9 and several Poisson's ratio's.

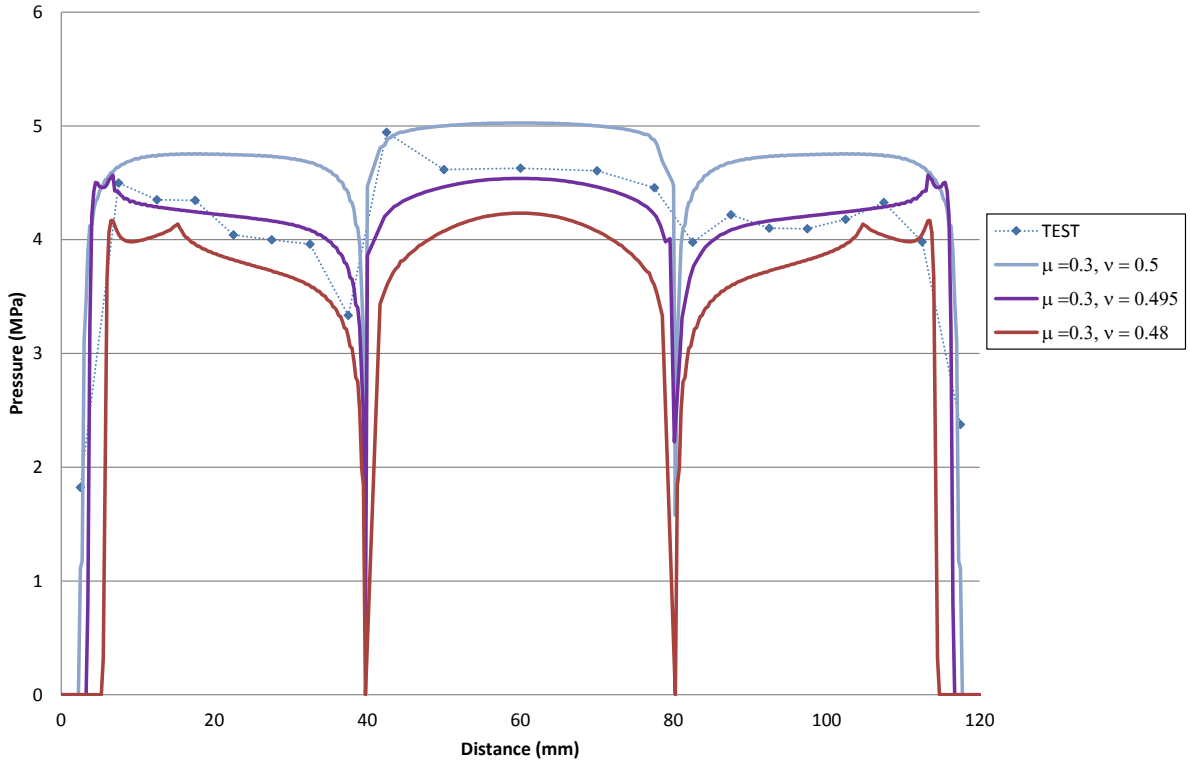

Figure 5.6 Pressure distribution for a coefficient of friction of 0.3 and several Poisson's ratio's.

5.3.2 3D solid Model

In order to reduce computational time, which, due to the complexity of the analysis, is quite large, one quarter of the model has been modelled making use of the double symmetry of the problem, as shown in Figure 5.7. The 3D model is built of solid elements. In the case of the rubber, only 8 nodes solid elements are used, while for the steel mould, due to its shape, tetrahedrons are used.

The material model used for the definition of the rubber, is the same that has been used in the 2D solid model. The material used to define the rubber with an hyperelastic material is in this case a C3D8RH, an 8-node linear brick, hybrid, constant pressure, reduced integration, hourglass control, whose definition can be found in [9], while for the steel mould, C3D4, a 4-node linear tetrahedron was used.

To simulate the pressure applied by the press, a concentrated force on one node was used, with the constraint that every node of the top surface of the rubber mould has the same vertical displacement of the node where the load is applied.

Appropriate symmetry boundary conditions are applied.

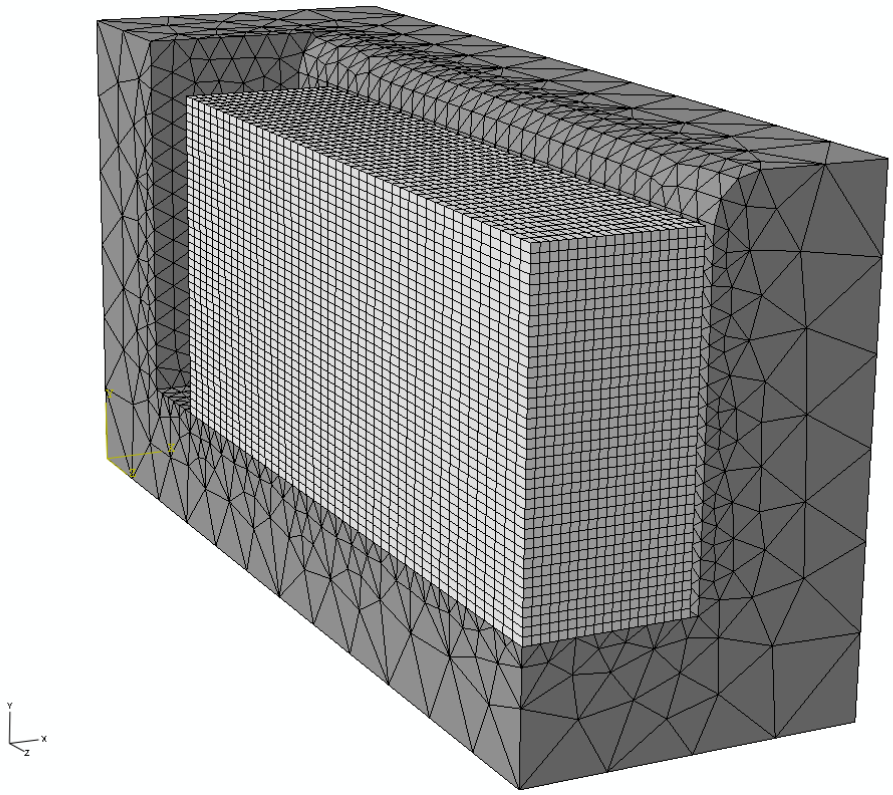

Figure 5.7 3D Finite Element Model.

The displacement of the rubber mould is shown in Figure 5.8 where the displacement of the rubber in the back of the mould is visible. The rubber is not in contact with the mould in that position. In the previously discussed two dimensional case, no displacement can occurr in the length of the mould. The difference between the 3D and the 2D case is thus that in 3D the rubber mould deforms in the direction perpendicular to its cross-section and therefore the rubber behaves less stiff than in the 2D case.

On the back of the mould, the effect of the high coefficient of friction on the edge of the rubber mould close to the steel mould is also visible: here the outer corner of the rubber mould is held against the side wall of the steel mould preventing it to follow the top side of the mould.

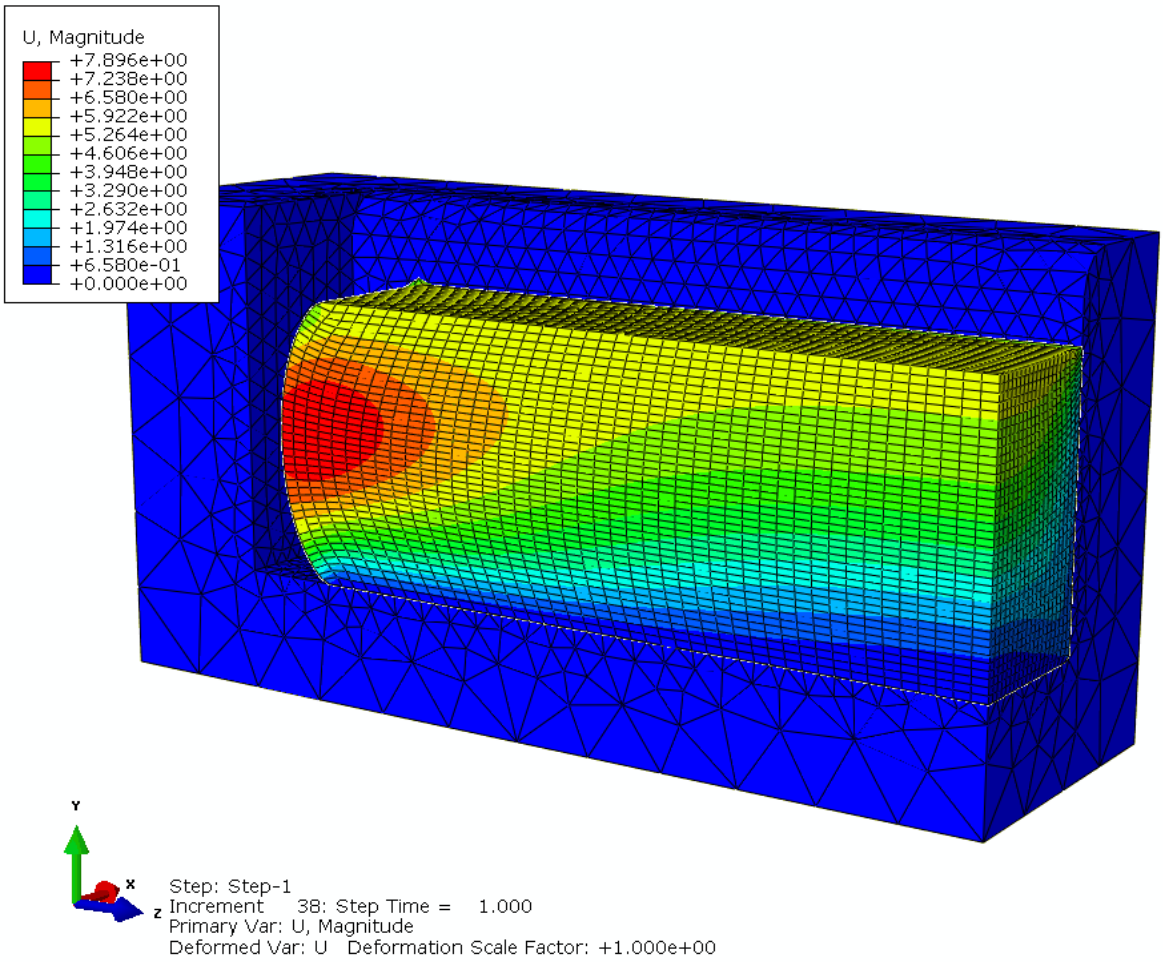

Figure 5.8 Deformation of the rubber block at the maximum pressure.

Figure 5.9 and Figure 5.10 show respectively the pressure distribution and the load vs. displacement plot for the case of a Poisson's ratio of 0.49 and a coefficient of friction of 0.9. In this case, the 3D model represents the test results better. In the pressure distribution plot of Figure 5.9 though, the pressure in the lower corner of the mould appears to be nearly 0.

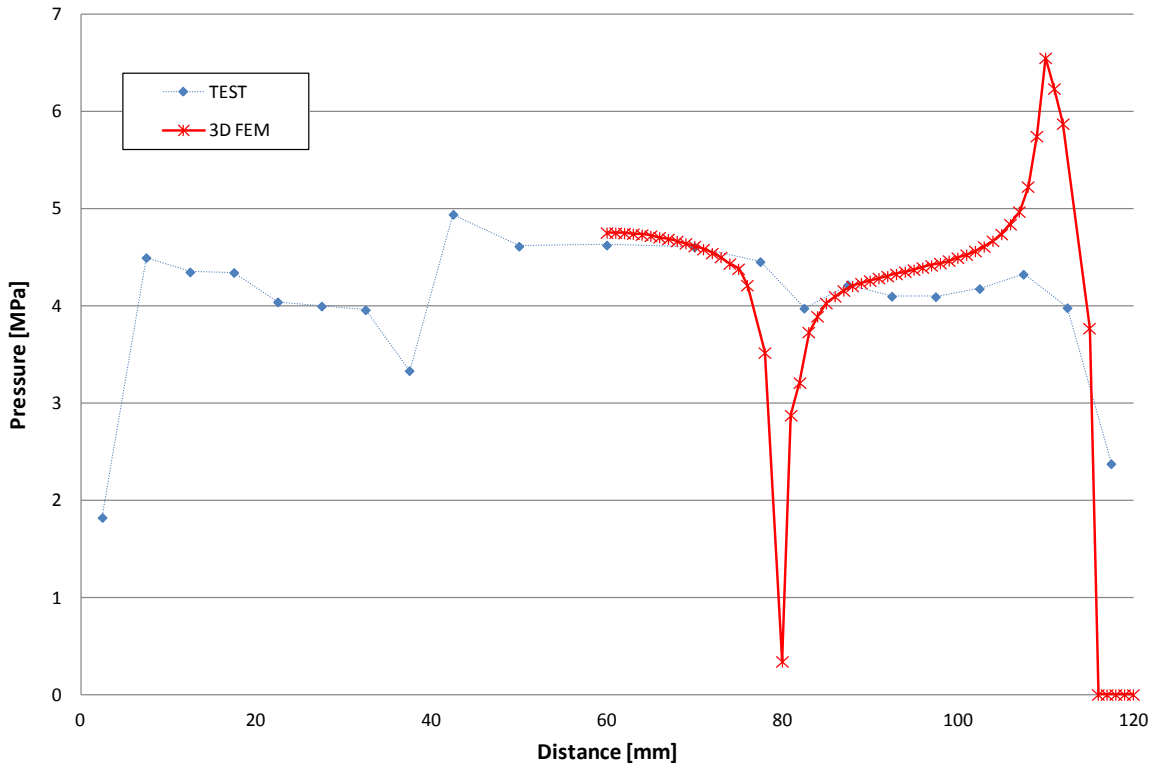

Figure 5.9 Pressure distribution in case in the 3D analysis.

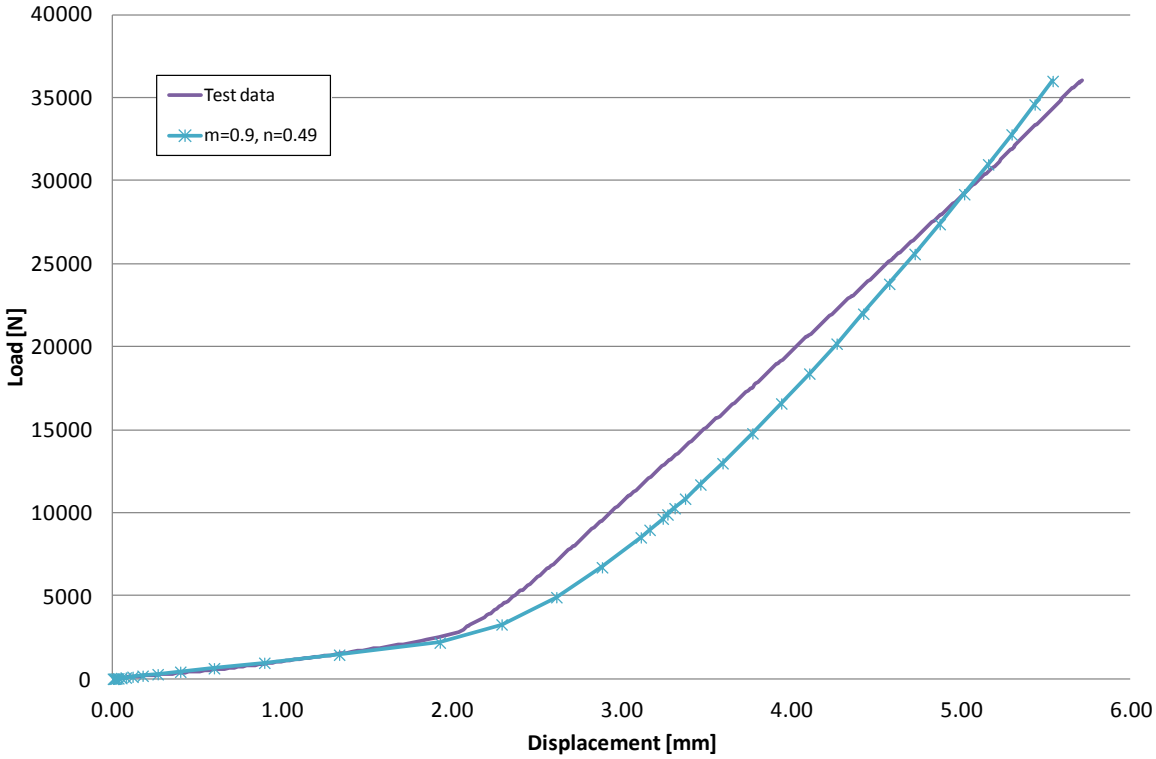

Figure 5.10 Load displacement diagram in the 3D analysis.

As the pressure is extrapolated to the nodes of each element, the contact pressure of the two elements perpendicular to each other does not seem to be calculated correctly. On the other hand, as the elements in the rubber mould have a width of 1 mm, the pressure calculated 2 mm away from the bottom corner already correspond to the measured one and is considered sufficient to press the corners in the correct way.

5.4 Case study: Eaglet rudder

Once the material model has been validated, it is possible to apply the material model to a real problem.

One of the projects at the Faculty of Aerospace Engineering at Delft University of Technology was the design and production of a full thermoplastic rudder for the Enaer Eaglet 2-seater recreational aircraft. Figure 5.11 shows the aircraft and the rudder structure.

Figure 5.11 The two seater "eaglet" (left) and an exploded view of its rudder with its components (right).

The thermoplastic composite rudder was chosen for its dimensions, namely 1.5 m length and about 0.1 m flat width, which allowed the "in house manufacturing" of all components on the available press. The main purpose of the project was to test various thermoplastic manufacturing techniques plus the joining of all components without the use of mechanical fasteners through for example resistance- and ultrasonic welding. Other techniques, such as the addition of an integrated ice-protection, were tested as well on the rudder.

All the components of the rudder are made of carbon fibre reinforced thermoplastic plates and in particular, the five ribs are produced by rubber pressure forming.

In this case, four different moulds were necessary, as shown in Figure 5.12. For two of the ribs the same mould could be used. In this application, it was decided to use a very large rubber mould, contained in a steel casing, and a metal die.

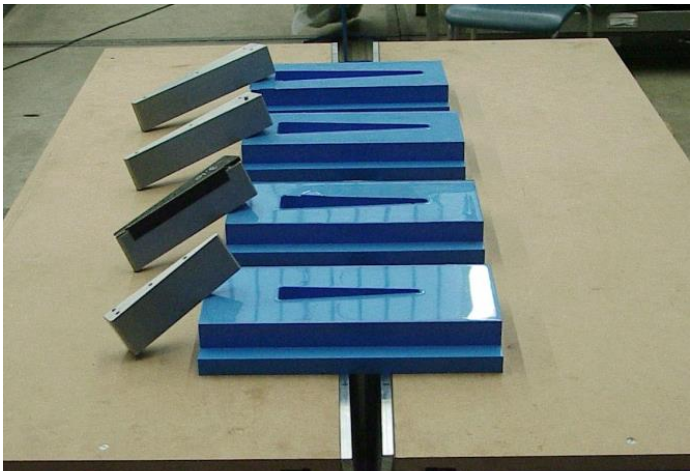

Figure 5.12 The four rubber moulds and steel dies used to produce the rudder's ribs.

The production set up is shown in Figure 5.13. The female silicon mould is contained in a steel casing attached to the press. The steel male mould lies on the bottom of the press. In this case, a thermoplastic preform was used, so that the corners of the flange' rib did not have to be formed and cut afterwards. The manufacturing of the ribs was therefore quite simple and the rubber mould was created using the steel mould as negative shape.

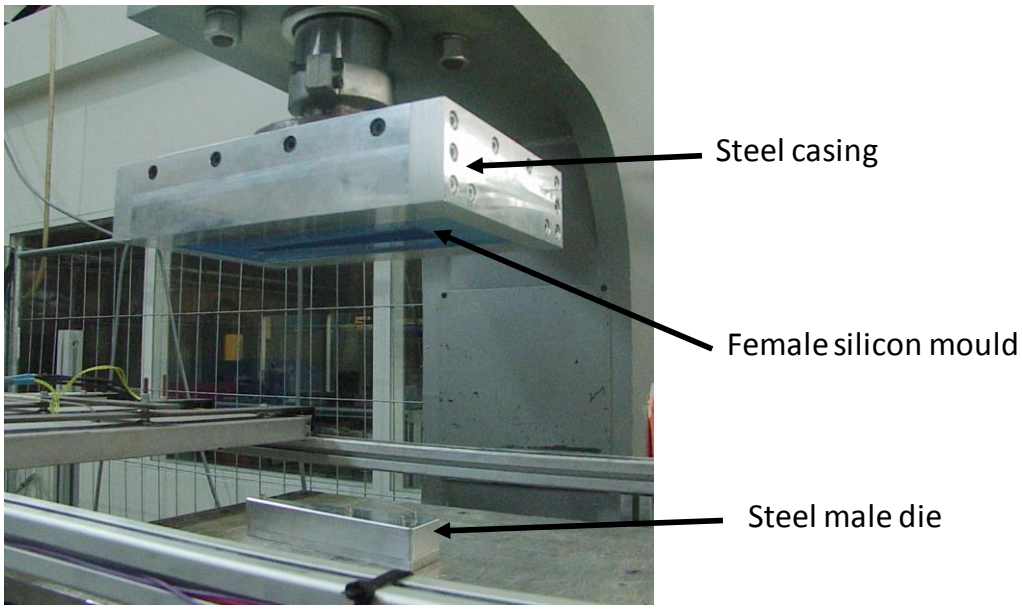

Figure 5.13 Set up for the production of one of the ribs.

Although the manufacturing of the ribs was a success, the rubber mould wore off after only ten cycles, as shown in Figure 5.14. The steel mould cuts the rubber along the whole perimeter.

Figure 5.14 State of the mould after 10 cycles.

In order to verify whether it is possible to model the same phenomenon through a Finite Element Analysis, a model of the test set up was created as shown in Figure 5.15. Steel and rubber moulds were modelled as well as a geometrical line to describe the uniformly distributed load on top of the steel mould.

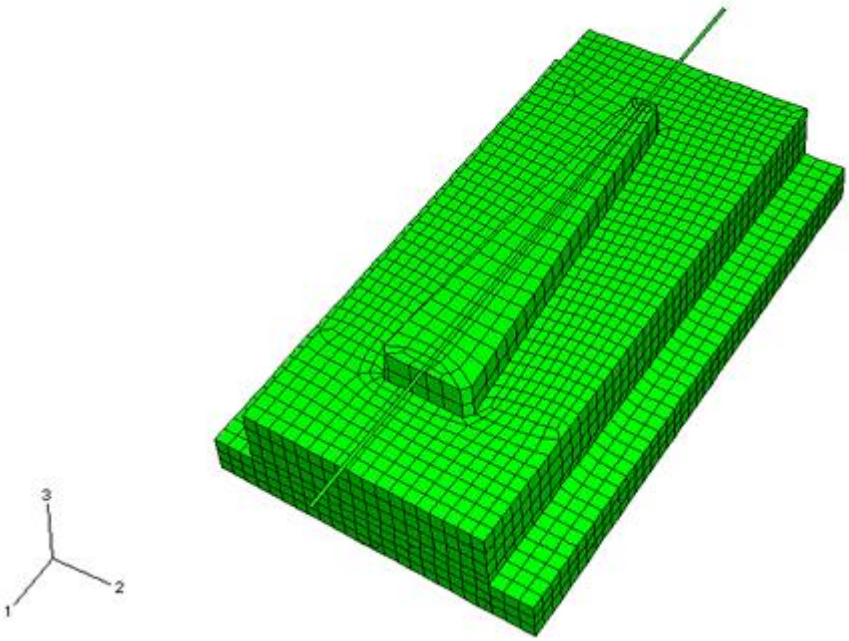

Figure 5.15 Model of the production of the CFRP rib.

In the FE-model, the steel mould is pushed inside the rubber mould. The material properties of the rubber are the same as those used in the simulation of the U-beam. In addition, in this case, no laminate has been modelled. Reason for that is that the laminate is forming easily and its forming does not influence the wear of the rubber mould.

The resulting stress distribution is shown in Figure 5.16. The figure shows the maximal stresses in the same position where the mould was cracked. Apparently, the edges of the hard mould press on the rubber causing a brittle failure.

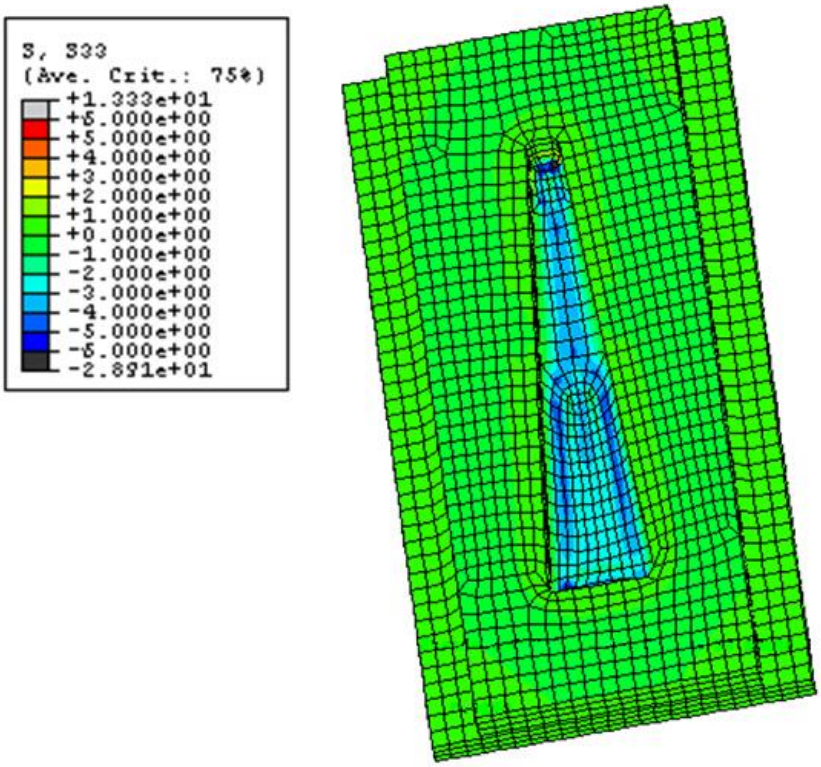

Figure 5.16 Stress distribution on the rubber mould.

5.5 Concluding remarks

The rubber model used to simulate the rubber pressure method works properly if parameters such as material characteristics, temperature, friction involved in the process are considered with sufficient accuracy.

In a preliminary design phase, it may be useful to use the rubber model in order to verify the homogeneity of the pressure distribution along the mould. When the pressure distribution is very inhomogeneous, it should be expected that problems occur at locations with low pressure in the form of dry spots or bad consolidation of the laminate and that contours differ (in particular in corners' areas) from expectations.

When the entire product needs to be analysed, the laminate should also be modelled.

Including the laminate in a model in female mould is flexible does not influence the pressure distribution on the mould, but increases the computational time. In case the male mould is flexible, the inclusion of a laminate, especially when a blanckholder is holding the laminate with a certain force, the pressure distribution on the hard female mould could be worse than in the case without laminate, depending on the force holding the blankholder. The purpose of the analysis, therefore, should be identified on forehand. The case without the laminate is a sort of "best case scenario" where the only parameters considered are the shapes of the two moulds. Once the rubber mould shape is optimised, the laminate might be included to verify the results and tune the force on the blankholder to obtain similar results.

5.6 Bibliography

[1]. H. Darijani, R Naghdabady and M H Kargarnovin. Hyperelastic materials modelling using a strain measure consistent with the strain enery postulates. *Journal of Mechanical Engineering Science*, Vol 223, Part C

[2]. R.S. Rivlin Large Elastic Deformations of Isotropic Materials. I. Fundamental Concepts. *Phil. Trans. R. Soc. Lond. A* 1948 **240**, 459-490.

[3]. R.S. Rivlin and D W Saunders Large Elastic Deformations of Isotropic Materials. VII. Experiments on the Deformation of Rubber. *Phil. Trans. R. Soc. Lond. A* 1951 **243**, 251-288.

[4]. S Kolling PA Du Bois DJ Benson WW Feng, A tabulated formulation of Hyperelasticity with rate effects and damage, *Comput Mech* (2007) 40:885-899

[5]. M Mooney, A Theory of Large Elastic Deformation, *Journal of Applied Physics* 1940

[6]. H.E.N. Bersee, B. Weteringe, M. Van Dongen, A. Beukers. Manufacturing of a Thermoplastic Composite Rudder. *SAMPE 2006 - Long Beach, CA April 30 - May 4, 2006*

[7]. T J Ahmed, Hybrid Composite Structures: Multifunctionality through Metal Fibres. An Exploratory Investigation, *PhD Thesis 2009, Ipskamp Drukkers B.V.*

[8]. V. Antonelli, R. Marissen, "FE-Modelling of the rubber mould behaviour during press forming of thermoplastic composites", 13th ESAFORM 2010 conference on material forming 2010, Brescia, Italy

[9]. ABAQUS user manual

Chapter 6
Rubber press forming with rubber particles as mould half

In Chapter 4 the basic problems associated with the rubber mould during press forming of thermoplastic composites are presented. The behaviour of the rubber during production can be simulated via Finite Element Analysis, as shown in Chapter 5, which allows the identification of the problematic areas.

Though the process can be well simulated via FEA and the stresses occurring in the rubber reflect the actual stresses during production, the simulations do not allow solving the problem sufficiently fast. The time spent in optimizing the production process and the consequent verification of the simulations would still require a long development time, decreasing though the costs for the production of a suitable rubber mould, as fewer trials during production will be necessary. Moreover, a numerical analysis of the problems hardly increases the technical options. In some cases, the problems are just too large and a numerical analysis would make these visible, but not always enable a solution.

The use of a soft material as mould half has still the advantage of allowing a quasi-hydrostatic pressure around the mould avoiding all the problems related to the use of a hard mould, mostly because a soft mould allows some deviations on the material thickness, which are inevitable when the product is doubly curved. However, some drawbacks like the effects of temperature on the dimensions of the rubber mould are intrinsic of the material used.

A new pressing technique, which uses rubber particles as mould half was first investigated in [1] and further developed in [2] and [3]. This process, unlike most of the press processes, replaces one of the two solid moulds with a collection of rubber particles creating a quasi-hydrostatic pressure distribution. The collection of rubber particles is used to press the

thermoplastic sheet in the metal mould in order to create the homogeneous pressure distribution needed during the reconsolidation phase. This technique provides a "rubber mould" without intrinsic shape or size. Thus, shape and size related problems like thermal expansion are not present. The technique is presented below.

6.1 Working principle

Figure 6.1 describes the whole production sequence as it is envisioned. The product mould is attached upside down on a stiff framework, directly beneath it a container filled with rubber particles is present (a). The reason for this set-up is that the rubber particles stay in the container under the influence of gravity. In (b), the heated thermoplastic composite material is brought between the product mould and the container. Directly after that, the container is pushed upwards until it creates an enclosed volume with the product mould (c). At this point the real pressurisation can start. When the piston moves up, it presses the particles towards the product mould. The particles press on their turn the sheet material towards the product mould (d). Because the particles can move freely and deform elastically, they will form a perfectly fitting rubber stamp as shown in (e). Once the thermoplastic is cooled down sufficiently, the piston and the container move downward as shown in (f). The rubber particles will fall back in the container under the influence of the gravity. At this point, the formed thermoplastic composite product can be removed and a new press cycle can start.

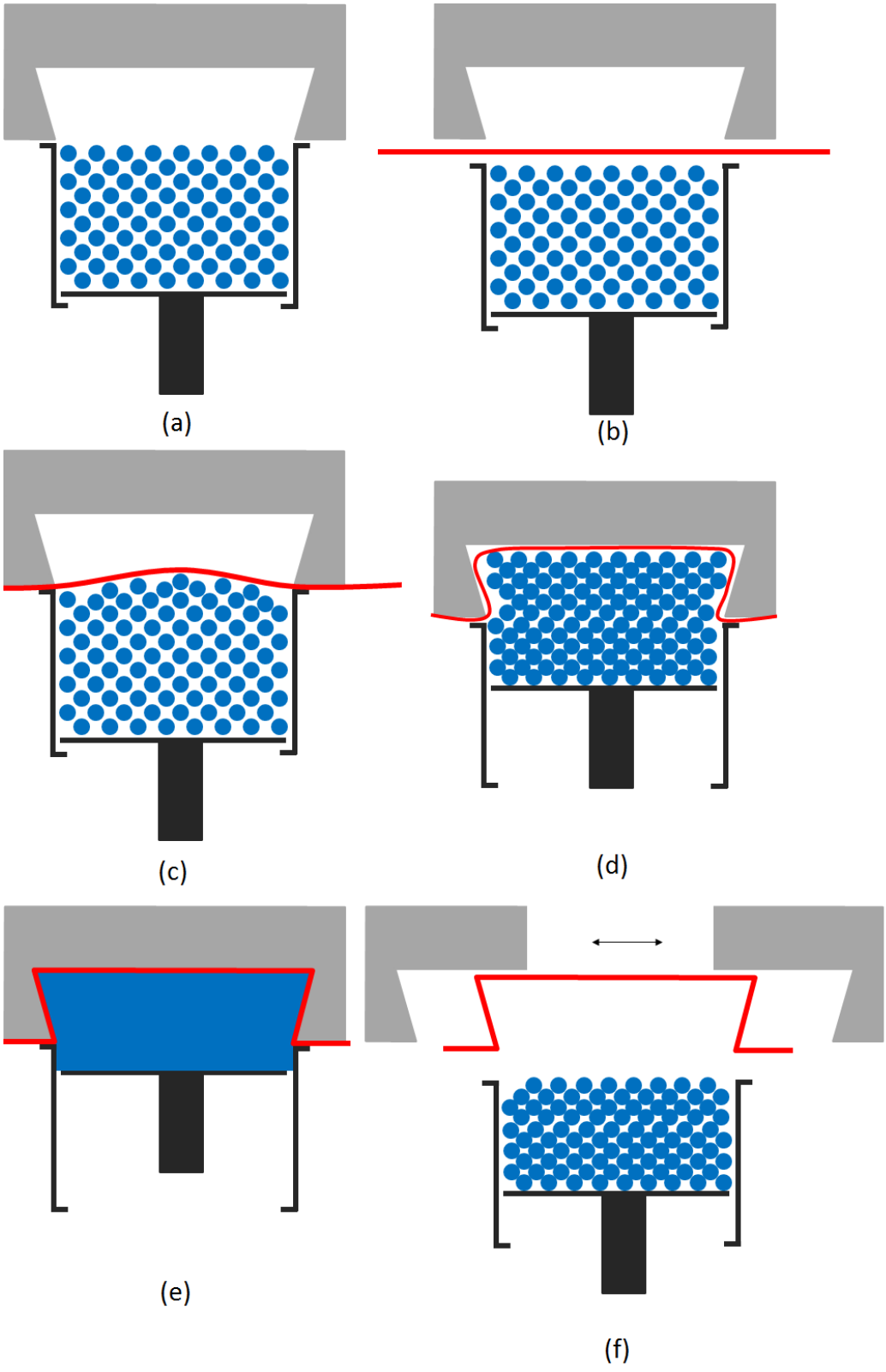

Figure 6.1 Working principle of the method with a collection of rubber particles. The container is filled with particles before the press cycle (a); the hot thermoplastic composite sheet material is transported between the container and the product mould (b); both container and piston are moved upwards (c); the laminate has reached the bottom of the mould but the particles are not fully compressed yet (d); the piston compresses the rubber particles to a full rubber stamp (e); the product is released from the mould.

6.1.1 Advantages of the method

The envisioned advantages are similar to the advantages of hydro forming. At the same time, the presented method eliminates the numerous disadvantages of application of real fluids: there is no leaking and in the case some of the rubber particles fall out of the mould when releasing the pressure, they could be either replaced or collected and used again in the following production processes.

Uniform pressure distribution – A uniform pressure distribution that is needed for the reconsolidation of the composite material is more easily created. This allows pressing with lower forces than with rubber forming or matched metal die forming.

Able to form complex shapes – it can form irregular shapes that may not be able to be formed using other press methods. For example, products with an undercut can be press formed.

Inexpensive tooling – it just requires one die that defines the product, the rubber particles act as a common die for all the different product shapes. The tooling costs are estimated approximately 50% less than for conventional press dies.

No accurate sealing needed – The rubber particles act like a fluid in the mould, but at the same time leakage is unlikely. The particles act like a cork. An open space between the container and the product mould is sealed by a particle. This is true on one condition: the opening must be considerably smaller than the single particle. This reduces even more the tooling costs. Tooling (container and piston) made by hand is sufficiently accurate for this forming process.

No need for precise calculations – As the rubber 'mould' is formed by itself, no precise calculations are needed the make a nicely fitting stamp. For composite products, this means a large cost reduction as the thickness of the composite does change and does not stay uniform during the forming process. These variables make it difficult to design a good fitting 'solid' stamp.

Adaptable to a large variety of materials – Almost all sheet materials capable of being press formed can be formed with this process. A big advantage above hydro forming can be found here. Hydro forming is mostly limited to materials that can be cold formed, as the rubber membrane that is enclosing the fluid cannot handle high temperatures. The present process can handle temperatures way above the melting point of most thermoplastics by using silicon rubber particles. Different material thickness as well as different types of materials can be formed for the same part without the need to modify the existing tooling.

Quick tool change – Due to the simplicity of the tooling the set ups can be changed quite quickly and easily.

Insensitive to wear – As the pressure medium is built up by individual rubber particles, the wear of one particle does not influence the whole collection of rubber particles on the contrary to rubber forming where a crack in the rubber stamp makes the whole stamp unusable after a short time. Because the particles are free to move, they will always be subjected to another load (heat and/or deformation) in the following press cycle. This makes that the whole collection of

rubber is subjected to the highest loads once in the system and not one particular part of a rubber stamp. If one particle is torn or broken, it will not influence the working of the principle.

No pressure limits – the process can be applied as long as the container and product mould can withstand the applied pressure forces. Once the rubber particles are fully compressed, the further loading is merely hydrostatic; this means that the particles are not subjected to other deformation forces. Therefore, the same rubber particles are applicable in low pressure forming processes and in high pressure forming processes.

Some advantages that do not count for the forming of thermoplastic composites, but might be important when considering forming of sheet metals are:

Eliminates multiple operations – compared to conventional press methods that may require two or three operations, it can often form the same part in a single cycle.

Minimal material thin out – it allows the metal to flow, unlike other forming processes that elongate or stretch the material very locally. Consequently, the reduction of thickness is smaller.

Easy to implement in existing factories – This production method is simple. With relative simple machines and little special education, it can be used to form products out of sheet material.

6.1.2 Disadvantages of the method

Because the pressure medium is made of rubber particles, the pressure will be slightly lower in between the particles. This will not have an influence on the overall pressure applied on the long fibres, as they are stiff enough to bridge this pressure drops, but it will have an influence on the thermoplastic resin, influencing the finish of the surface in contact with the particles on one side only. In order to minimise the imprint of the particles, this effect has been further investigated in the next section.

During press forming the hot thermoplastic matrix has a low viscosity, which makes it flow in this low-pressure regions. When the thermoplastic composite is hardened, small bulges of matrix material might be visible on the surface. The roughness of the surface due to the imprint of the rubber particles will depend on the dimensions of the particles and on how dense they can be packed. The fibre reinforcement is not disturbed by this disadvantage, it is therefore believed that this is rather an aesthetic problem than a mechanical engineering problem.

A bigger problem does occur when the fibre layout is not chosen well. When the fabric becomes unstable during forming, for example when the fibres reach their maximum shear angle, the fabric can show some wrinkles. If these wrinkles nest between the rubber particles, a very rough surface finish can be expected. On the other hand, this can also turn to an advantage, due to the fact that no wrinkles are pressed flat, as in the case of rubber forming and matched die forming.

6.2 Optimisation of the geometrical and mechanical characteristics of the rubber particles

Once the method has been defined in theory and proven feasible, there is the need to define the best parameters to press a thermoplastic composite sheet into a product obtaining the best surface quality possible.

One of the first questions to be answered is which shape of the rubber particles is the best in order to obtain the densest packing. According to [5], there is a difference in density between shaken and not shaken spheres according to the following formulas:

$$\rho = 0.636 - 0.33N^{-\frac{1}{3}}\ shaken$$

$$\rho = 0.6 - 0.37N^{-\frac{1}{3}}\ not\ shaken$$

Being N the number of balls.

More in general, [6] states that when a granular material, like sand or rice, is poured into a container, its density is relatively low and it flows like an ordinary fluid. If the vessel is shaken, the level of the material decreases and the packing density increases. In the utmost case, the sand behaves as a solid. This idea fits perfectly with the rubber pressing method with rubber particles. When the particles are poured into the mould, they are like a fluid; therefore, they can fill any corner of the mould. When they are pressed together, they behave like a massive mould, giving the hydrostatic pressure needed.

In theory, the best shape to obtain the most compact and smooth surface is a collection of solids with rounded edges, in particular it has been demonstrated [7] that ellipsoidal shapes placed randomly in a container contain the least empty space in between them.

Simple experiments to verify the effect of the particle dimensions on the pressure distribution were made with the use of Pressurex® foil (Figure 6.2), which gives a quantitative evaluation of the pressure distribution on a surface after a certain amount of pressure. In the picture, it is visible how the ellipsoids give a finer imprint with less and smaller voids in-between particles compared to cubic particles.

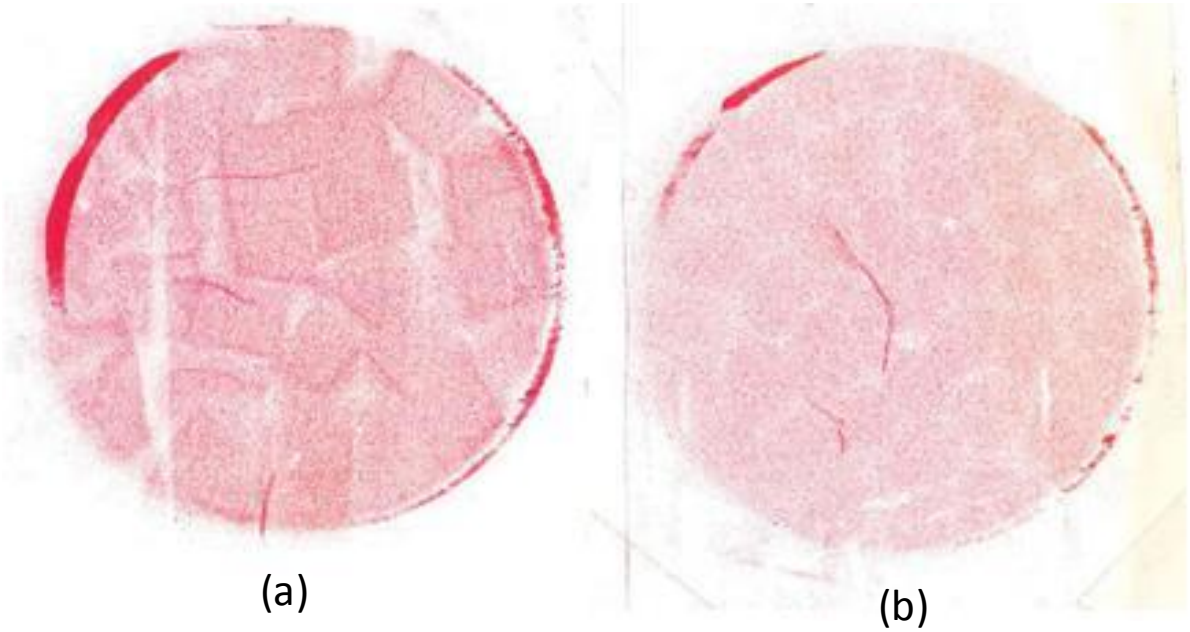

Figure 6.2 Pressure distribution using Pressurex® foil: cubic particles (a) and ellipsoidal particles (b).

In order to verify the effective necessity of such a shape and the influence on the dimensions and the hardness of the rubber particles, a series of tests was carried out to investigate the influence of these parameters on the pressure distribution during the forming process.

Figure 6.3 Rubber particles

A summary of the tested shapes and dimensions is listed in Table 6.1. Two hardness grades of ellipsoid particles were considered. Dimensions and hardness were chosen based on the availability of the producer. The rubber particles are produced via injection moulding; in this case, a major first investment is necessary. This would imply the knowledge of the best dimension and hardness on forehand. The cubic particles, instead, are hand cut from a large block of the same silicon rubber used to produce the solid rubbers for rubber pressing. The blocks are not as regular as the ellipsoidal ones but can be made in-house and do not require a large investment.

Shape	Type	Hardness (Shore A)	Dimension 1 (mm)	Dimension 2 (mm)	Dimensions 3 (mm)
Ellipsoid		20	8 x 10 x 12.5		
Ellipsoid		35	8 x 10 x 12.5		
Cube	Zermack ZA 22 Mould	22		5 x 5 x 5	10 x 10 x 10
Cube	Zermack HT 33 TRANSP	33		5 x 5 x 5	10 x 10 x 10
Cube	Zermack SA 50 LT	50		5 x 5 x 5	10 x 10 x 10
Cube	Silastic S	37		4 x 4 x 4	8 x 8 x 8
Cube	Silastic M	59		4 x 4 x 4	8 x 8 x 8

Table 6.1 Summary of tested rubber types and shapes

6.2.1 Test set up

The test set up is practically the same as the one used for determining the pressure distribution of a solid rubber mould, as described in Chapter 4.

The container for the rubber particles is a Plexiglas box stiffened at its bottom with thick aluminium reinforcement. In order to push the particles inside the mould, an aluminium piston is inserted in the Plexiglas mould as shown in Figure 6.4. It should be noted that the arrangement is upside-down compared to the description of the method in section 6.1. The reason is that neither the optimal configuration was established when these tests were carried out, nor was it necessary for these specific tests where most of the test-up was already available.

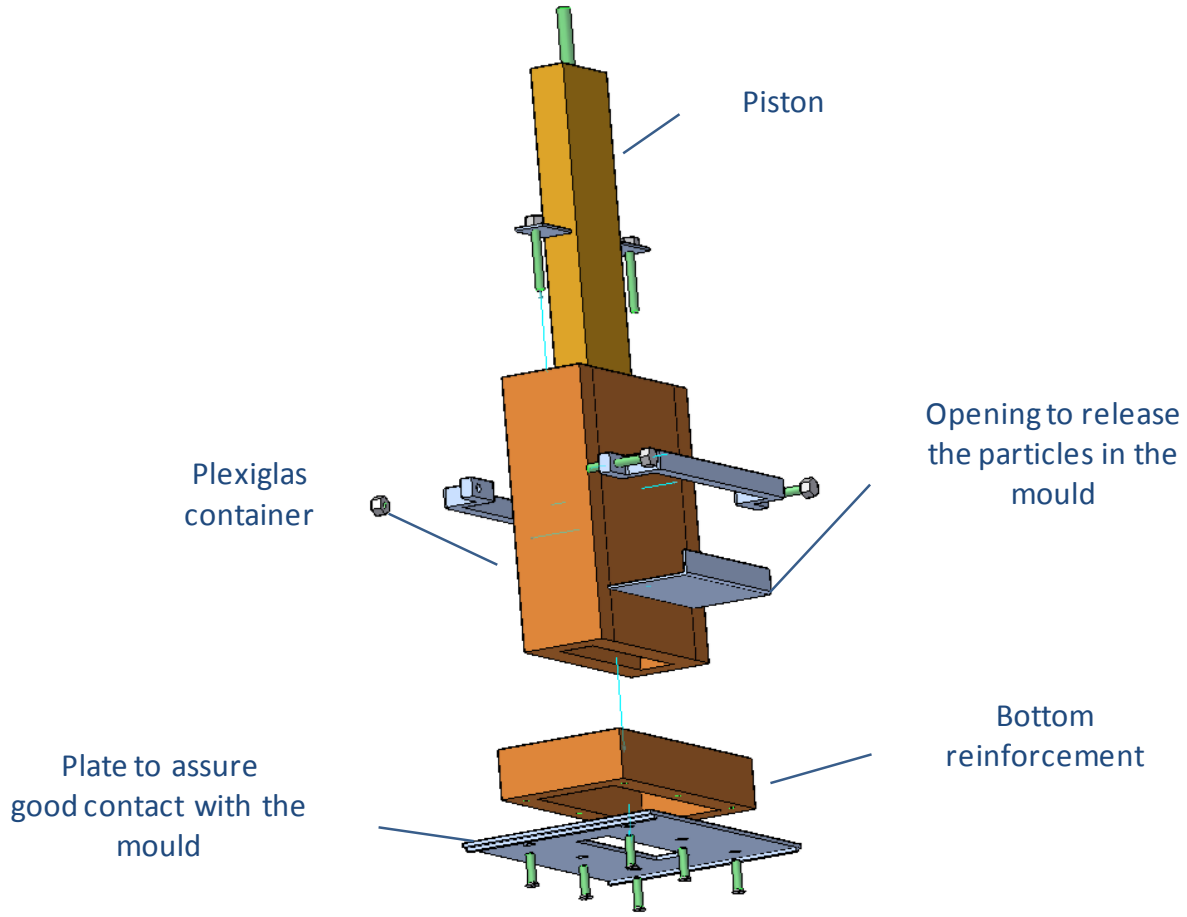

Figure 6.4 Container designed to press the rubber particles.

At the bottom of the container, a plate is positioned to be able to clamp the container for the rubber particles to the steel mould as shown in Figure 6.5 together with the entire set up.

The tests are carried out on a force controlled Zwick machine. The force is varied in steps of 500 N from 0 up to a maximal applied force of 5 kN. This maximal force depends on the set up. The compressed particles exert a hydrostatic force on the piston as well as on the Plexiglas container. The latter is too weak to sustain a very high pressure. During the test the applied force on the piston is recorded together with its displacement. The pressure distribution on the side walls of the mould at several load steps is measured, using strain gauges, as well.

Figure 6.5 Test set up.

6.2.2 Discussion of the results

For each rubber type, at least five tests are carried out. An example of the rubber particles behaviour during compression is shown in Figure 6.6. Here large solid blocks of medium hardness are shown. It is visible that the higher the pressure, the more compact the rubber gets, filling all the voids between the particles and becoming similar to a solid mould. The same is visible, to a smaller or greater extent, in all cases or rubber types and dimensions.

It has to be noted that the larger the dimensions of the particles, the larger the container should be. The amount of air entrapped between the particles before the start of the test is in fact more when the dimensions of the particles increase.

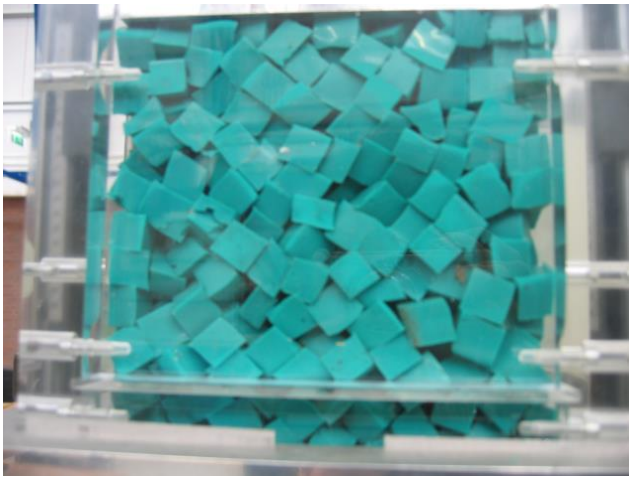

(a)

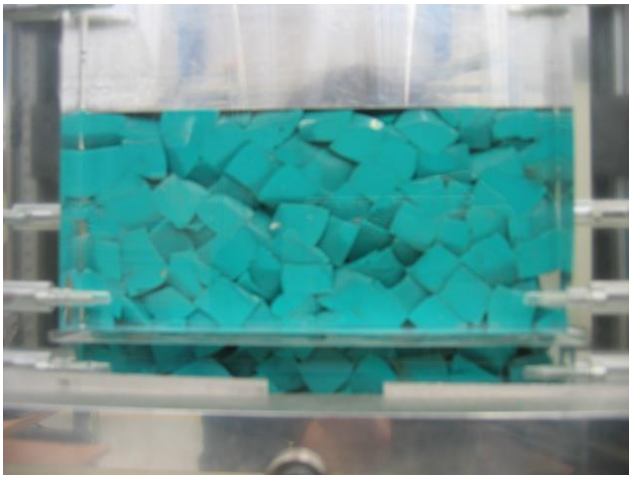

(b)

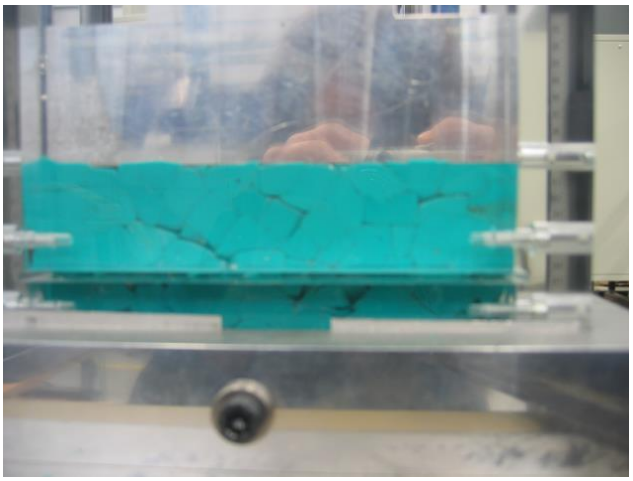

(c)

Figure 6.6 Example of pressing sequence: a) no pressure, b) partially closed, c) almost at full pressure.

As an example of the improved pressure distribution, the results of a test carried out with small cubical particles of 20 Sh A is shown in Figure 6.7, where the pressure distribution around the mould is shown at increasing values of the applied load. The low peaks corresponding to the loss of pressure around the corners of the mould have disappeared. Moreover, the higher and lower pressure values for different tests do not correspond to the same place in the mould but depend on the particle position inside the mould, as it is also visible in Figure 6.6, c) where voids in-between the particles are still visible.

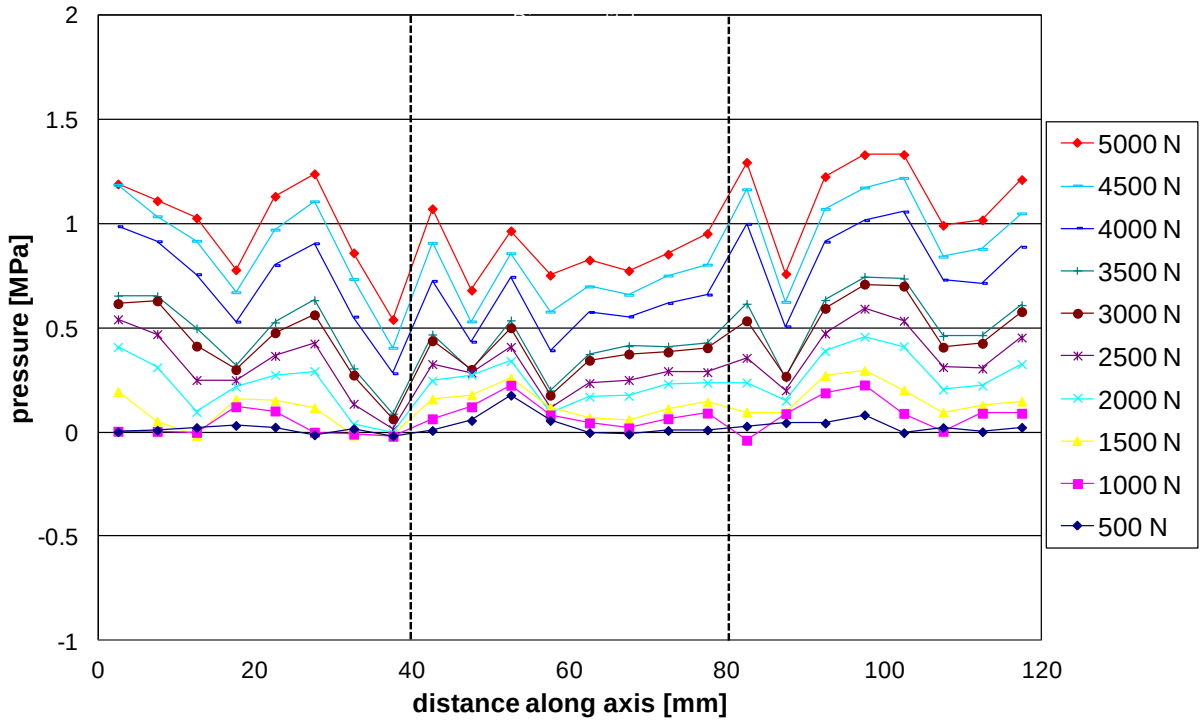

Figure 6.7 Pressure distribution a tests made with small square particles of hardness 22Sh A.

In order to decide which shape, dimension and hardness provide the most constant pressure distribution, the average pressure of each strain gauge and the standard deviation are calculated for the last load step of 5 kN for all rubber shapes and hardnesses tested. The summary of the results is shown in Figure 6.8 and Figure 6.9.

The two figures indicate that, for equal particle dimension, the average normal pressure on the walls of the mould is inversely proportional to the particles' hardness. In fact, the lower the normal pressure, the higher the tangential component and therefore an increased friction exerted on the mould walls. This means that the harder the rubber, the higher the increase of friction on the walls of the mould. At the same time, the amount of scatter in the data increases with the increase of hardness, which implies a less constant pressure distribution on the mould.

The tests pointed out that the most important parameter is the rubber hardness; it should be as soft as possible. The rubber particles shape is not very important as long as the dimensions of the particles are kept constant. A rounder shape appears to perform somewhat better than a squared one at equal volume, but it has to be established during actual production to which extent the effect is important. A rounder shape involves higher starting costs, due to the cost of

production of the rubber particles, therefore a smaller size of cubic particles might be a more attractive option.

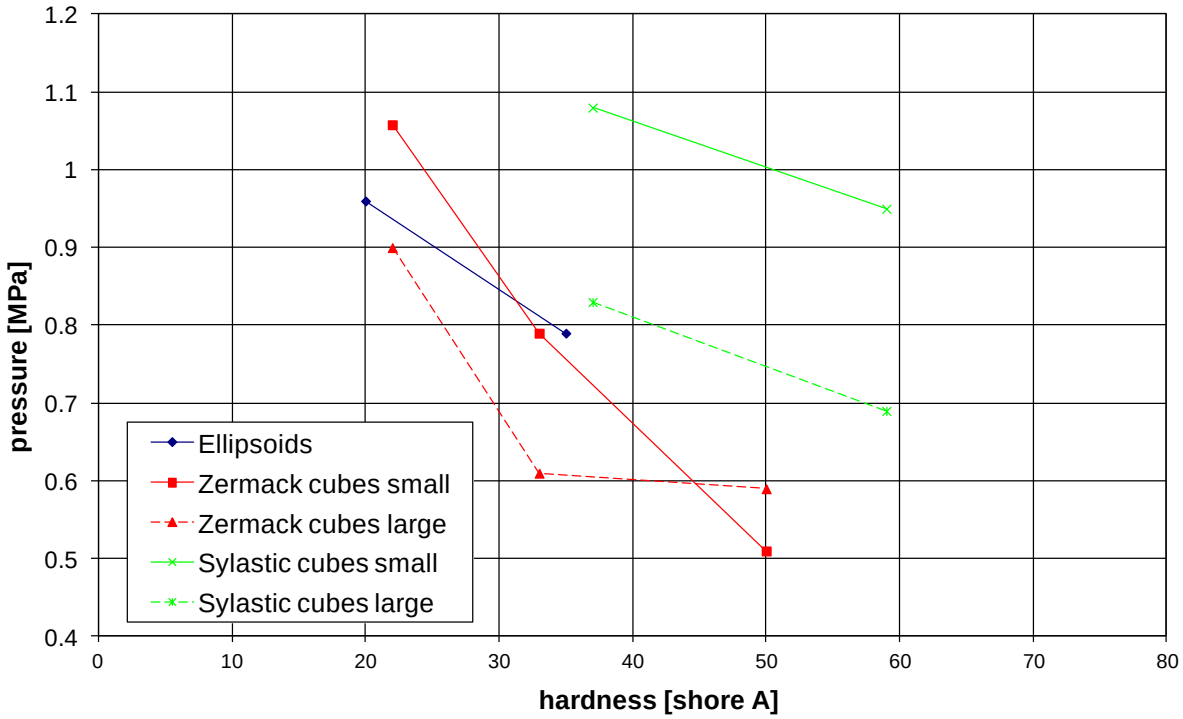

Figure 6.8 Average pressure values on the mould walls for the performed tests.

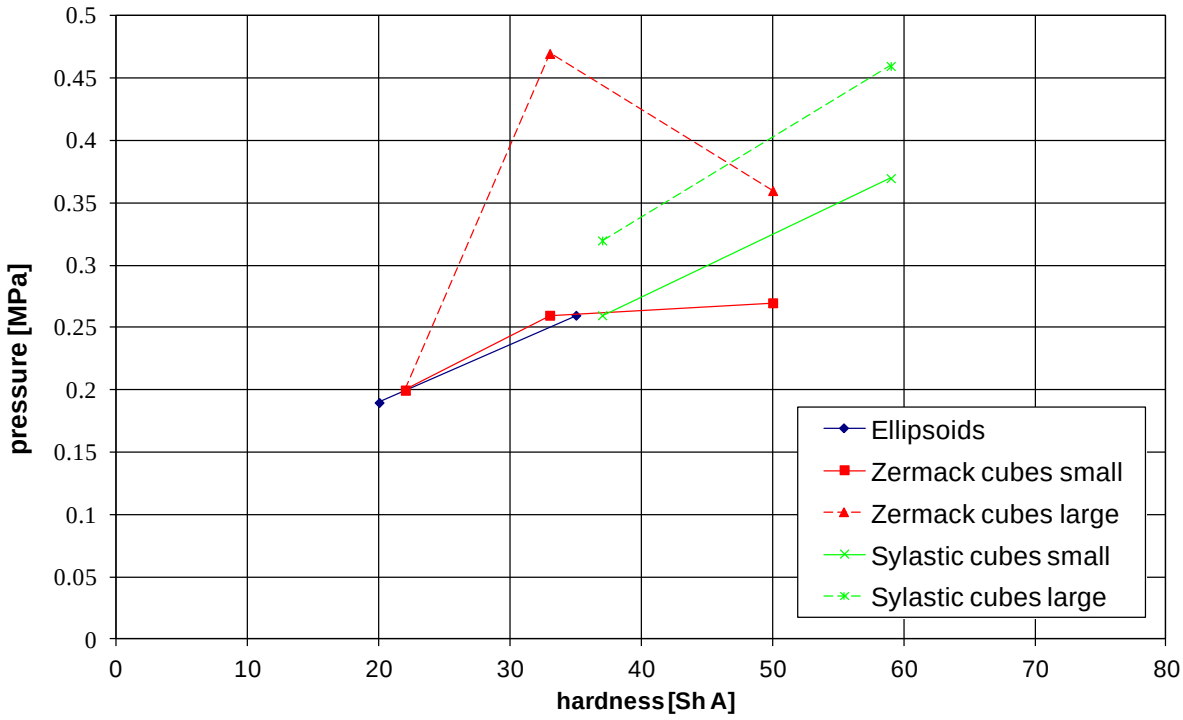

Figure 6.9 Standard deviation of the average pressure on the mould surface for the performed tests.

6.3 Production of parts

The parts produced with the present technique are all pressed with the Alfamatic press described in Chapter 2. The complete setup is shown in Figure 6.10. Two infrared panels are used to heat the thermoplastic composite material. In order to heat the different metal moulds, a heat plate is used, heated with five electric resistors. The temperature on the panel is controlled via a thermocouple.

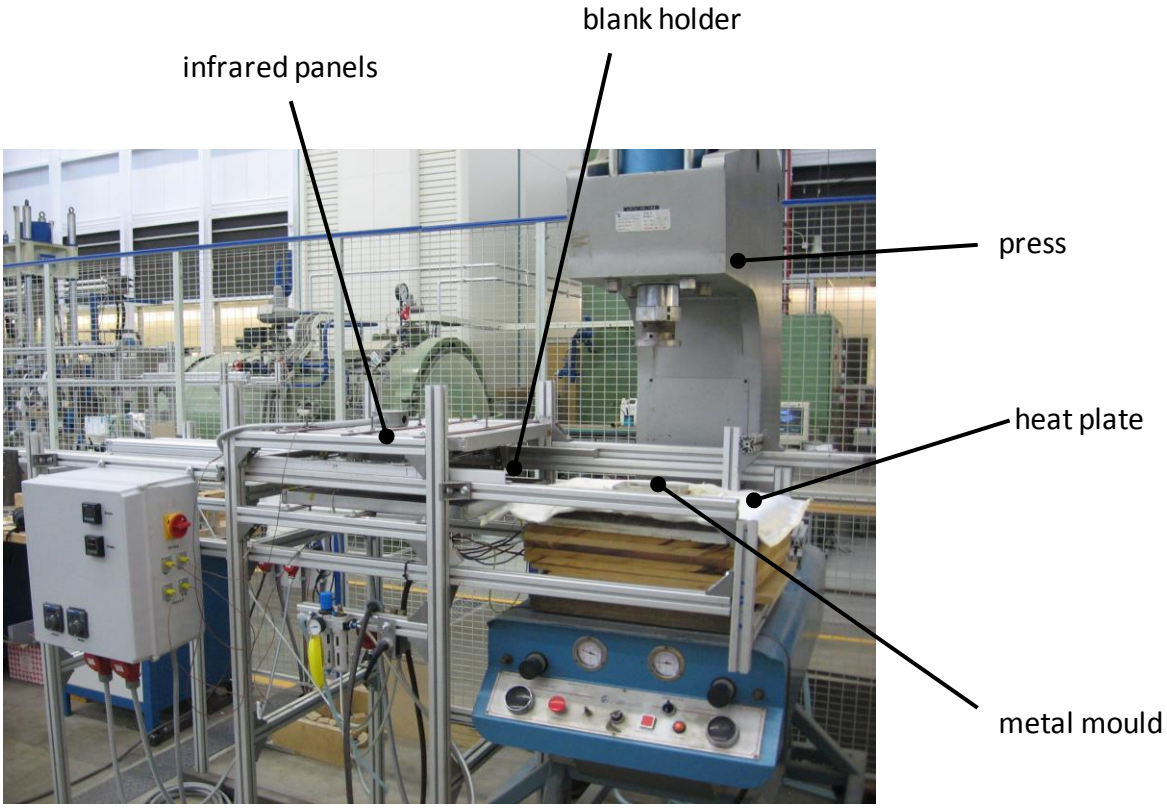

Figure 6.10 Total production set up.

6.3.1 Pressing of hemispherical composite specimens

The hemisphere is the typical thermoplastic part that is produced via rubber press forming to study the behaviour of the thermoplastic material. Although being a simple part, it presents many challenges as the shearing angle of the thermoplastic laminate to form an hemisphere is very high. Therefore, the forming pressure has to be high enough to form the part without wrinkles but also not too much in order to avoid breaking the laminate.

Figure 6.11 shows the product mould as well as the container for the rubber particles and the piston that is attached to the press. The container has exactly the same diameter of the outer diameter of the hemisphere and is attached to the piston so that it cannot fall down. This allows a downward movement when the pressurization of the rubber starts.

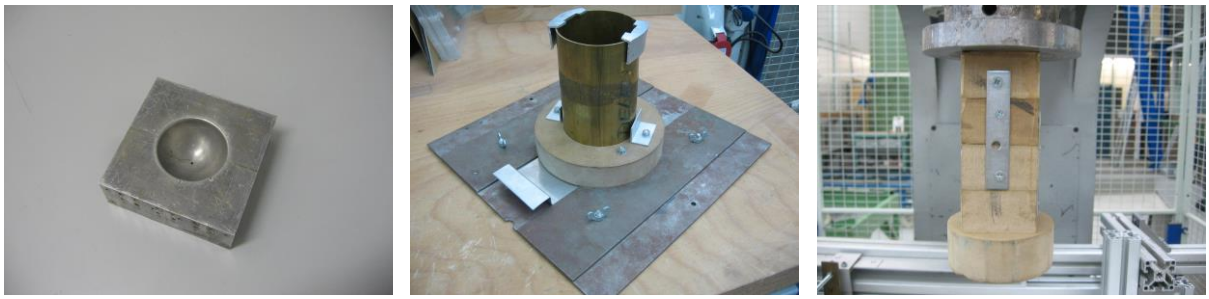

a b c

Figure 6.11 Mould (a), particles container (b) and piston (c) used for the production of the hemispheres

In order to verify the experimental results on the effect of the shape of the particles and the hardness needed on the pressing process of an hemisphere, several hemispheres have been produced using different composite thermoplastic materials and rubber particles types. Figure 6.12 shows a hemisphere produced with woven glass fibre PPS. The outer surface is well formed and no visible difference between hemispheres produced by the standard method is present.

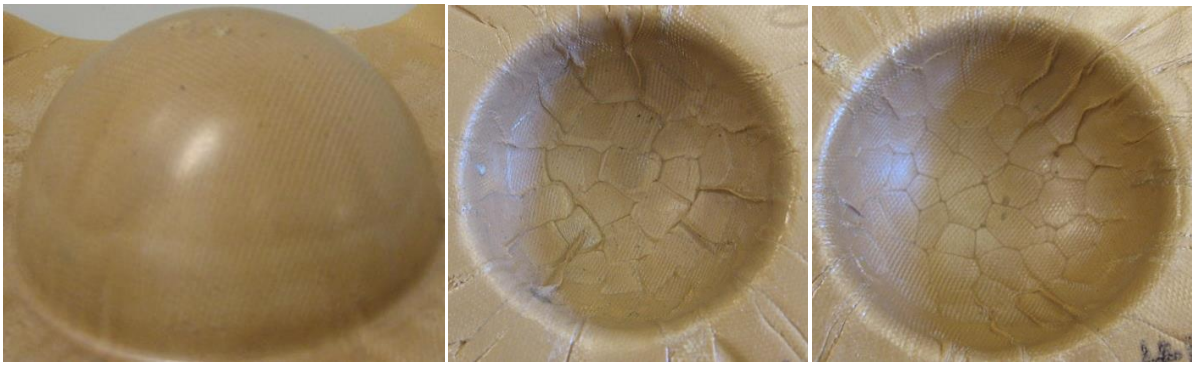

Figure 6.12 Surface quality. Difference of imprint between cubical (large 37 Sh A) and ellipsoidal (20 Sh A) particles.

When looking at the quality of the inner surface, though, the imprints of the particles are clearly visible. In particular, the imprint of the large cubical particles of medium hardness is more visible than that of the ellipsoidal ones, which confirms the previous findings of the quasi-static experiments on the influence of particles shape and hardness on the pressure distribution presented in 6.2.

In order to verify that the process is valid for every type of material, also carbon fibre PPS plates where pressed by means of rubber particles. The result is shown in Figure 6.13. Pressing with rubber particles works well also in the case of a stiffer fibre. In addition, in this case the square particles leave a visible imprint at the back of the product, while the external surface is smooth and perfectly formed. In order to verify the quality of the laminate one produced hemisphere is cut to verify the good consolidation of the thermoplastic. This is shown in Figure 6.14. In addition, in this case the consolidation of the part is very good and delaminations are

not visible. This is a confirmation that the particles are able to exert enough pressure on the laminate during both forming and consolidation phases.

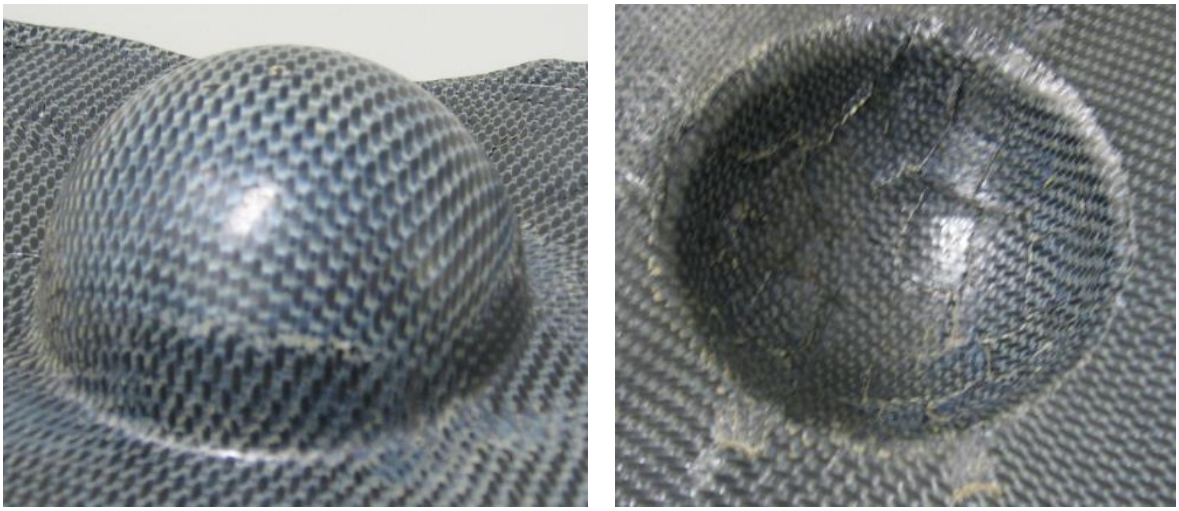

Figure 6.13 Surface quality in case of carbon fibre PPS pressed with large Silastic S cubic particles.

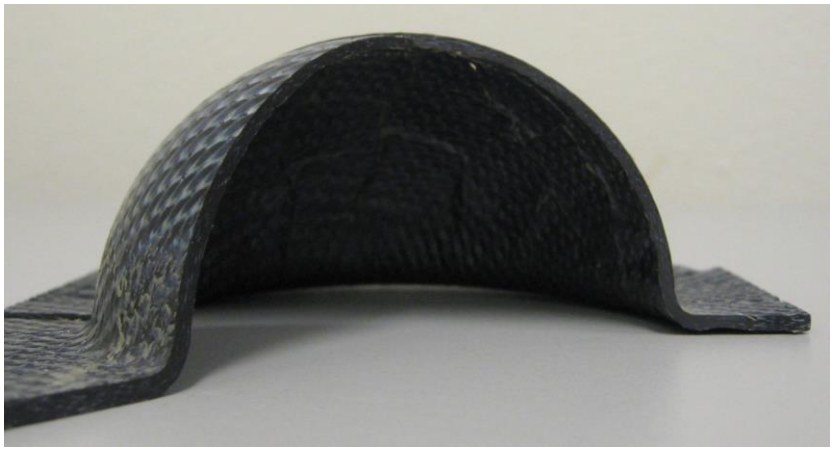

Figure 6.14 Quality of thermoplastic laminate after pressing with a collection of rubber particles.

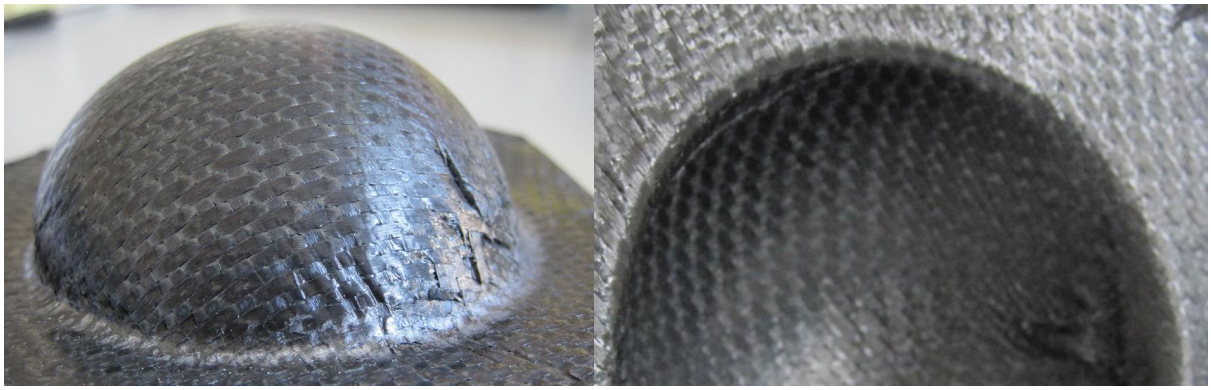

Figure 6.15 Surface quality in case of carbon fibre PPS pressed with small Zermack ZA 22 Mould cubical particles

Finally a hemisphere is produced with small, soft (22 Sh A) rubber cubes in order to investigate the hypothesis that the dimensions of the rubber have an influence on the more constant pressure distribution and therefore the final surface quality of the product on the side of the rubber particles (Figure 6.15). Although the product presented some defects due to wrong production parameters, both inner and outer surface are smooth a no imprint of the particles is visible.

6.4 Conclusions and recommendations

Although pressure forming of thermoplastics using rubber particles instead of a solid rubber mould is still in a development phase, it already presents several advantages to the classical rubber pressing method. Not only is it more versatile, as a wider range of products can be formed; including pieces with an undercut, but it also allows the reduction of development costs related to the definition of the right rubber mould.

Using the right combination of shape and hardness of rubber particles it is possible to form a product of high quality, which is expected to be better than the optimised rubber pressed product. From this study, it appears that the best particles for a smooth product have to be with the smallest possible size, with a typical dimension in the range of millimetres instead of centimetres, and with a low hardness. The shape of the particles plays a role, but it is not dominant. Ellipsoidal particles with the same volume of cubical particles perform better, but might be easily substituted by smaller cubical ones.

More work has to be carried out in the definition of the right parameters during production and the design of the optimal container for the rubber particles that can allow a fast series production.

6.5 Bibliography

[1]. Decoster D., Novel, universal pressure moulding process for thermoplastic composites, using a collection of rubber particles as pressure medium, Master Thesis, Delft University of Technology 2007

[2]. Decoster D, Marissen R, Antonelli V, “Method and Device for manufacturing a moulded part from a Sheet-like material”, patent WO2008147185

[3]. Decoster D, Antonelli V, Marissen R, Beukers A, “Hylid Forming, an Innovative Production Method for the Forming of Thermoplastic Composites”, 11th ESAFORM2008 conference on material forming. April 2008, Lyon, France

[4]. Antonelli V, Decoster D, Marissen R “Improvements in the pressure distribution during the forming of thermoplastic composites”, 11th ESAFORM2008 conference on material forming. April 2008, Lyon, France

[5]. Schott GD, “Packing of Spheres”, Nature 188, 908-909, 1969

[6]. Aste T, Weaire D, “The Pursuit of Perfect Packing” Institute of Physics Publishing, Second Edition 2008

[7]. Man W., Donev A.,Stillinger F.H., Sullivan M.T., Russel W.B., Heeger D., Inati S., Torquato, S. and Chaikin P.M., “Experiments on Random Packing of Ellipsoids”, Physical review letters, 20 May 2005

[8]. V. Antonelli, R. Carbone, S. Lindstedt, R. Marissen, "Pressure distibution and surface quality during forming of thermoplastic composites with a collection of rubber particles as mould half", 17th International Conference on Composite Material ICCM 2009, Edinburgh, UK

Chapter 7
Characterisation of a collection of rubber particles

7.1 Introduction

Although the pressing method with a collection of rubber particles is more versatile and needs much less optimisation, it is still worthwhile being able to model the process, in order to acquire more understanding and explore the limits of the process. The present chapter presents the first steps for the development of such a model.

The collection of rubber particles behaves in a way similar to that of a fluid during the pressing process. It has the advantage of filling the mould completely so that there is always contact between the rigid and the flexible mould. Once the cavity of the mould is filled completely with rubber particles, the collection of particles has the same characteristics of a solid with an initial very low stiffness and an unconventional shear stiffness.

The scope of the present chapter is to describe the collection of rubber particles as a homogeneous material of which the specific mechanical characteristics have to be determined. To be able to characterize the rubber particles behaviour as a continuum, a series of tests has been designed for the determination of some of their physical parameters.

Homogeneous isotropic linear elastic materials have their elastic properties uniquely determined by any two modules among the Bulk modulus (K), the Young's modulus (E), the Lame's first parameter (λ), the Lame's second parameter or Shear modulus (G) and the Poisson's ratio (ν) through the relationships shown in Table 7.1.

	(λ, G)	(K, G)	(G, ν)	(E, ν)	(E, G)
λ		$K-\frac{2}{3}G$	$\frac{2G\nu}{1-2\nu}$	$\frac{\nu E}{(1+\nu)(1-2\nu)}$	$\frac{G(E-2G)}{3G-E}$
G				$\frac{E}{2(1+\nu)}$	
K	$\frac{3\lambda+2G}{3}$		$\frac{2G(1+\nu)}{3(1-2\nu)}$	$\frac{E}{3(1-2\nu)}$	$\frac{E}{3(3G-E)}$
E	$\frac{G(3\lambda+2G)}{(\lambda+G)}$	$\frac{G(3\lambda+2G)}{(\lambda+G)}$	$2(1+\nu)G$		
ν	$\frac{\lambda}{2(\lambda+\mu)}$	$\frac{3K-2G}{2(3K+G)}$			$\frac{E-2G}{2G}$

Table 7.1 Elastic modules for linear, homogeneous and isotropic materials.

Measurement methods for collections of particles are not widely described in literature, although tests methods are available for measuring the mechanical properties of soils [1]. It has been shown, though, that the behaviour of the collection of particles is similar to the one of a liquid, therefore bulk modulus tests can be carried out in a similar way.

In order to estimate the shear modulus, several tests have been carried out to be used to evaluate the shear behaviour of the collection of particles when pushed together. The tools were designed to fit in the Zwick 2 tonnes machine.

7.2 Bulk modulus dominated tests

The bulk modulus gives the change in volume of a solid substance as the pressure on it is changed, in other words it measures the degree of stiffness or the energy required to produce a given volume deformation.

The bulk modulus (K) is the inverse of the compressibility. It is also called the ***incompressibility***: if a solid or fluid (liquid or gas) has a high bulk modulus, then it is difficult to be compressed.

The bulk modulus is defined by:

$$K = V\frac{\partial P}{\partial V}$$

where V is the volume, which is decreased when a pressure P is exerted uniformly in all directions. Usually, the temperature is kept constant during the compression. K can be measured directly by exerting a known pressure and measuring the change of volume.

7.2.1 Test method

Confined compression tests are carried out to determine the longitudinal bulk modulus of the collection of rubber particles. The test set up is shown Figure 7.1. It is a 10 mm thick cylinder of 30 mm inner radius and 120 mm height. The top and bottom closures are 20 mm thick; therefore, the effective height is 80 mm.

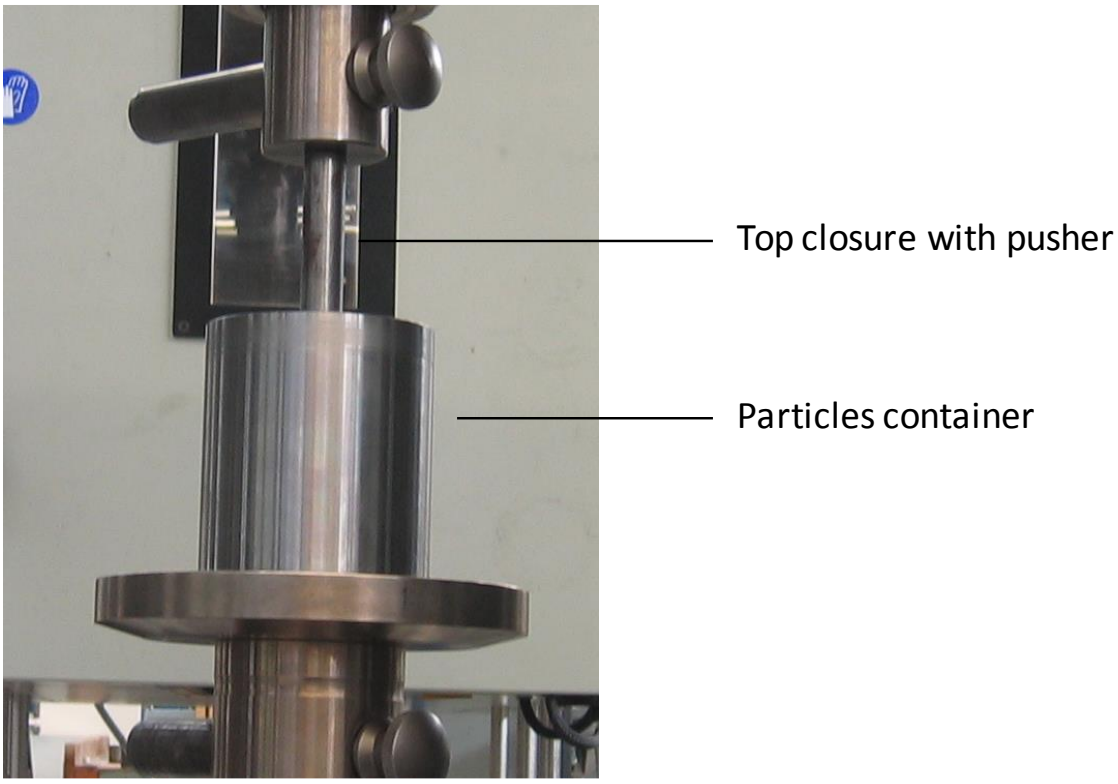

Figure 7.1 Test set up for the bulk modulus test.

The procedure for the series of tests is the following:

- A certain amount of particles is placed in the container so that the top closure is at the same height of the edge of the cylinder, but the particles are not yet squeezed in the container (there is still a large amount of air in it).
- When a preload of 20 N is reached, the displacement is set to 0.
- The test machine records force and displacement until a defined maximal value is reached (this value varies from 2.5 kN up to 8 kN depending on the hardness of the particles).
- The particles are removed after the test, then placed again inside the container, so that they are always the same amount, and randomly placed in the container without being squeezed.

Code	Shape	Type	Hardness (Shore A)	Dimensions (mm)	Number of tests
e20	Ellipsoid	(silicon)	20	7.5 x 10 x 12.5	5
e35	Ellipsoid	(silicon)	35	7.5 x 10 x 12.5	10
c37	Cube	Silastic S	37	8 x 8 x 8	6
c37small	Cube	Silastic S	37	4 x 4 x 4	6
c59	Cube	Silastic M	59	8 x 8 x 8	7
c59small	Cube	Silastic M	59	4 x 4 x 4	5

Table 7.2 Summary of the carried out tests for bulk modulus calculation (the silicon type of the ellipsoidal particles is not known, as they were not produced in-house).

7.2.2 Results

A typical load-displacement diagram of the tested rubber particles is shown in Figure 7.2.

In the present case, the longitudinal bulk modulus *K'* can be found with:

$$K' = H\frac{\partial F}{\partial h}$$

where H is the height of the part of the container filled with rubber particles, F is the force and h is the reduction in height relative to the applied force.

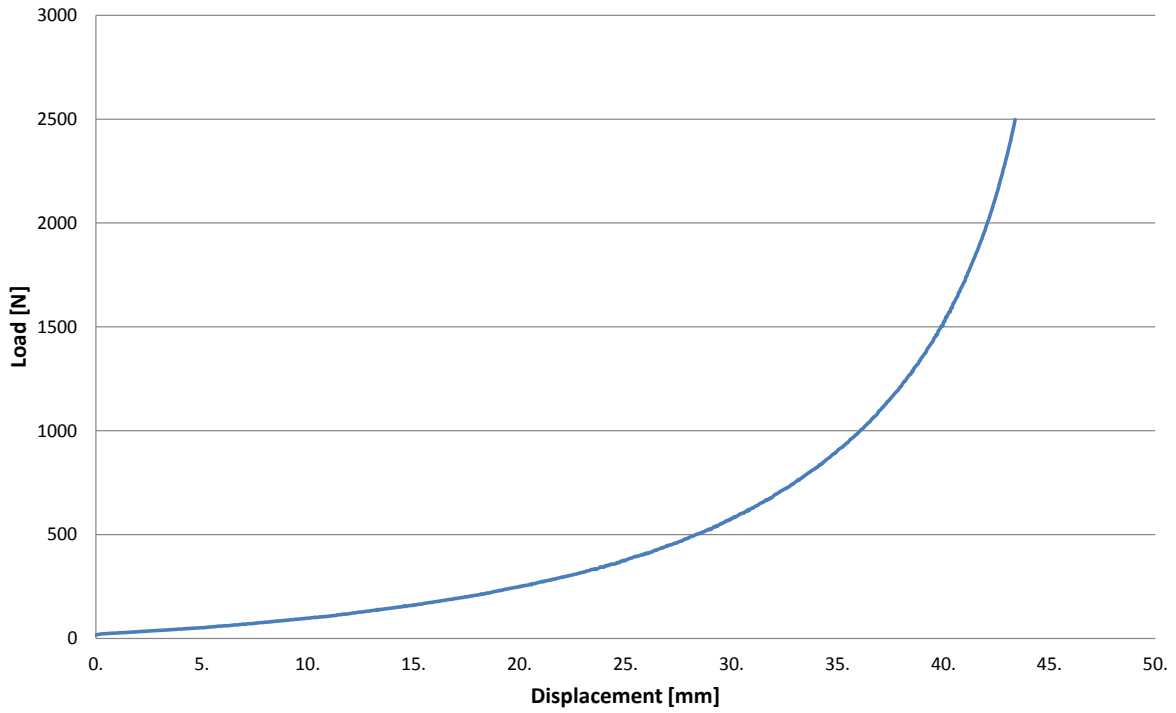

Figure 7.2 Load vs. displacement plot for the confined compression tests of the rubber particles.

An overview of the results for all the carried out tests is shown from Figure 7.3 to Figure 7.5. The plots show the bulk modulus versus the strain for the tested rubber particles. In particular, Figure 7.3 shows the results obtained for the ellipsoidal particles of two different hardness values, while Figure 7.4 and Figure 7.5 show the same results for particles of the same hardness but two different sizes. It has to be noted that the value of H is slightly different at every measurement, as the amount of air in the container depends on the random position of the rubber particles when placed in the container. When this effect is considered, the measured bulk modulus values of the same particle collection are very close to eachother.

Common to every grade is the biphasic behaviour, slowly parabolic in the beginning, turning into exponential once the particles start to behave as a solid rubber.

The particles of same hardness and different dimension present a very similar behaviour, where the first almost linear part is longer for larger particles. This is due to the amount of air that is entrapped between the particles that has to be squeezed out before the particles get in contact to each other.

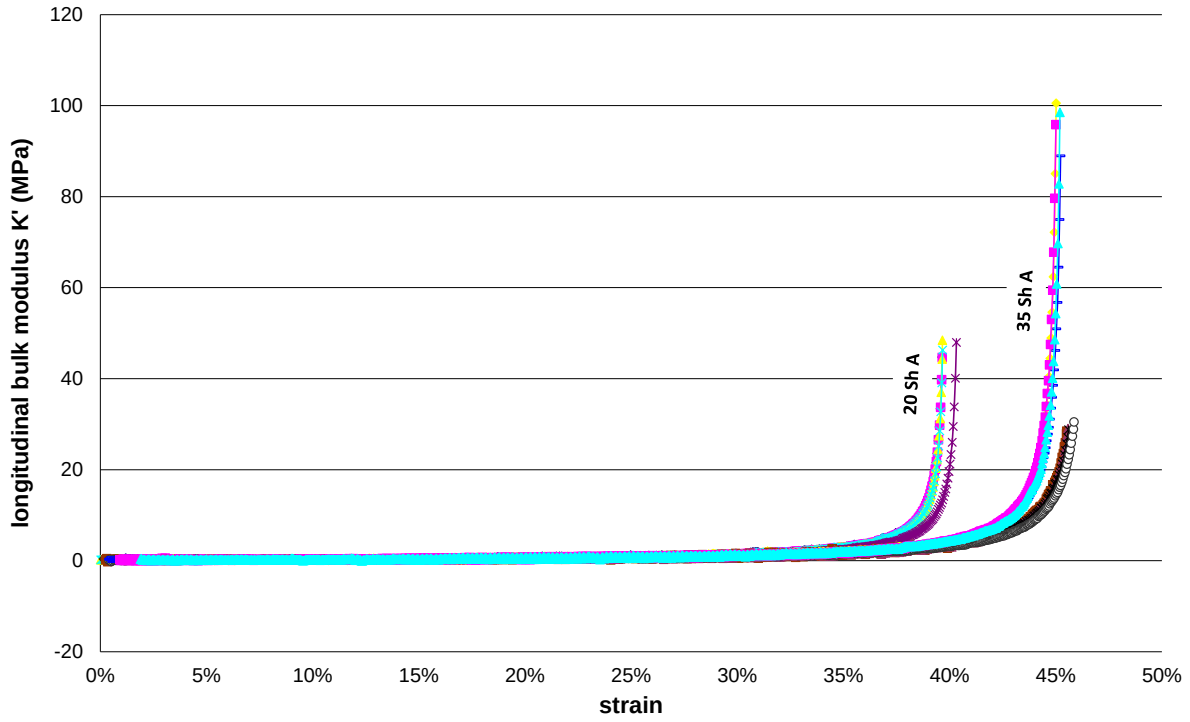

Figure 7.3 Overview of the bulk modulus as a function of strain for two collections of ellipsoidal particles with different hardness.

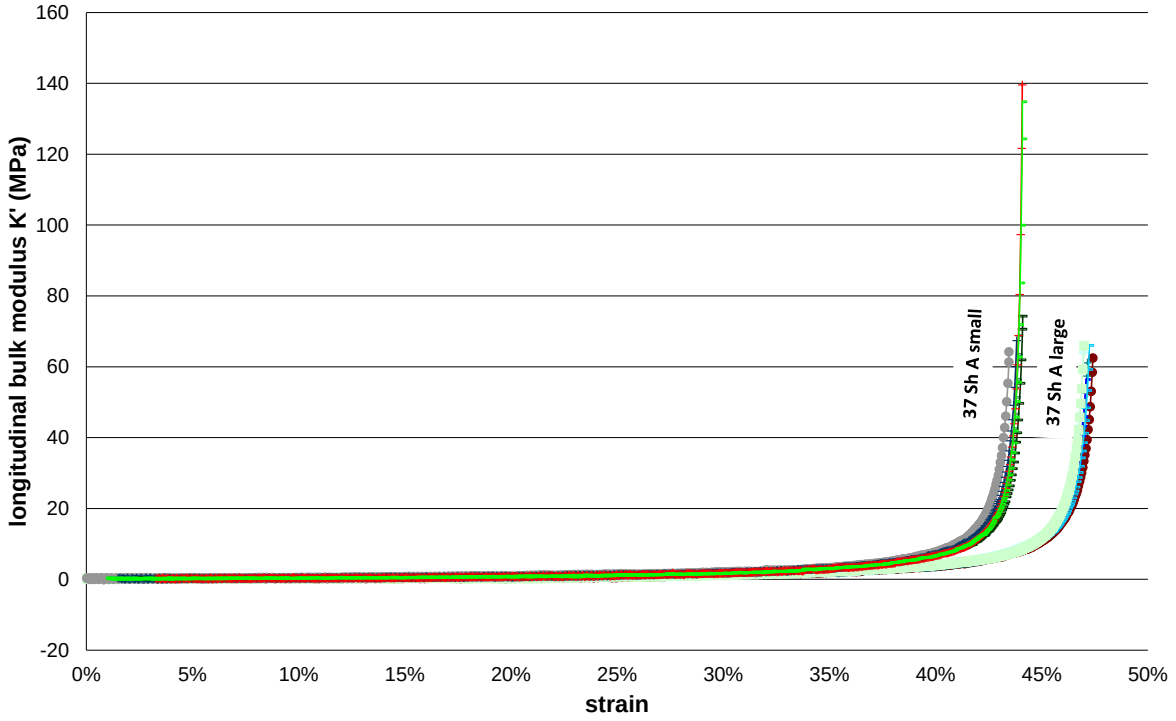

Figure 7.4 Overview of the bulk modulus as a function of strain for two collections of 37 Sh A cubical particles of two different sizes.

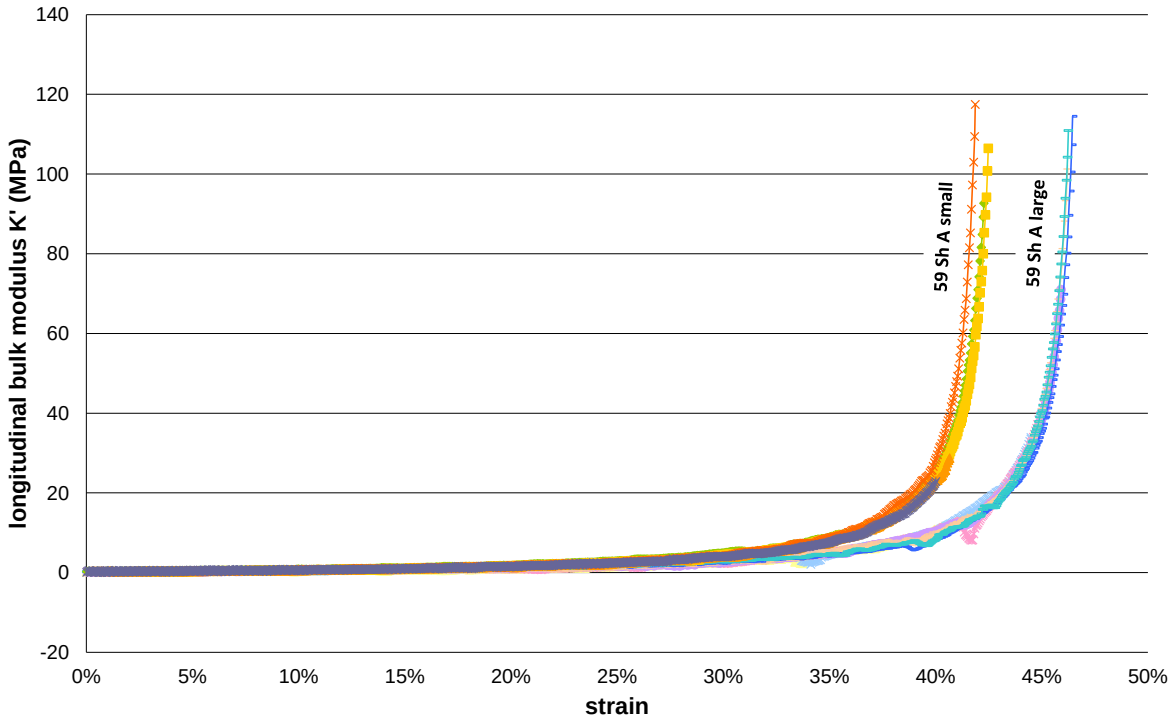

Figure 7.5 Overview of the bulk modulus as a function of strain for two collections of 59 Sh A cubical particles of two different sizes.

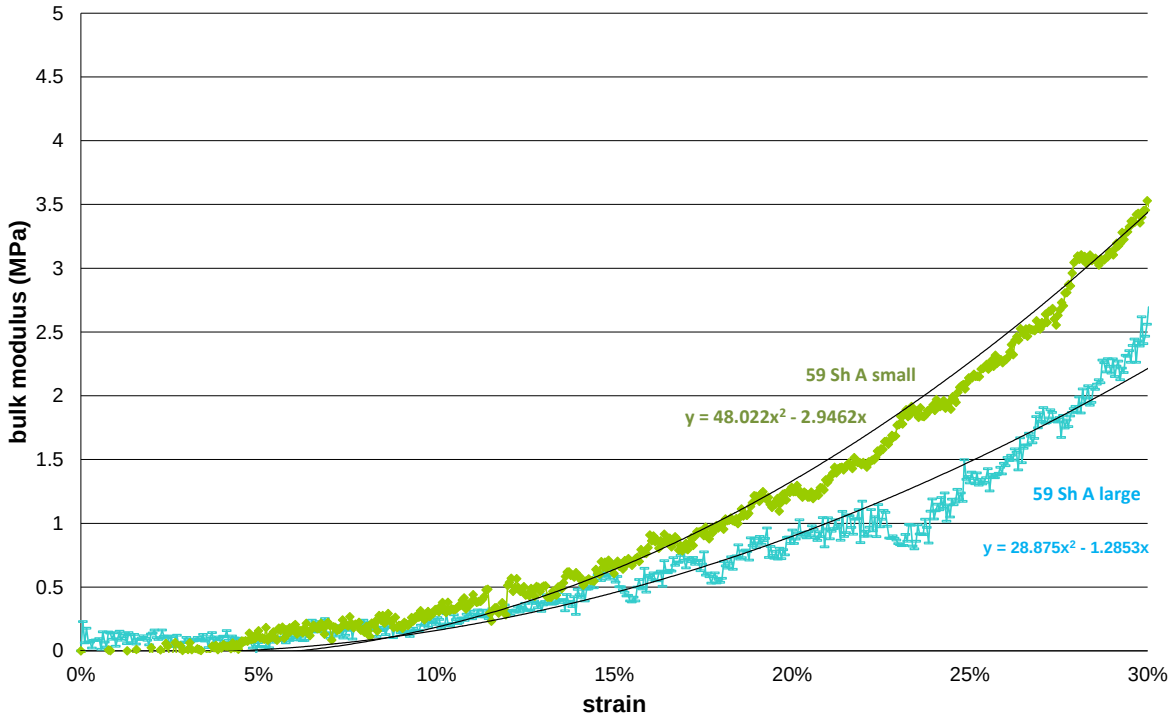

Figure 7.6 Detail of the bulk modulus as a function of strain for two collections of 59 Sh A cubical particles of two different sizes.

Figure 7.7 shows an overview of all bulk modulus test results carried out on rubber particles collections. The plot shows that there is no unique correlation between hardness and bulk modulus. The behaviour also depends on both shape and hardness. From the picture, it is possible to conclude that smaller particles are preferred to large ones, as this would allow the particles to be compacted in a shorter time to their minimum volume.

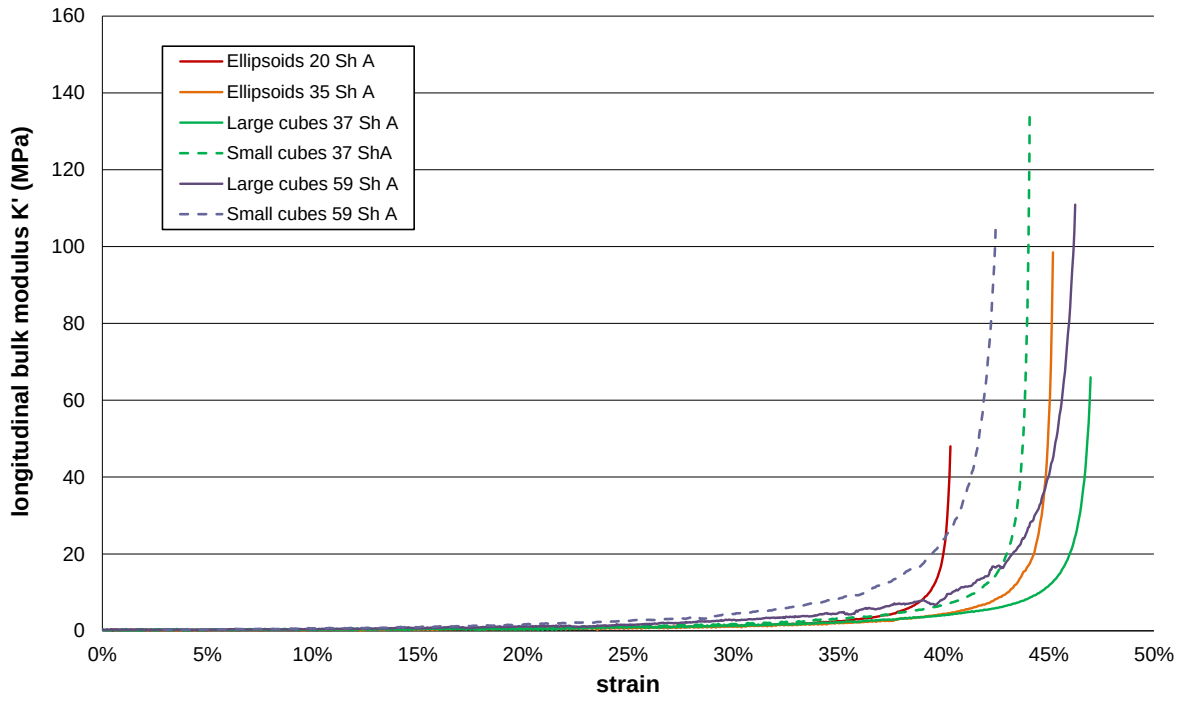

Figure 7.7 Overview of all bulk modulus results.

Figure 7.8 shows a representation of what happens in the different phases of the tests. Before starting the test (figure a) the particles are separated by air. When the air is pressed outside (figure b) the real compression of the rubber starts, until the particles form a compact block of rubber (figure c). From this moment on, the particles behave like a massive rubber block.

The pressing away of the entrapped air corresponds to the initial very low bulk modulus of all figures. After the first very low-modulus region, the bulk modulus increases up to the point where the formed block is hardly able to deform (nearly incompressible region).

It is notable that smaller particles have a smaller “low modulus” region. This is probably because the particles are more compacted at the beginning of the test; therefore, the air left in the container is less from the beginning. After the low-modulus region, the particles have the same behaviour. The same consideration can be made for softer particles: the “low modulus” path is shorter compared to harder particles of the same dimensions. The softer particles can deform easier under the weight of the column of particles above them; the collection of particles is therefore more compact from the beginning of the test.

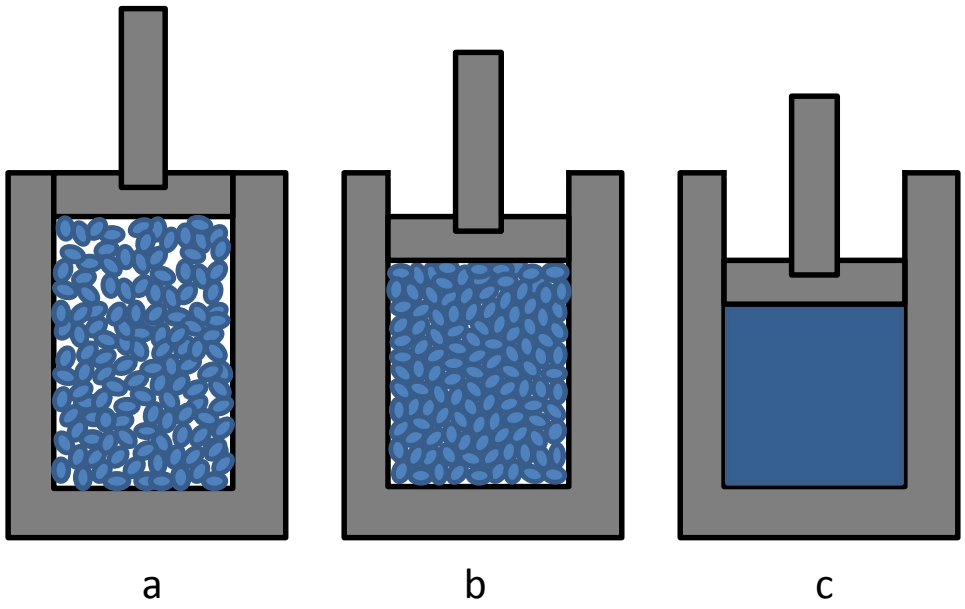

Figure 7.8 Schematic of the different phases of the compression.

7.3 Shear dominated tests

A completely new tool has been designed to measure the shear stiffness of the particles and it is shown in Figure 7.9. It has the same cross section of the classical picture frame for in-plane shear tests [7], but it is in practice a box, in which the particles can be contained. The four sides of the box are connected together by four corner hinges. Since the hinges can rotate freely, it changes the angle between the arms, resulting in a pure shear deformation. Each arm consists of two plates with four screws.

In the set up as it is, the first displacement of the system, and consequent compression of the particles, is due to the own weight of the container. It gives the initial load and displacement values that need to be considered in order to obtain the absolute load-displacement values of the further recorded data.

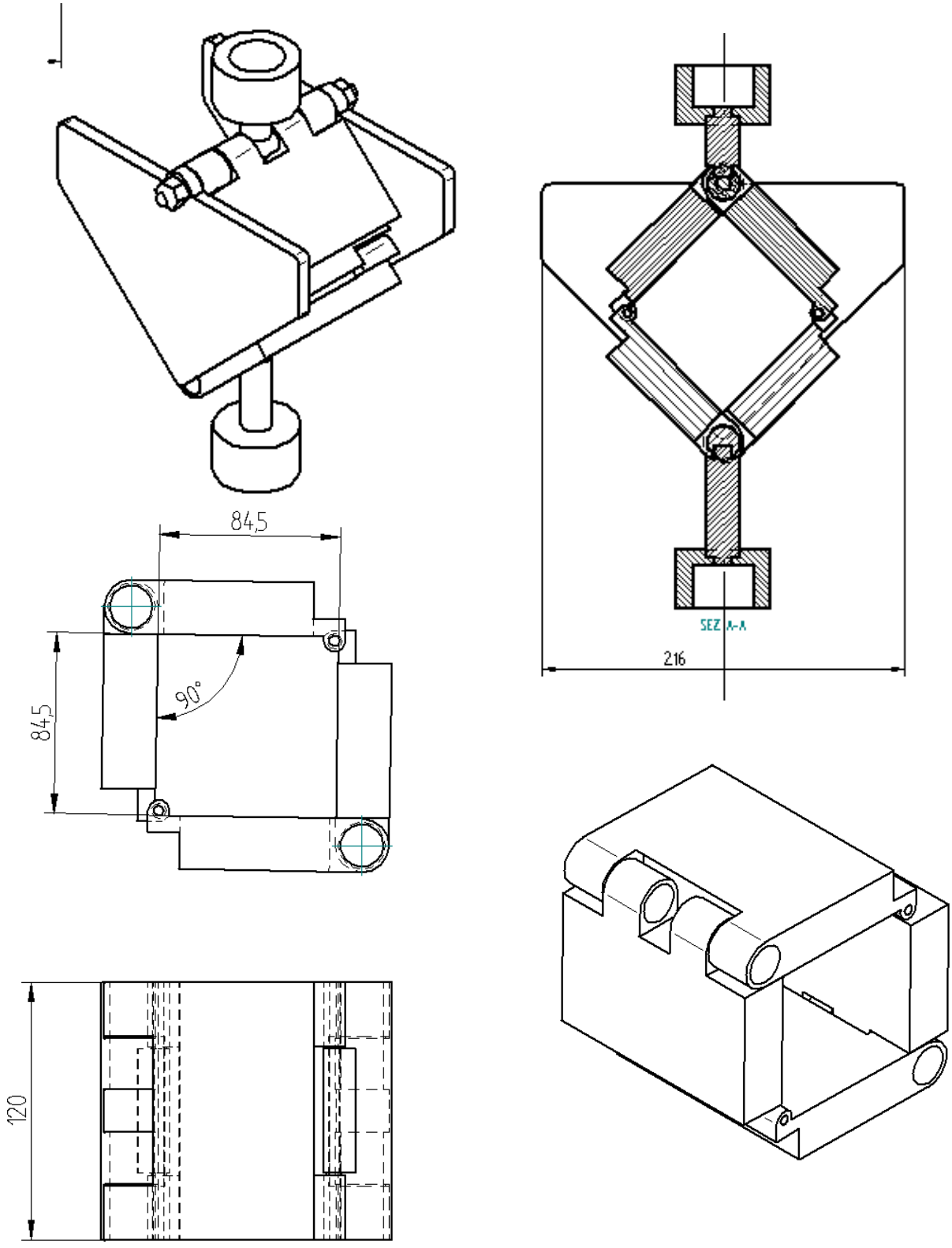

Figure 7.9 Shear test equipment.

7.3.1 Shear modulus calculations

A compressive force is applied at the crosshead mounting. The initially square frame thus becomes of rhomboid (or diamond) shape.

Material inside the rig is initially subjected to pure shear deformation kinematics. The force required to deform the material is recorded at the crosshead mounting as a function of crosshead displacement. From this information, the shear force (or stress) can be determined as a function of shear strain and shear strain rate.

During an oriented picture frame test, the deformed configuration can be expressed as shown in Figure 7.10.

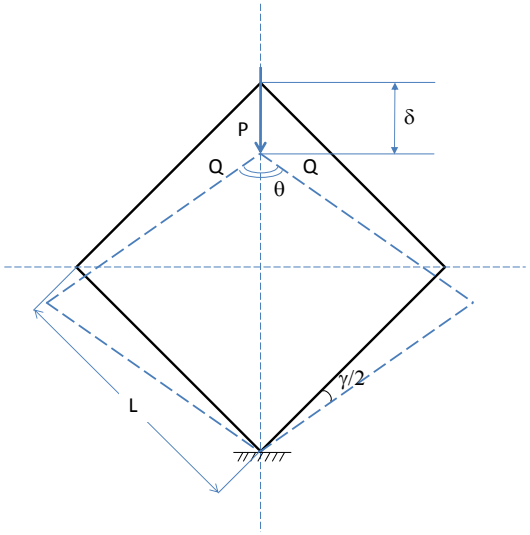

Figure 7.10 Deformed configuration of the shear test specimen.

Therefore, shear force Q and shear angle are calculated through the following formulae:

$$\begin{cases} Q = \dfrac{P}{2\cos\dfrac{\theta}{2}} \\ \gamma = \theta - \dfrac{\pi}{2} \end{cases}$$

and

$$\cos\frac{\theta}{2} = \frac{\sqrt{2}L_{frame} - \delta}{2L_{frame}}$$

Where:

L_{frame} =84.5 mm is the side length of picture frame,

δ is the recorded displacement between two crossheads,

P is the effective load at each displacement point,
Q is shear force acting along each arm of the picture frame,
θ is the current angle
γ is the shear angle.

The shear stress can be directly calculated from the shear force. Note that after deformation, the area of the specimen reduces, while, based on the assumption of volume conservation, the thickness of the specimen should increase. In this case, though, the particles are contained in a closed box, therefore the volume changes and the particles are under compression. In the case of the tests, though, the change in volume is only 5 % and it is initially neglected. It will be accounted for in a later stage during the modelling of the complete assembly of particles.

With this assumption, the shear stress can be calculated as:

$$\tau = \frac{Q \cdot \sin\theta}{L \cdot t} = \frac{P \cdot \sin\theta}{2 \cdot \cos\theta/2 \cdot L \cdot t}$$

in which L is the side length of deformed specimen. The shear strain remains the same as the shear angle γ.

Three types of rubber have been tested, the two ellipsoidal rubber particles (respectively 25 and 25 Sh A) and small cubes of hardness 50 Sh A.

7.3.2 Test method for shear

The procedure for the series of tests is the following:

1. A certain amount of particles is placed in the container and weighted, in order to have always the same amount of rubber particles during the test, Figure 7.11 (a).
2. The sides of the container are closed, so that the particles cannot drop out the container during testing.
3. The container is placed in the test machine, which records force and displacement, Figure 7.11 (b) shows the set-up.
4. After the test the particles are removed from the container and placed in it again, taking care that the amount is always the same

The shear modulus G can be calculated from the derivative of the regression equation determined from the data points on the shear stress versus shear strain plot, if the units of shear strain are in radians.

For the case of small rubber cubes of 50 Sh A hardness, the shear stresses versus strain curves are almost linear, as shown in Figure 7.12. In this case, a linear regression curve has been chosen. The shear modulus is found as the average modulus calculated from the test results.

In the case of the ellipsoidal particles, as shown in Figure 7.13 and Figure 7.14, the shear stresses versus shear angle have a somewhat parabolic behaviour and the curves are better represented by a third order polynomial.

In Figure 7.15 the plot of the shear modulus versus the shear angle is shown. The shear modulus has been averaged from all tested values. In the case of the small cubic particles the shear modulus can be considered constant and equal to 657 Pa, while for the ellipsoidal particles it is increasing for higher shear angles and a second order polynomial should be used.

(a)

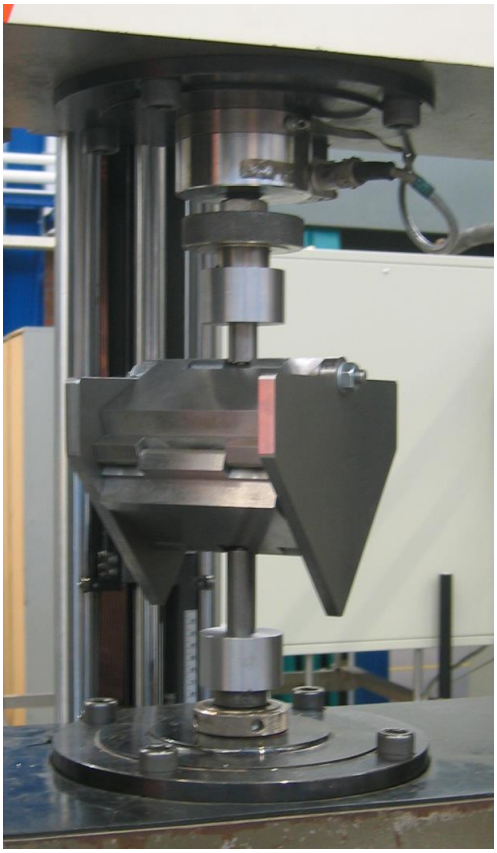

(b)

Figure 7.11 Test set up for the pure shear tests.

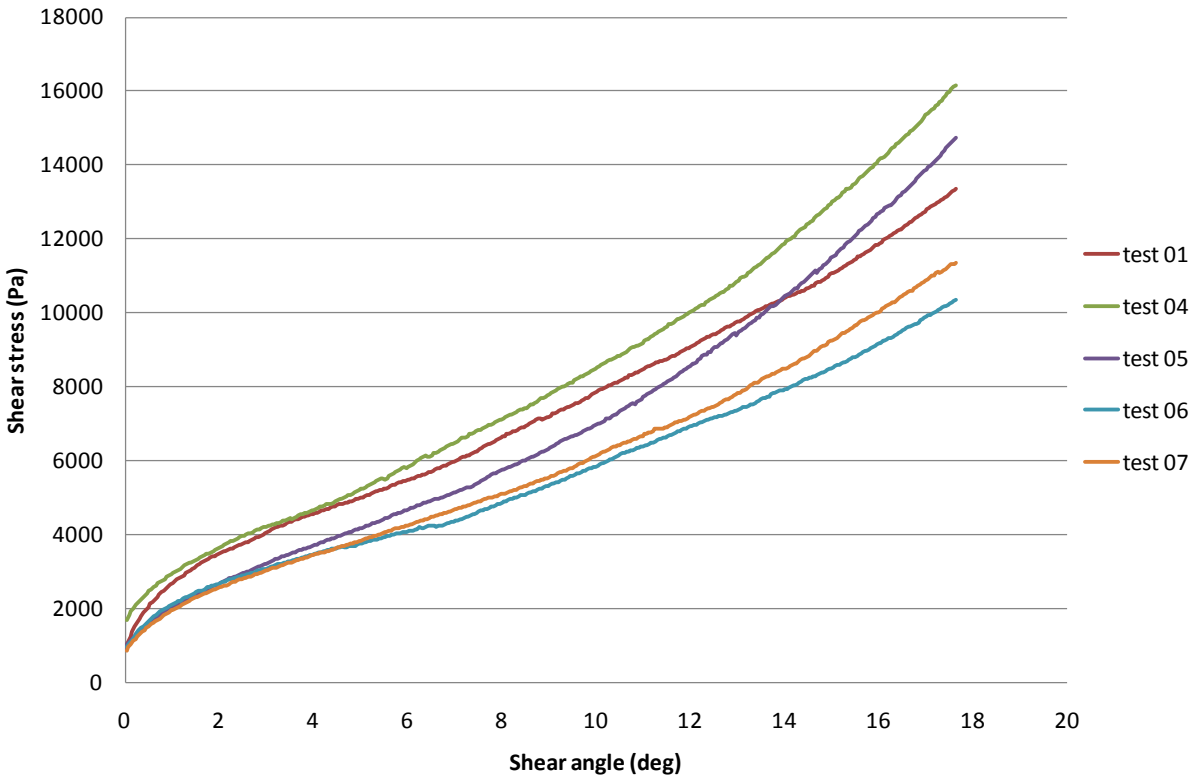

Figure 7.12 Shear stress- shear angle curves for small cubic rubber particles of 50 Sh A hardness.

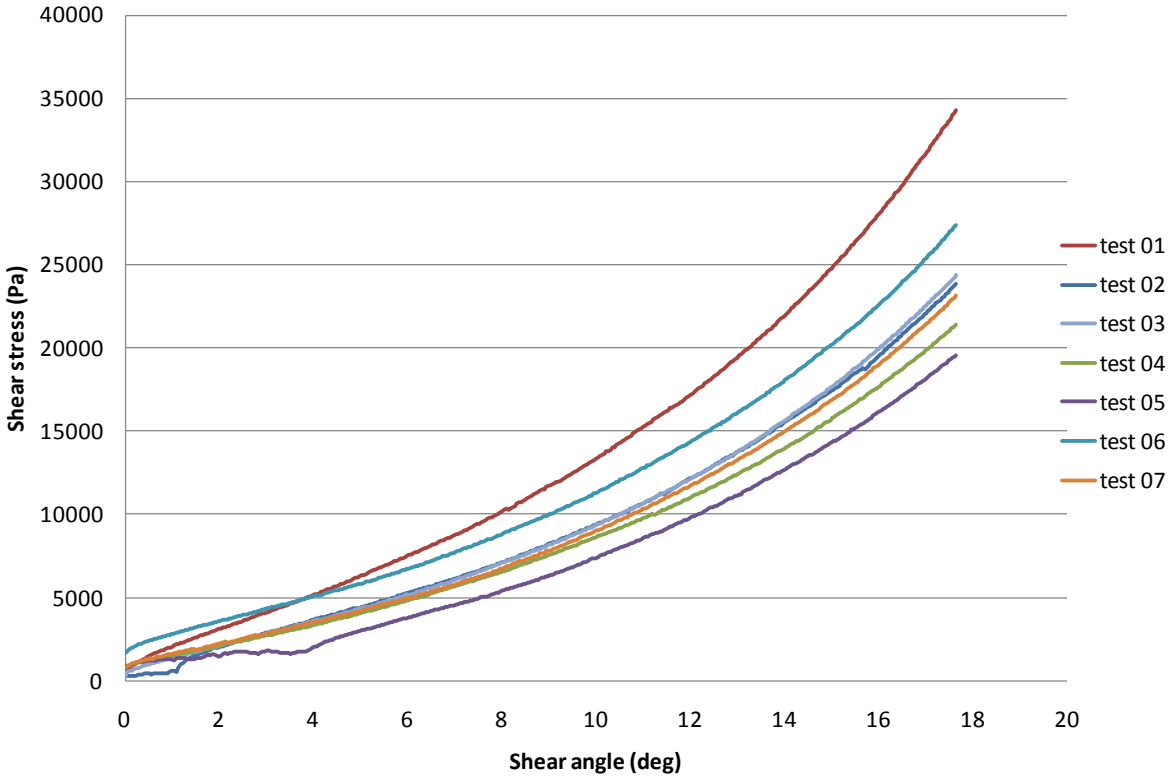

Figure 7.13 Shear stress- shear angle curves for ellipsoidal rubber particles of 20 Sh A hardness

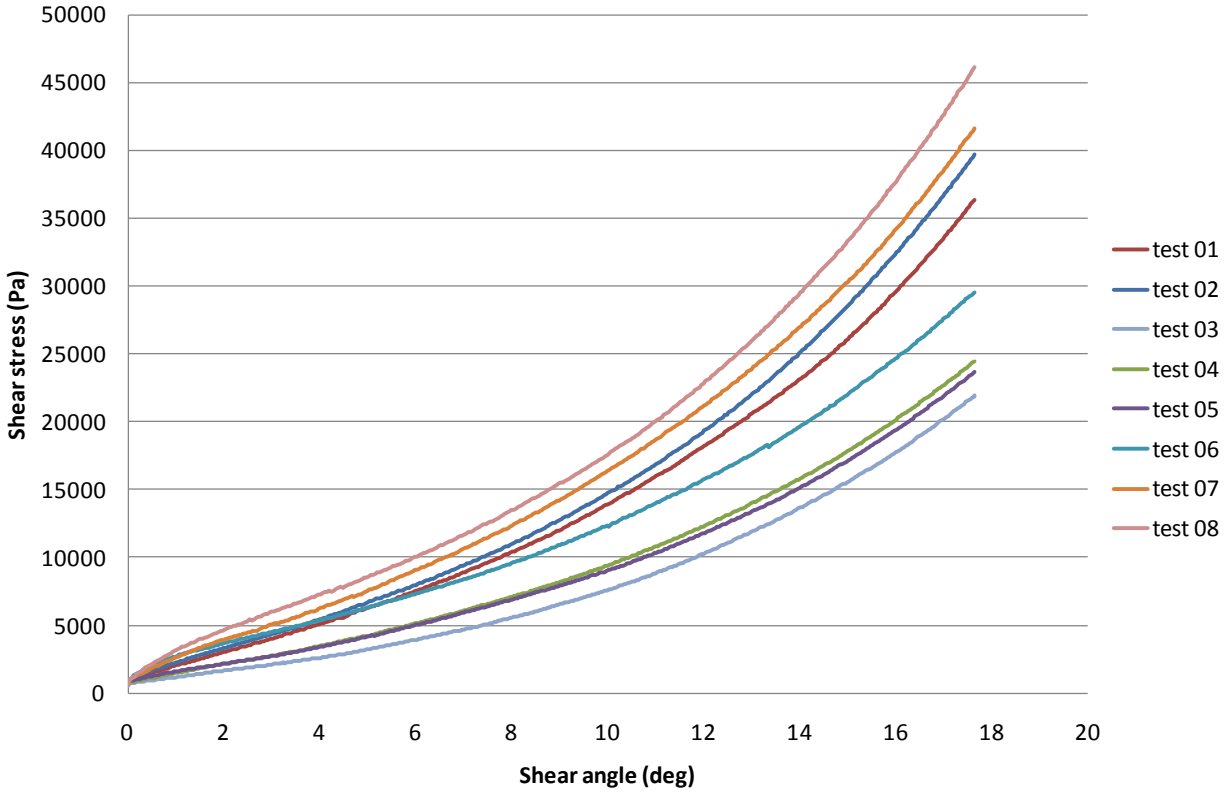

Figure 7.14 Shear stress- shear angle curves for ellipsoidal rubber particles of 35 Sh A hardness

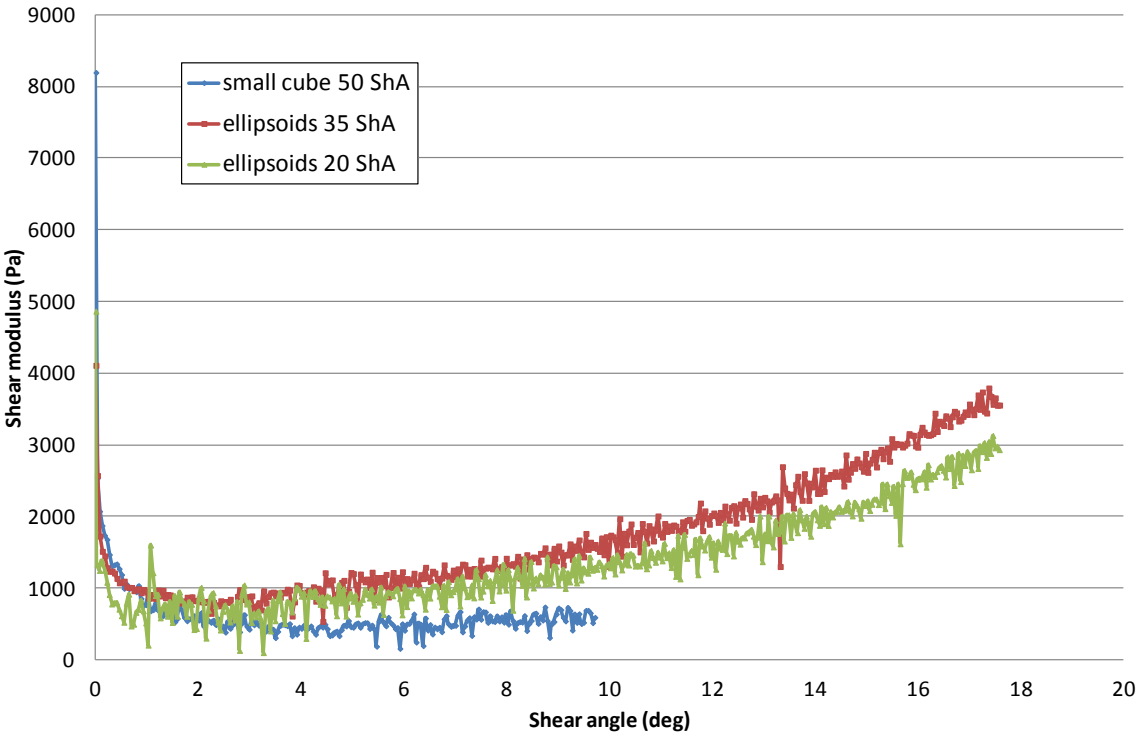

Figure 7.15 Average shear modulus versus shear angle for the tested rubber particles collection.

7.3.3 Discussion of the results

At first sight, the test did not seem to give good results, due to the initial deformation of the "box" under its own weight. For this reason, tests were carried out only for three particles types and grades. The problems encountered are mainly due to the own weight of the container of the rubber particles. Being free to rotate around the hinges, it tends to compress the particles before testing, therefore a lot of effort is needed to properly start the measurements and be able to record the real strain. The results though appear to be reasonable; therefore, the set up could be used again with some modifications allowing the "box" not to deform before the test starts.

7.4 Evaluation of the developed testing methodology

The tests presented above allow obtaining the mechanical characteristics of the rubber particles' assembly in the case they are considered as a continuum.

The first two tests of bulk modulus and shear modulus are a valid way to determine these values. The bulk modulus test can be used without any further change, while for the shear test set up a few modifications might be necessary in order to make it easier to handle. The set-up, moreover, appears to be too heavy to be easily handled by one person alone.

7.5 Discussion of the results

In the case of the ellipsoidal particles, that were tested for both bulk modulus and shear modulus it is possible to obtain two values of K and G for no compaction strain and 5% compaction strain.

The Poisson's ratio is calculated by:

$$\frac{3K - 2G}{2(3K + G)}$$

The results shown in Table 7.3 show that while the modulus of elasticity slightly increases for a low compaction strains, the shear modulus increases more rapidly. The Poisson's ratio, on the other hand, has an almost constant value, which is close to 0.5 and thus implies an almost incompressible material.

	K (MPa)		**G (Pa)**		**ν**	
	no comp.	5%	no comp.	5%	no comp.	5%
20 Sh A	0.22	0.28	777	3046	0.498	0.494
35 Sh A	0.18	0.20	912	3673	0.497	0.489

Table 7.3 Mechanical properties of the ellipsoidal collection of rubber particles as a continuum.

For small values of compaction strains, though, the compressibility is very high, as the volume of the continuum made of rubber particles is drastically reduced due to the elimination of the air in-between the particles. This high value can be justified by the fact that the shear modulus is also extremely low when the particles are not compacted.

7.6 Conclusions

The purpose of the experimental work shown in the present chapter is to be able to represent the collection of rubber particles as a continuum.

From the tests, several material models can be considered, from an simple one, which considers the material as isotropic, whose material properties are presented in Table 7.3, to more elaborated ones as shown in [8].

With these test results, especially the results obtained with the bulk modulus tests, it is also possible to create a rubber model and verify its behaviour with the other tests presented in 6.2, before implementing the material model in the simulation of the production process.

7.7 Bibliography

[1]. ASTM Standard D2435 - 04 Standard Test Methods for One-Dimensional Consolidation Properties of Soils Using Incremental Loading

[2]. E Kim, C Chen, "Calculation of bulk modulus for highly anisotropic materials", *Physics Letters A* 326 (2004) 442-448

[3]. K Phani, D Sanyal, "The relations between the shear modulus, the bulk modulus and Young's modulus for porous isotropic ceramic materials", *Material Science and Engineering A* 490 (2008) 305-312

[4]. S S Kushwah, H C Shrivastava, K S Singh, "Study of pressure-volume relationships and higher derivatives of bulk modulus based on generalised equations of state", *Physica B* 388 (2007) 20-25

[5]. Mehdi S. Kiasat, "Curing shrinkage and residual stresses in viscoelastic thermosetting resin and composites", PhD Thesis, Delft University of Technology, 2000

[6]. D Tabor, The bulk modulus of rubber, *Polymer,* Volume 35 Number 13 1994

[7]. ASTM Standard D 7078-05, "Shear Properties of Composite Materials by the V-Notched Rail Shear Method," ASTM International (W. Conshohocken, Pa.), first issued in 2005

[8]. Shulmeister V. "Modelling of the mechanical properties of low-density foams", PhD thesis, Delft University of Technology, 1998

Chapter 8
Finite element modelling of rubber particles

8.1 Introduction

In the same way as presented in Chapter 5, it is possible to create a material model that fits the behaviour of the rubber particles as presented in Chapter 7. In Chapter 5, a hyperelastic model was used to simulate rubber. Though any stress strain curve can be simulated through a hyperelastic model, hyperelasticity implies an almost incompressible behaviour. This is not the case of the rubber particles considered as a continuum, as shown in the compression tests, due to the amount of air that is present in-between the particles. On the other hand, if incompressible behaviour is considered in a relative sense, namely the ratio bulk versus shear modulus and accompanying Poisson's ratio, the collection of rubber particles is also an almost incompressible medium. The actual perceived absolute compressibility is just a matter of initially very low moduli.

8.2 Collection of particles as cellular solid

A way to describe the collection of particles as a continuum is to consider them as a cellular solid. The definition of a cellular solid as given in [1] is the following: „a solid made up of an interconnected network of solid struts or plates which form the edges and faces of cells".

There are many examples of cellular solids, both natural ones and synthetic. Two classical examples are shown in Figure 8.1.

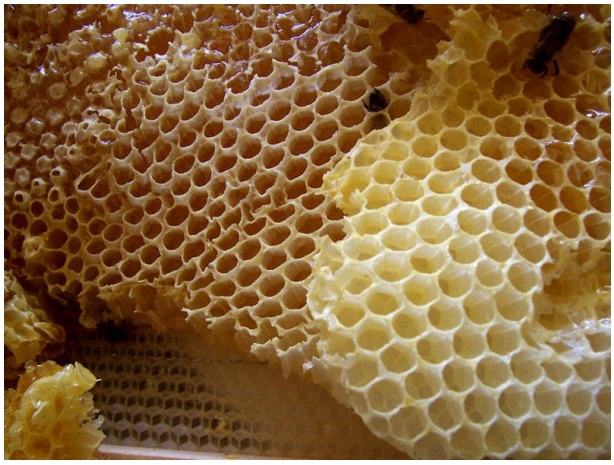

a) natural honeycomb

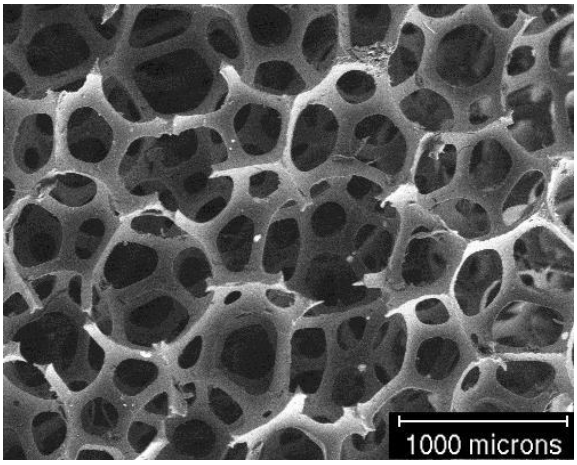

b) polyurethane foam

Figure 8.1 Example of a natural cellular solid a) [2] and an engineering cellular solid b) [3].

Differently from the real cellular solids, the collection of rubber particles is not completely interconnected, but it shares with a cellular solid its most important characteristic: its *relative density*, ρ^*/ρ_s (the density of the collection of particles ρ^* divided by that of the rubber it is made of: ρ_s). The fraction of pore space in the collection of particles is its *porosity* $(1-\rho^*/\rho_s)$.

	Density rubber [g/cm^3]	Average dimension of the single particle	Density of the collection of particles [g/cm^3]	Relative density
Silastic M 59 Sh A	1.29	Large	0.65	0.51
		Small	0.71	0.55
Zermack 50 Sh A	1.2	Large	0.62	0.51
		Small	0.69	0.57
Zermack 33 Sh A	1.09	Large	0.56	0.51
		Small	0.58	0.53
Zermack 22 Sh A	1.1	Large	0.58	0.53
		Small	0.61	0.56
Ellipsoids 20 Sh A	1.05	8 x 10 x 12.5 mm	0.60	0.57
Ellipsoids 35 Sh A	1.05	8 x 10 x 12.5 mm	0.61	0.58

Table 8.1 Density measured rubber particles.

A summary of the obtained results is shown in Table 8.1. The table shows that the relative density of the particles varies between 0.5 and 0.6 and is higher for smaller particles. On the other hand, the relative density is more dependent on the dimensions of the particles than their hardness. The ellipsoidal particles present a higher relative density compared to the volume of the single particles as expected.

8.3 ABAQUS material model

In order to account for large deformations, it is possible to describe the rubber particles as elastomeric foam. The elastomeric foam material model [8] is isotropic and non-linear and is valid for cellular solids whose porosity permits very large volumetric changes and can deform elastically up to 90% strain in compression.

Three stages can be distinguished during compression, as shown in Figure 8.2:

1. At small strains ($<5\%$), the foam deforms in a linear elastic manner due to cell struts bending and in-plane and out-of-plane cell wall deformation

2. The next stage is a plateau of deformation at almost constant stress, caused by the elastic buckling of the "struts columns" or "membrane plates" that make up the cell edges or walls. In closed cells, the enclosed gas pressure and membrane stretching increase the level and slope of the plateau.

3. Finally, a region of densification occurs, where the cell walls crush together, resulting in a rapid increase of compressive stress. Ultimate compressive nominal strains of 0.7 to 0.9 are typical.

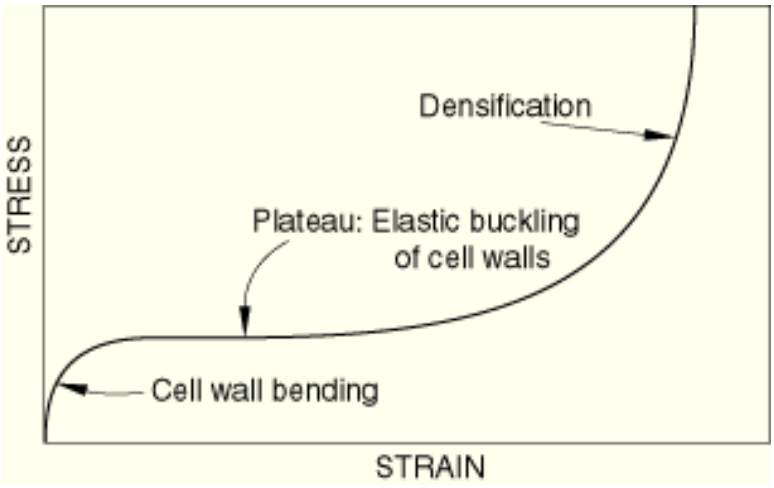

Figure 8.2 Typical compressive stress-strain curve for an elastomeric foam [8].

The behaviour of the rubber particles is slightly different as the first two stages of the curve shown in Figure 8.2 are substituted by a long, almost linear, behaviour representing the squeezing of the air in-between the particles and subsequent deformation of the rubber particles. After which the same densification of the rubber, tending to an "incompressible behaviour" follows.

8.4 Model prediction of material behaviour versus experimental data

In ABAQUS, it is possible to define the elastomeric foam using an existent material model defined as "hyperfoam" and defining the material either giving the constant for the already

existing material or from test data. In this case, ABAQUS automatically translates the test data in the coefficients of the curve. Thus an optimal fit is obtained, minimising the effect caused by the difference between the collection of particles and real foam.

The Hyperfoam potential, accurately described in [7], has the following form and can be fitted up to order N=6:

$$U = \sum_{i=1}^{N} \frac{2\mu_i}{\alpha_i^2}\left[\hat{\lambda}_1^{\alpha_i} + \hat{\lambda}_2^{\alpha_i} + \hat{\lambda}_3^{\alpha_i} - 3 + \frac{1}{\beta_i}\left(J_{el}^{-\alpha_i\beta_i} - 1\right)\right]$$

The deformations modes are characterised in terms of the principal stretches and the volume ratio J. The elastomeric foams are not incompressible: $J=\lambda_1\lambda_2\lambda_3\neq 1$. The transverse stretches λ_2 and are independently specified in the test data either as individual values depending on the lateral deformations or through the definition of an effective Poisson's ratio.

Given experimental data, the material constants are determined through a least-square-fit procedure, which minimises the relative error in stress.

In the present case, the input of the material behaviour is given by the results obtained during the bulk modulus tests, described in section 7.2. The input is given in the form of data points of the volume ratio versus the applied pressure. Furthermore, the order of the curve that is describing the model has to be defined together with the Poisson's ratio and eventually the shear test data. These last values have not been inputted as they were only available for two rubber particles grades and shapes. In the case of the Poisson's ratio, the one that is automatically calculated by ABAQUS seemed to yield the best results in every analysed rubber case, while the order of the energy potential that best fitted the results was the first order one.

Once the elastomeric foam constants are determined, the behaviour of the hyperfoam model in ABAQUS is established. However, the quality of this behaviour must be assessed, as ABAQUS cannot automatically apply the ebst material model representing the stress strain curve as obtained during the experiments. The prediction of material behaviour under different deformation modes must be compared with the experimental data. It must be judged whether the elastomeric foam constants determined by ABAQUS are acceptable, based on the correlation between the ABAQUS predictions and the experimental data.

Test cases are used to calculate the nominal stress–nominal strain response of the material model and are presented below. In both cases, a square block is modelled.

8.4.1 Verification of unidirectional compression data

The model is shown in Figure 8.3. It is a solid block subjected to a vertical pressure on the top surface. The block can only be compressed in the vertical direction, as if contained in a box. No friction is applied on the sides of the block.

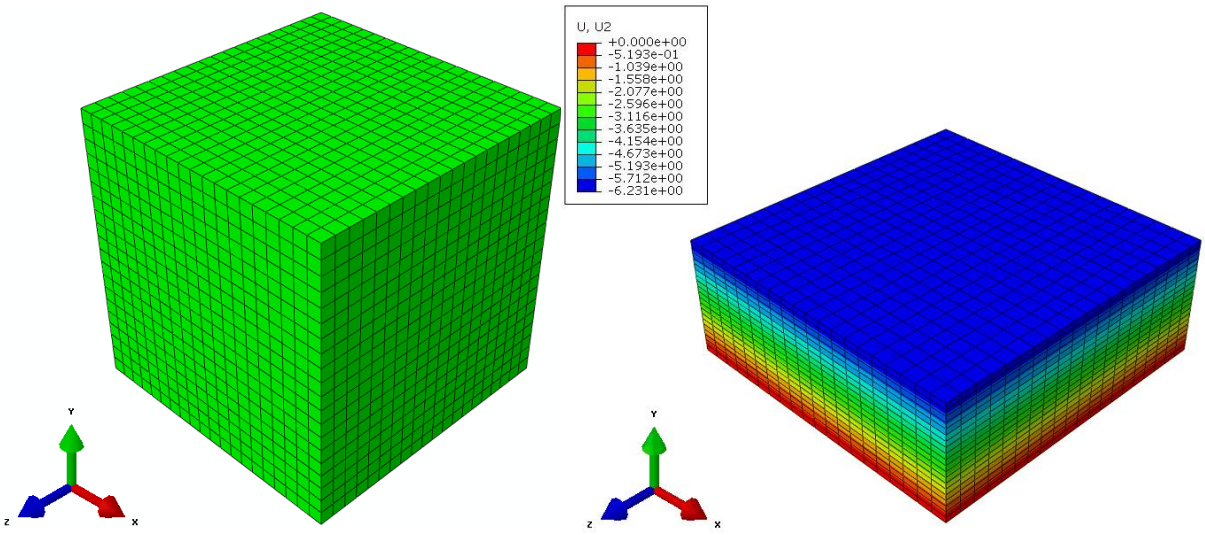

Figure 8.3 Solid model to verify bulk material properties (left) and its deformed shape (right).

Figure 8.4 shows the results obtained using the volumetric test data of the bulk modulus tests. For all types of particles the first part of the slope, when the particles are pushed together, is represented very well by the hyperfoam model of ABAQUS.

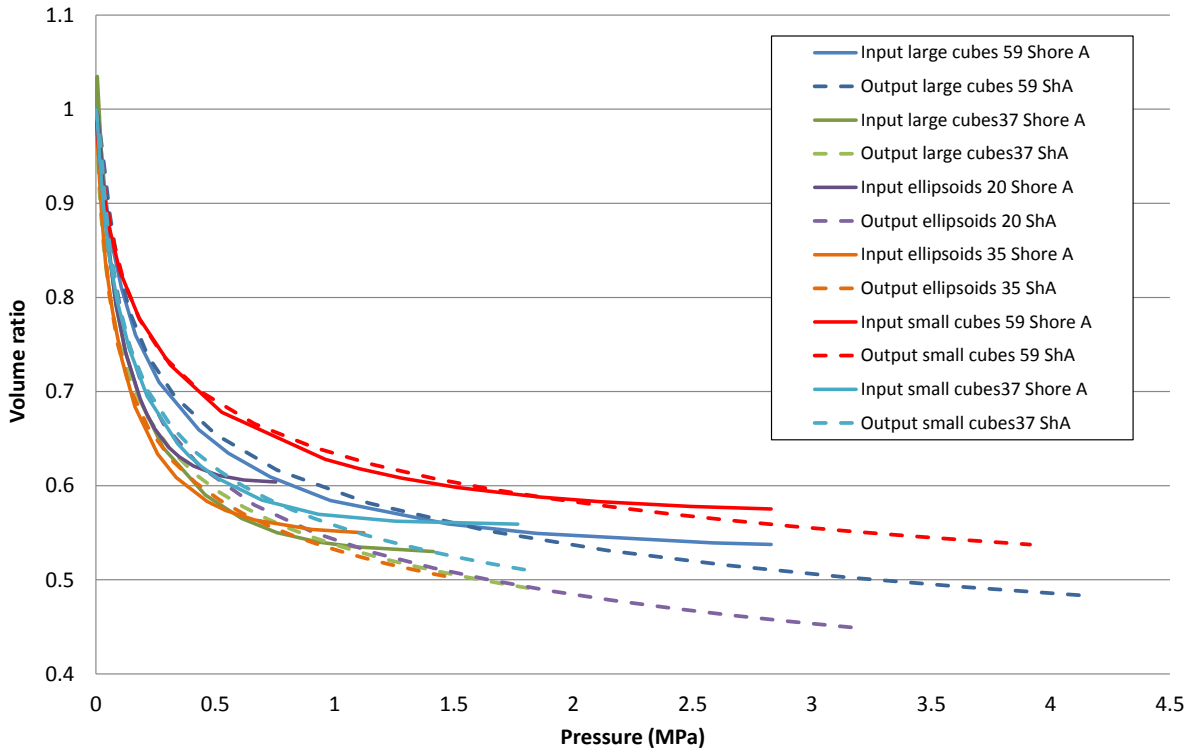

Figure 8.4 Comparisons between volumetric test data and FE-results using the hyperfoam option, where with "input" is intended test data and "output" is the result obtained by ABAQUS.

The second part of the slope, when the rubber particles are becoming incompressible, though, does not completely represent the volumetric test data for every rubber particles' hardness and dimensions. In particular, in the cases of softer and smaller particles, as the ellipsoidal particles of hardness 20 ShA, the compressivity drop appears to be too sudden to be followed by the hyperfoam curves and the two solutions are diverging after the first part of almost linear behaviour.

In the case of larger and/or harder particles, the curves obtained numerically are following the test data more accurately.

The case of the stress-strain curve as inputted in the material model and as output of the analysis of the cube is different, as shown in Figure 8.5. In addition, in this case the first part of the curve, where the air is pushed out from the material, is well represented by the model. The model does not represent the second part of the curve, though, as the particles stiffen more slowly than in reality.

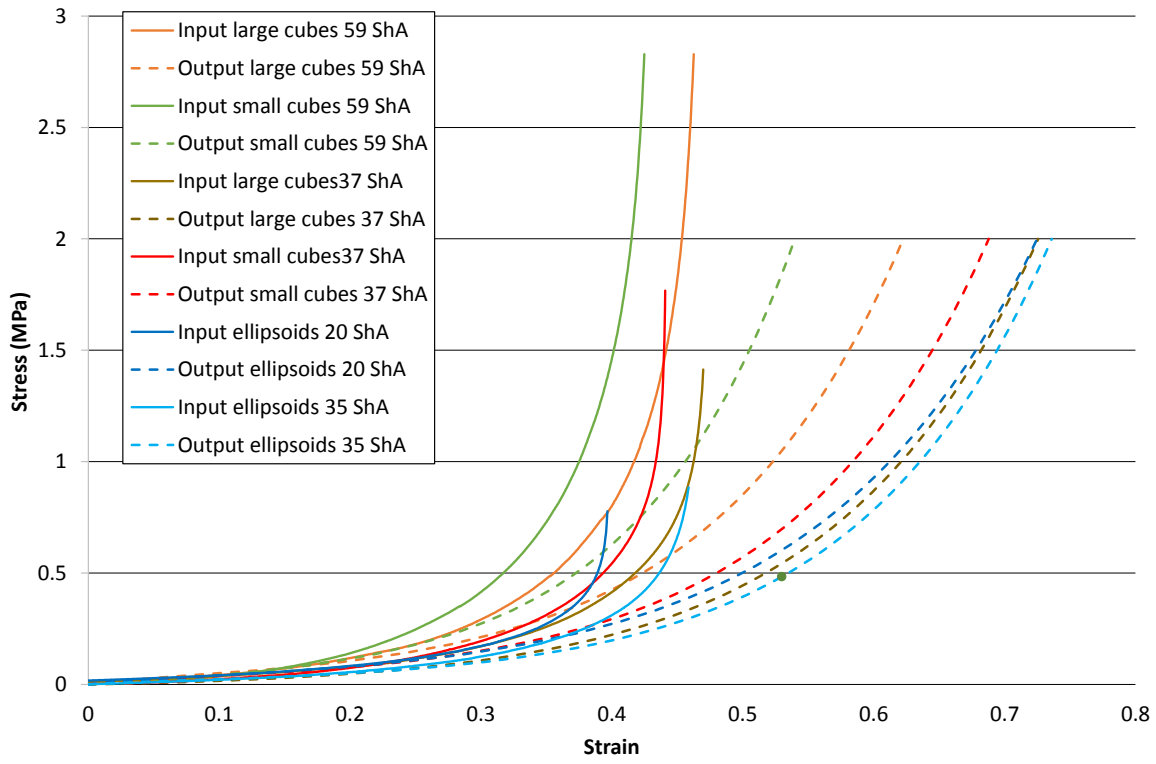

Figure 8.5 Comparison between the stress strain input and output data

It has to be noted that in the Finite Element calculations, the boundary conditions do not consider any friction on the sides of the container. Including the effect of the coefficient of friction, which is very high, should improve the results of the second part of the curve. Nevertheless, having considered two different dimensions and without considering the influence of friction in both cases, the results give a sufficiently good estimation of the behaviour of the rubber particles as a continuum.

8.4.2 Verification of shear load data

To be able to verify the behaviour in shear of the rubber model, the same block is loaded in shear, with the appropriate boundary conditions and load, as shown in Figure 8.6 in its undeformed (left) and deformed (right) shape.

The material model used is the same as for the compression load, therefore the same material data, given by the longitudinal test used.

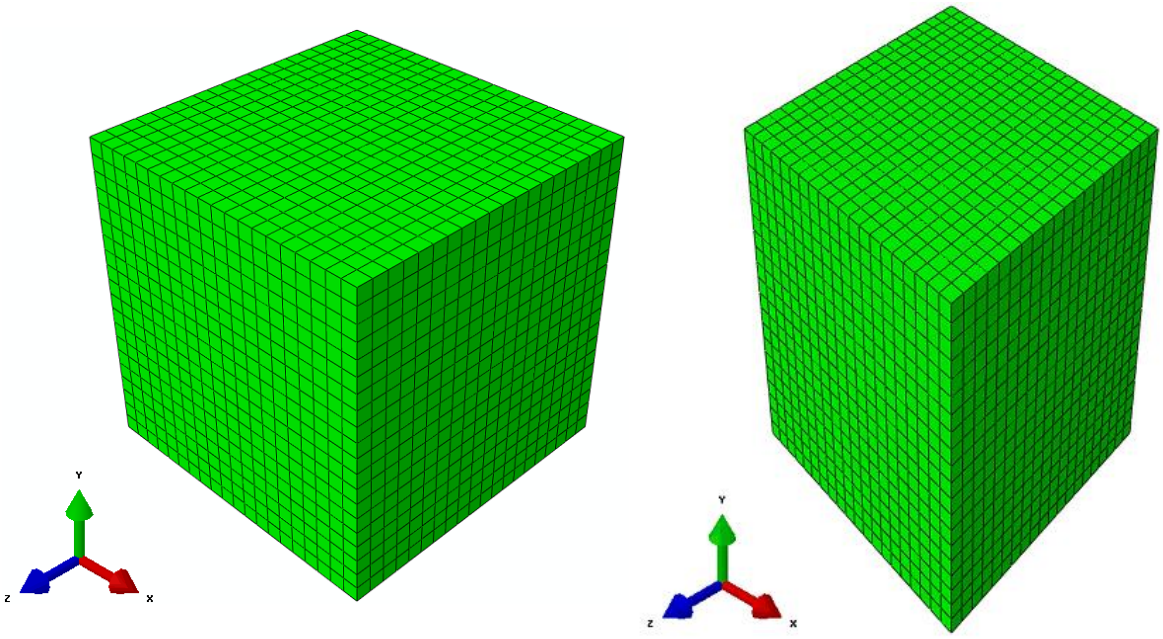

Figure 8.6 Solid model to verify the shear material properties (left) and its deformed shape (right).

Figure 8.7 shows the results obtained using the volumetric test data of the bulk modulus tests on the shear behaviour of the material. In this case, only the two collections of ellipsoidal particles were modelled, as both material behaviour, in compression as input and shear for the verification, was tested. The plot shows that the shear behaviour is very well represented for both particles.

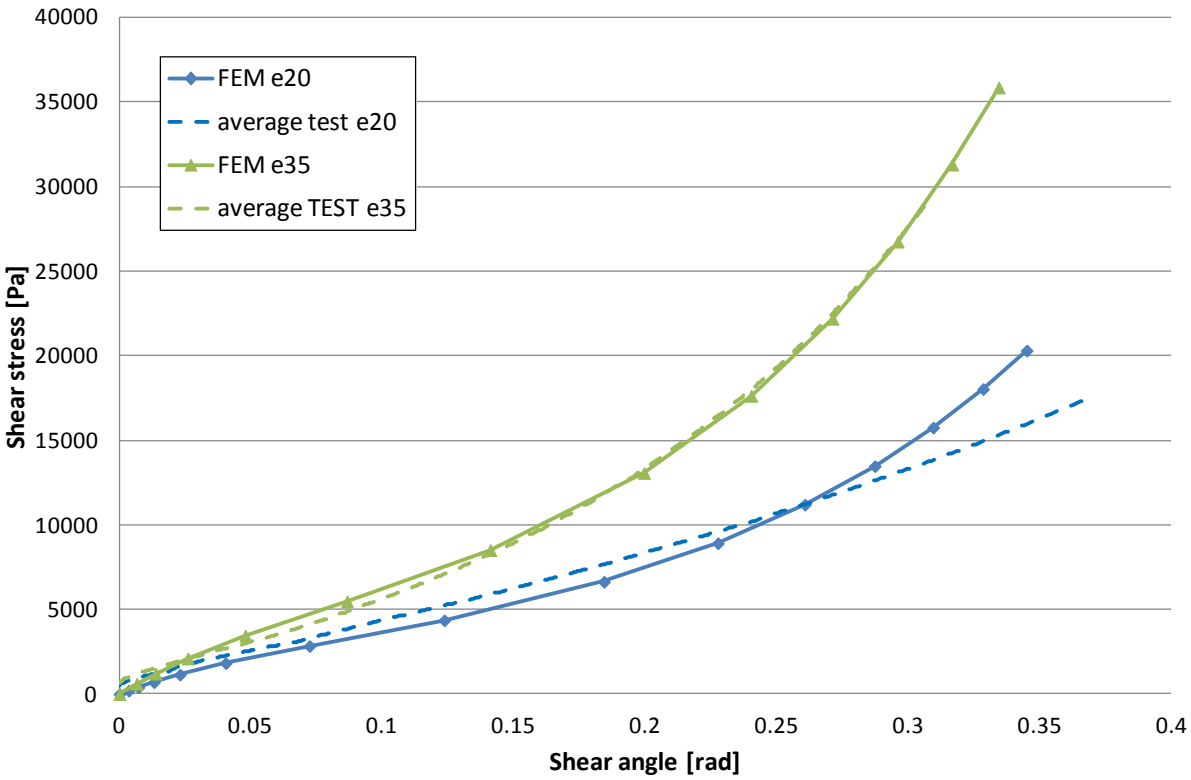

Figure 8.7 Comparisons between shear test data and FE-results using the hyperfoam option.

8.5 U-beam

From the calculations presented in the previous rection, it can be concluded that the rubber particles' behaviour as a continuum can be approximated with a reasonable accuracy as a cellular solid. This motivates the application of the model to the real case of the collection of particles used in a moulding process. At first, the material model will be applied to the pressure distribution tests on the U-beam described in Chapter 4.

The geometrical model of the U-beam is similar to the one described in Chapter 5. The major difference being that the mass of the rubber particles occupies the entire space available in the mould and no gap between steel mould and rubber particles is considered, as the particles are filling all the space available in the mould, just like a liquid would do.

As the volume of the rubber particles reduces a lot in the first part of the compression, a column of particles, higher than the mould, is considered in order to assure enough material when the particles are fully compressed.

Symmetry boundary conditions are considered on both moulds as only half of the test set up has been modelled. Between the moulds, a contact with friction is considered. The value of the friction has been varied as in the case of the rubber block to verify its influence. Although the coefficient of friction of the rubber is usually very high and previously in this thesis has been set as 0.9, the coefficient of friction of the rubber particles should be much lower until the

particles are completely compacted. The particles, in fact, are not always completely in contact with the surface, especially not until they are fully compressed.

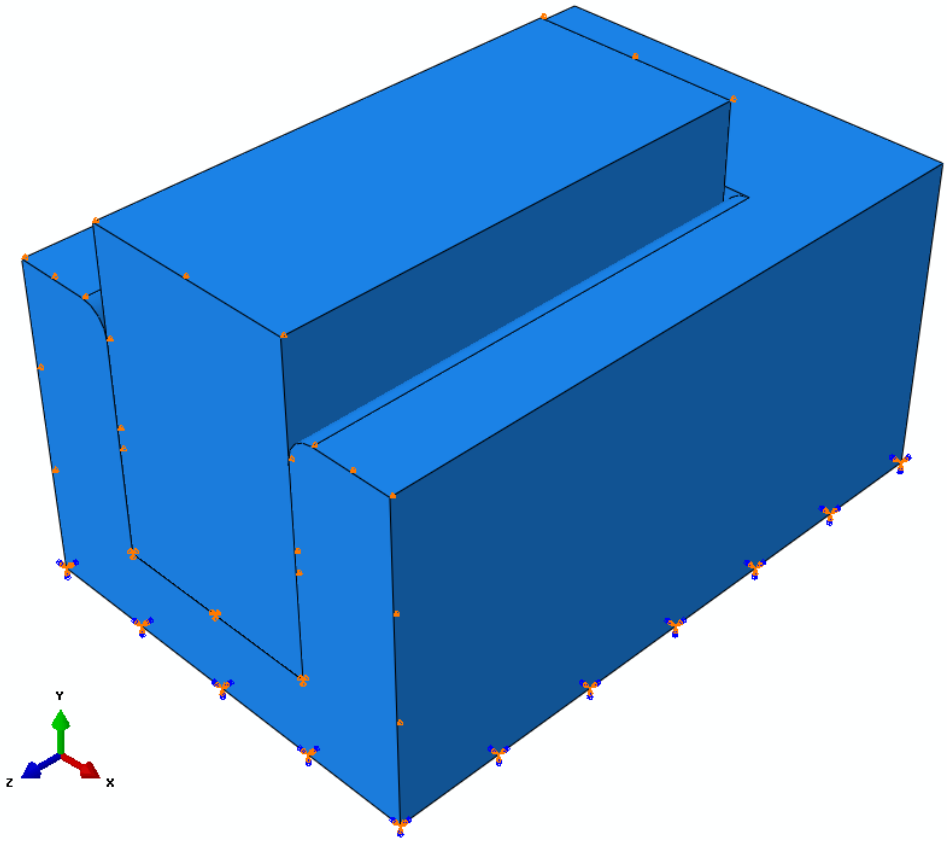

Figure 8.8 U-beam model with rubber particles.

In the Finite Element results, a value of 0.5 for the coefficient of friction seems more realistic than the 0.9 used in the case of a rubber block, as shown in Figure 8.9 in the case of cubical particles of hardness 59 ShA. The same is confirmed for the case of the collection of ellipsoidal rubber particles, as shown in Figure 8.10.

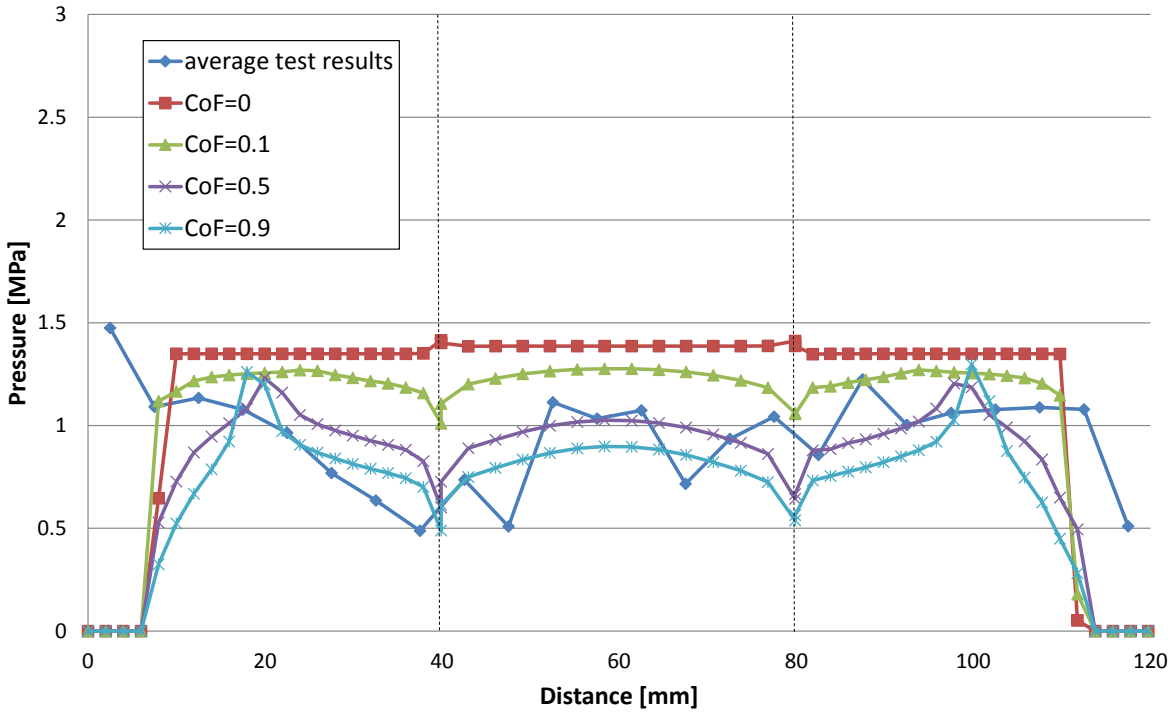

Figure 8.9 Effect of friction on the pressure distribution of the collection of small cubical rubber particles of hardness 59 Sh A.

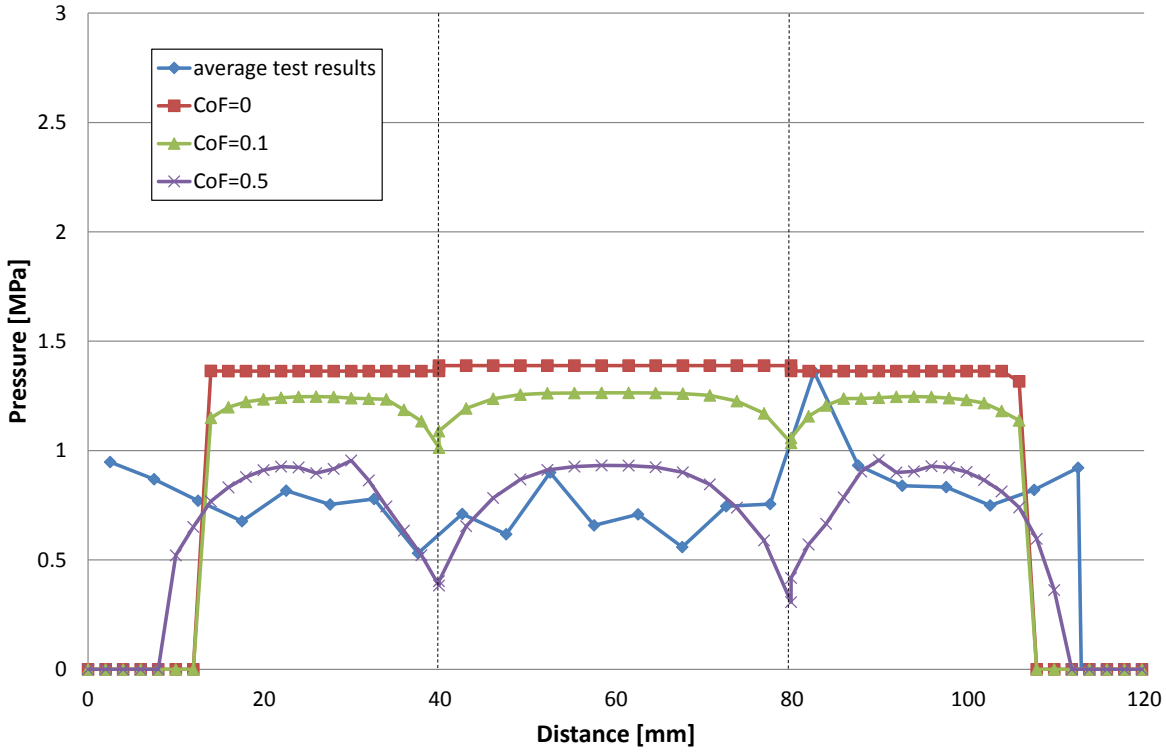

Figure 8.10 Effect of friction on the pressure distribution of the collection of ellipsoidal rubber particles of hardness 35 Sh A.

It has to be noted that, independently from the value of the coefficient of friction, the volume of the rubber particles is drastically reduced during compression; therefore, there is no pressure on the top sides of the mould.

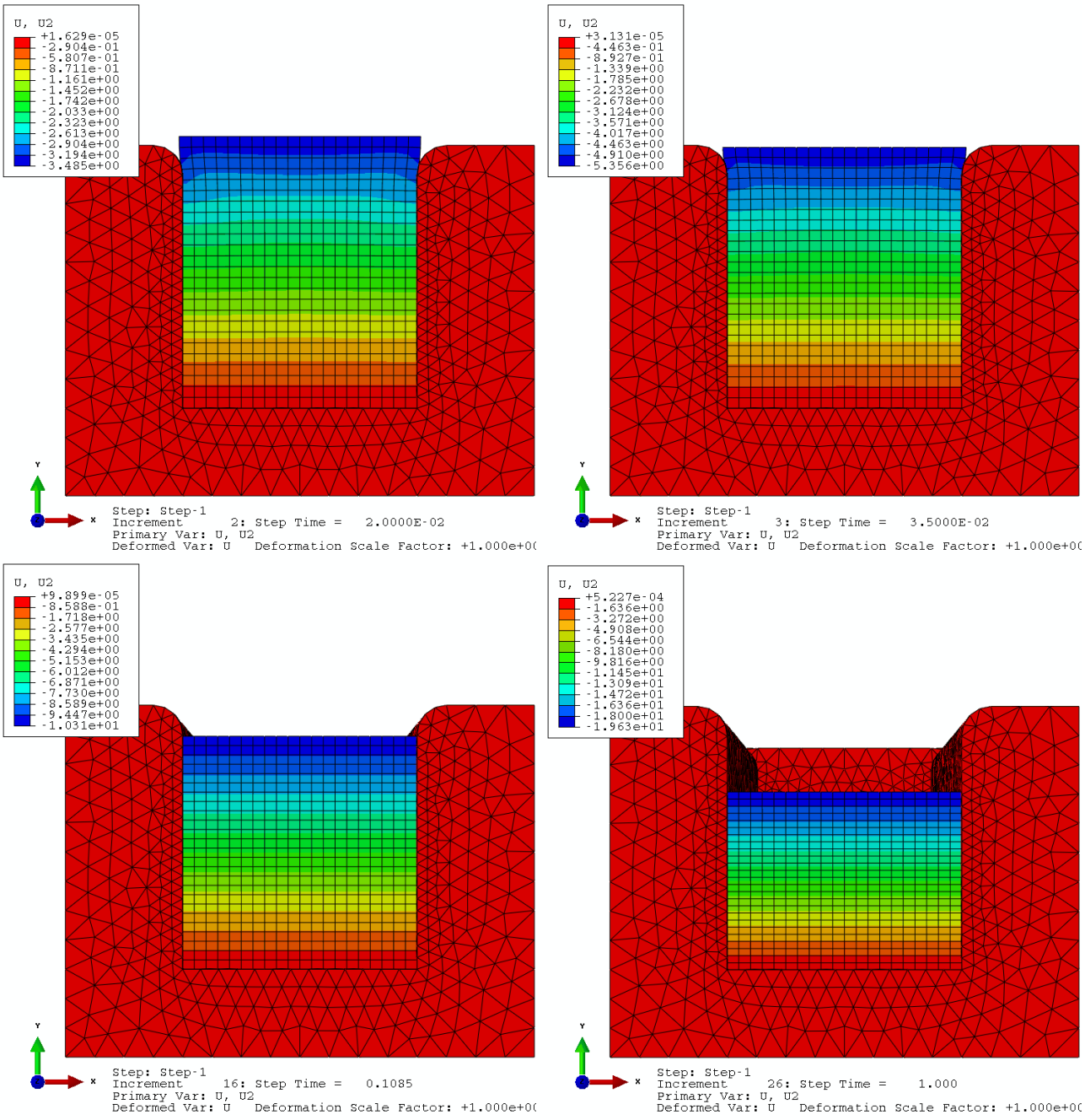

Figure 8.11 Compression sequence of the rubber particles in the U-beam

This effect is something that has to be taken into account when using the collection of rubber particles. Also in practice, in fact, the volume of the compressed particles is considerably reduced. This is shown in the calculations of the relative density, but also visible during the real tests, where the volume of the uncompressed particles had to be at least twice as much as

the volume of the compressed particles in order to have pressure also on the top edges of the mould.

8.6 Real product: non releasable shape

An example of a product that could not be manufactured with the standard rubber mould is, for instance, a beam with a cross section shown in Figure 8.12. This is a relatively simple product whose production is not influenced by the shearing of the fibre inside the thermoplastic material during forming. At the same time, the classical rubber forming method cannot be applied to produce it. It is in fact not possible to press a negative rubber mould into the female steel female mould during production and therefore it is not possible to obtain an almost constant pressure distribution on the side walls of the steel mould.

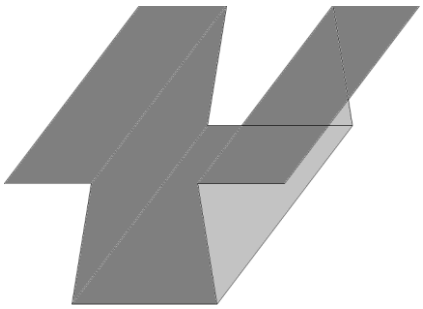

Figure 8.12 Non-releasable product: U-beam.

With the collection of rubber particles, on the other hand, it is possible to insert the particles in the section even if the top cross-section is smaller than the bottom one and to extract the particles once the product is formed.

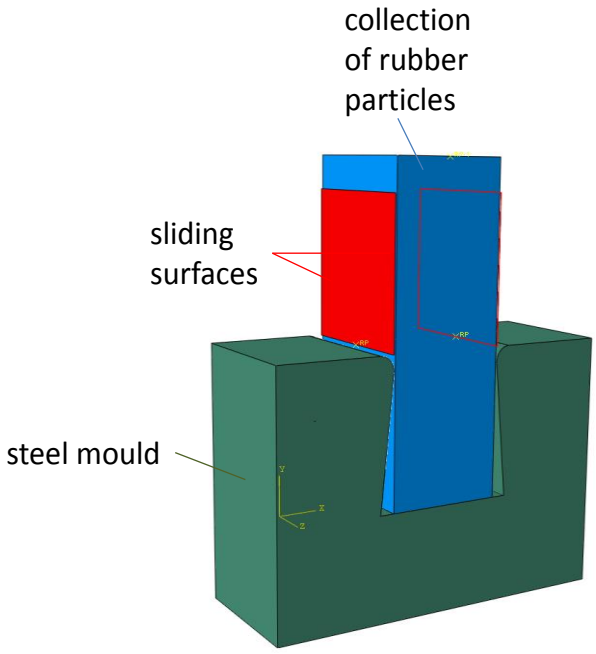

Figure 8.13 Definition of the finite element model.

In order to verify the possibility to produce such a product, a simple model has been built in ABAQUS, as shown in Figure 8.13. A small portion of a mould to fabricate a long hat stiffener has been modelled, using symmetry boundary conditions on both sides of both moulds. The top of the flexible mould is subjected to a pressure force and bound to the same vertical displacement.

Due to the large reduction in volume, a high column of particles has been modelled, which is constrained to follow two perpendicular "guides" when outside the mould, as shown in Figure 8.13. The guides are represented by two rigid surfaces. Only a small section has been modelled considering symmetry boundary conditions on both sides of the cross section, in order to simulate a long beam. This configuration actually represents the worst-case scenario, as the particles will most likely follow the contour of the female mould once they are in contact to it. Nevertheless, Figure 8.15 shows the compression sequence once the column of rubber particles is compacted: The rubber particles completely fill the mould assuring pressure also on the vertical sides of the mould.

Figure 8.14 shows the pressure distribution on the female mould wall at increasing pressure values in the case of the mould made of a collection of rubber particles. At the increase of the forming pressure, the particles fill the cavity of the mould and consequently the pressure on the mould walls increases.

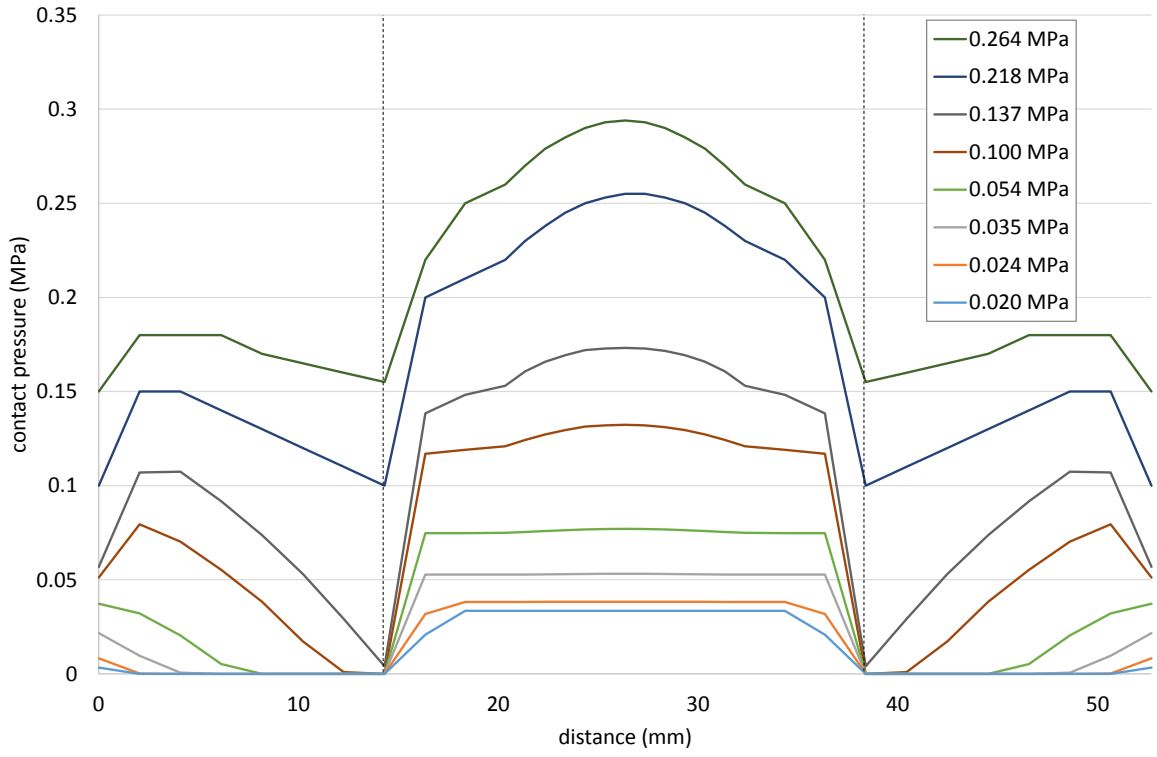

Figure 8.14 Pressure distribution due to the collection of rubber particles at increasing applied pressure.

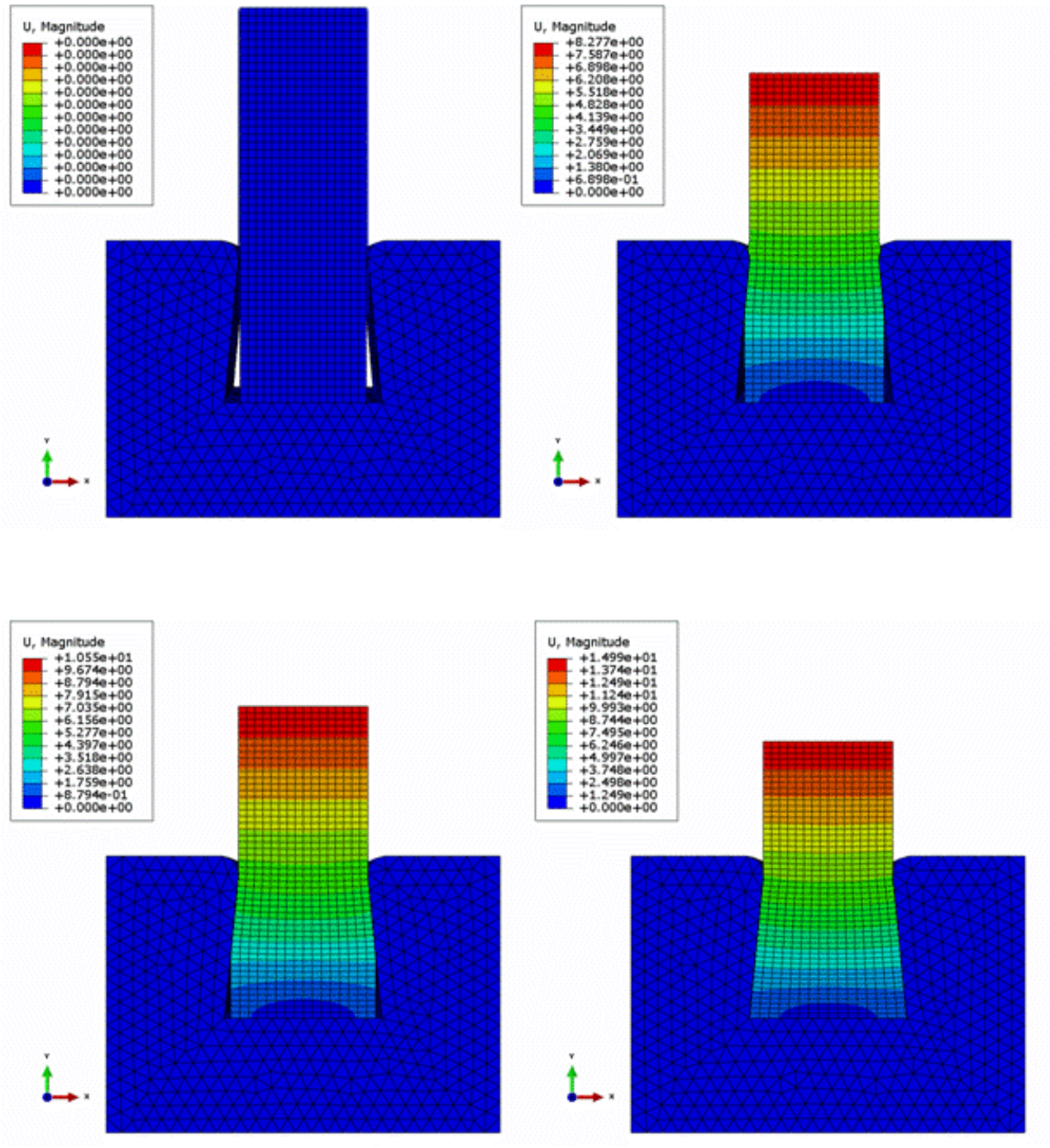

Figure 8.15 Compression sequence of the rubber particles during the forming process of a product with a non-releasable negative solid male mould.

In order to compare the results, the same set-up has been used to simulate the production of the same object using a solid rubber mould as female mould. The same rubber type of the rubber particles has been considered, namely a silicon rubber of 59 Sh A hardness.

The results are shown in Figure 8.16 where the plot of the contact pressure due to a solid rubber mould on the female mould walls is shown at increasing applied pressure values. Even if the applied pressure is higher than the case of the collection of rubber particles, there is no pressure on the lower part of the mould's side walls.

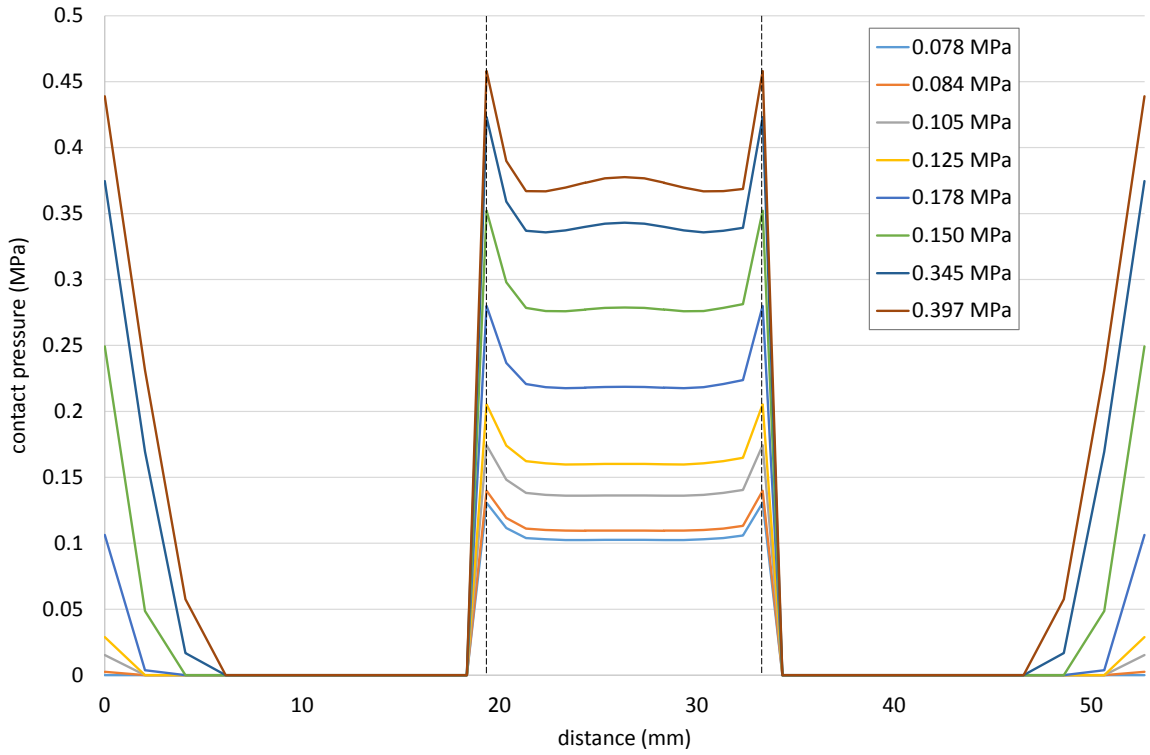

Figure 8.16 Pressure distribution due to the solid rubber mould at increasing applied pressure.

The results of the calculation are also shown in Figure 8.17. The solid rubber mould cannot deform as much as the collection of rubber particles as the mould will soon take a barrel shape, which prevents filling the corners of the female mould.

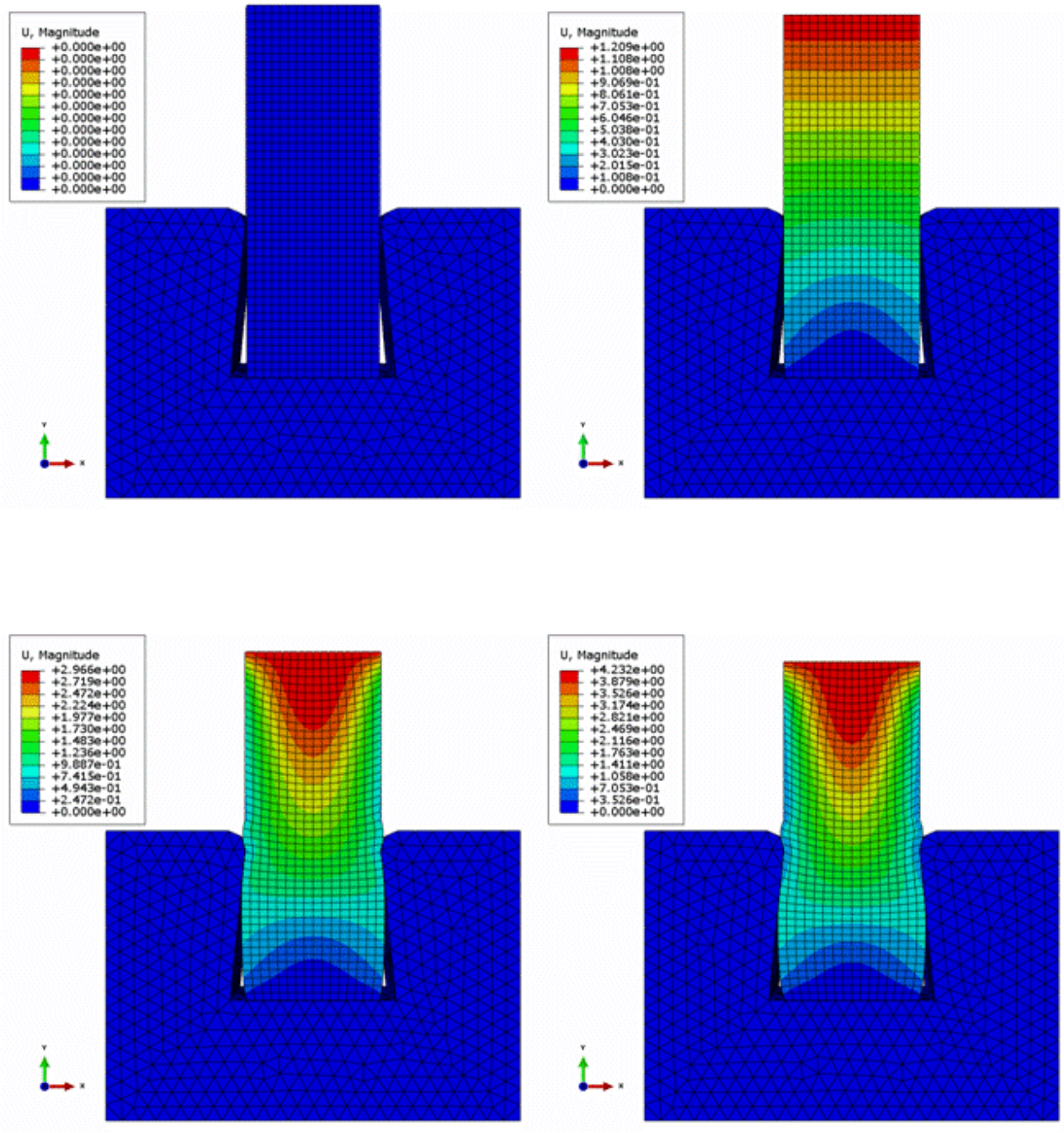

Figure 8.17 Compression sequence of a rubber mould during forming process of a product with a non-releasable negative solid male mould.

8.7 Conclusions

The cellular solid model within ABAQUS allows to predict with a reasonable accuracy the behaviour of the collection of rubber particles as a solid mould while rubber forming. It also demonstrates that the collection of rubber particles performs better than the solid rubber mould, as it is possible to obtain a more uniform pressure distribution on all sides of the product allowing for a better consolidation. Moreover, the collection of rubber particles allows the production of products that cannot be produced with a solid rubber mould as products with an undercut.

The next step in the simulation would be the addition of a laminate, in order to simulate the entire process with a better accuracy and be able to predict how well the product can be manufactured, given a certain rigid mould. This next step, though, is beyond the scope of the present thesis; not in view of fundamental difficulties, but because establishing the model input data of the laminate under high temperature gradients is an effort that requires the period of another PhD project.

8.8 Bibliography

[1]. L.J.Gibson, M.F.Ashby, "Cellular solids: structure and properties", Pergamon Press, Oxford, 1988
[2]. http://en.wikipedia.org/wiki/File:Honey_comb.jpg accessed on 2012/04/10
[3]. http://allthumbsdiy.com/ accessed on 2012/11/21
[4]. W.W. Feng, R.M. Christensen, "Nonlinear deformation of elastomeric foams", International Journal of Non-Linear Mechanics, Volume 17, Issues 5-6, 1982, Pages 355-367
[5]. G. Ben-Dor, G. Mazor, G.Cederbaum, O.Igra, "Stress-strain relations for elastomeric foams in uni-bi- and tri-axial compression modes", Archive of Applied Mechanics 66 (1996) 409-418
[6]. G. Ben-Dor, G.Cederbaum, G. Mazor, O.Igra," Well tailored compressive stress-strain relations for elastomeric foams in uni-axial stress compression" Journal of Material Science 31 (1996) 1107-113
[7]. ABAQUS Theory Manual (6.12)
[8]. ABAQUS Analysis User's Manual

Chapter 9
Conclusions and recommendations

The aim of this thesis was to understand the behaviour of the rubber mould during pressure forming of thermoplastics and to reduce the development costs of the thermoplastic products produced by thermoforming, improving the design of the rubber mould. This chapter summarises the outcomes from the thesis and outlines areas for future work.

9.1 Conclusions

9.1.1 Background

The increase of use of composites and in particular thermoplastics, not only in aerospace and aviation, but also in the automotive industry, was presented in Chapter 1. The need to improve those manufacturing techniques that would allow for (large) series production, such as the case of thermoforming, was clear. An overview of the state of the art on thermoforming of thermoplastics was presented in Chapter 2. It was shown that all difficulties could be divided into two large categories, the definition of a suitable rubber mould and the limitations due to the type of shape that was possible to manufacture based on the drape-ability of the fabric embedded in the thermoplastic resin. The focus of this thesis was set on understanding of the behaviour of the rubber mould during the forming phase and its improvement.

9.1.2 Rubber behavior

The rubber parameters relevant to better understand the behaviour of the pressure forming of thermoplastics were analysed in Chapter 3. It was shown that the coefficient of friction, together with the hardness of the rubber very much influence the ability of the rubber to deform in a desired way, especially in corners. The coefficient of friction could be improved in a substantial way with the use of lubricants, though this might negatively influence the performances of the melted thermoplastic, which cannot be accepted. The third parameter that has to be considered is the very high coefficient of thermal expansion. This parameter should be taken into account while designing the mould. During series production, in fact, when the rubber mould has reached its maximum temperature, the change of shape of the rubber modifies significantly the position of the details that have to be pressed. This is particularly evident in the case of large products. The effect of the three rubber parameters in the rubber mould during pressing has been thoroughly investigated in Chapter 4, where the pressure distribution in a mould to produce a U-beam has been measured. Here both effects of the rubber hardness and of lubrication on the pressure distribution exerted on the metal mould have been investigated at different temperatures for several rubber mould shapes. From this study several conclusions could be drawn:

- the rubber mould needs to be designed for its use at higher temperature, therefore when it is already expanded. Only this way it is possible to better approximate a uniform pressure distribution for series production,
- the thickness of the laminate has to be included in the mould design considering the thermal expansion, otherwise the laminate will not be pressed correctly into the mould,
- the addition of a filler with a negative coefficient of thermal expansion, like Twaron pulp, gives positive results in the reduction of difference in pressure distribution at different temperature. This could be investigated further in order to obtain the optimal amount of filler which assures the same pressure distribution at any temperature
- a lubricant is very effective in the reduction of pressure loss, though the effect of lubrication on the mechanical performances of the thermoplastic laminate should be considered.

The outcomes of Chapter 4 were verified in ABAQUS using the material data obtained in Chapter 3 and a hyperelastic material formulation based on the test results. These results are presented in Chapter 5. As pressure distribution and load-displacement diagram fit the test data very well, the material model is used to verify a real life problem. Also in this case, the material model fits the results obtained during production very well, which means that such a material model could be used before starting production to determine if critical points are expected.

9.1.3 Rubber pressing with a collection of rubber particles

Although several possibilities for the improvement of this production method exist, the developments time of such a rubber mould is still quite long. Moreover some practical limitations remain, even after modelling. A full alleviation of the limitations appears just impossible due to the actual limits of the process. The use of a mould made of a collection of rubber particles is considered a better option as shown in Chapter 6, where the method is described and demonstrated through the production of several products. The dimensions of the particles and the rubber type have been investigated in order to determine the combination needed to obtain a well-formed product. It is shown that shape of the particles and hardness of

the rubber are less important than the particles dimensions. In general, the smaller the particle, the better is the quality of the product.

In Chapter 7, the rubber particles have been tested in order to obtain their characterisation as a continuum. Bulk and shear modulus have been determined, as well as an equivalent shear related test to determine a shear value which is valid for different compaction levels of the particles.

The bulk modulus results show that:

- the bulk modulus is very low for low strain levels, when the assembly of particles are mainly separated by air;
- at higher strains, also depending on dimensions and hardness of the rubber particles, the particles behave as a solid block of rubber becoming almost incompressible.

The shear modulus increases almost parabolically at higher values of compaction strains for the collection of ellipsoidal rubber particles, while it is almost constant for the cubical particles.

When calculating the Poisson's ratio from the bulk and shear modulus values, it appears that the Poisson's ratio is almost constant and very close to that of an incompressible material (slightly below 0.5). These material data make it possible to describe the collection of rubber particles as a continuum.

It turns out that considering the collection of rubber particles as a continuum solid results in a material with a very variable stiffness. Stiffness expressed as moduli results in moduli that vary over more than two orders of magnitude, from very small values when the collection is still hardly compressed, to high values where compaction is (almost) complete. The bulk- and shear modulus are related by the Poisson's ratio. In retrospect it turns out that the Poisson's ratio is not varying much over the entire range from hardly compacted particles to almost completely compacted particles. It is always slightly below the value of 0.5. This value of 0.5 is often related to incompressible materials. This conventional language is also used in the present thesis in order to give the readers an engineering feeling. However, it should be noted that all materials are compressible. The really striking property of a material with a Poisson's ratio of 0.5 is the very low shear modulus as compared to bulk modulus, down to a shear modulus of zero for fluids. So incompressible should be understood as hardly compressible as compared to shearing. So the collection of particles shows a behavior implying that compressibility is always much lower than "shearability", even in the hardly compacted region where compressibility is high in an absolute sense.

The Poisson's ratio being nearly constant and slightly below 0.5 is consistent indeed to the fluid-like behavior at the beginning of the process where the particles behave is such a way to provide the advantages of hydroforming. It is also consistent to the behaviour at the end of the process where the collection acts as a solid "incompressible" rubber block.

Indeed, polymer foams do show an almost constant Poisson's ratio over the entire deformation range and have in common with the collection of particles that the moduli may vary over wide

ranges and may increase progressively if compaction becomes important. So in retrospect, it can be understood that modeling the behavior of the particle collection as a foam yields realistic results for the pressure distributions in the mould, if the model starts with a filled mould situation. The filled mold situation as a starting point can be motivated as a trivial consequence of the more liquid character of free flowing particles at the very beginning of the process. Free flowing particles will tend to fill a mould completely. Yet, this very beginning of the process may be considered a modeling challenge for future investigations where the melted composite is incorporated as well. The low "near liquid" stiffness, compared to the low stiffness of melted thermoplastic composite may still require detailed modeling for complex mould shapes where the "just-filling' assumption is not adequate anymore.

In Chapter 8, the material data obtained in Chapter 7 are used to simulate the production process in ABAQUS. The rubber particles are modelled as cellular foam with the volume change defined as the one of the bulk modulus test and the shear modulus derived from the shear tests. The results were first compared with the test results and then a real case has been modelled in which the producibility is proven of a more varied number of products with promising results.

The novel moulding process with the collection of rubber particles is a considerable improvement over the conventional process with a solid rubber mould. Many problems of the conventional process are just eliminated to such an extent that modeling may become unnecessary. On the other hand, even with the extended possibilities of the novel process, limits will be apparent on product geometries that can be made. Modeling will still be very useful if those limits are approached. The present modeling of the collection of rubber particles during moulding is a first step towards that exploration of new production limits.

9.2 Recommendations

The rubber press forming with a collection of rubber particles as mould half has been proven feasible from a production point of view and it has been shown that it is possible to model the entire process with the use of a Finite Element Analysis. Although the method has been patented, it still needs more research in order to be commercialised. Some of the envisioned points to be addressed are described below.

From a production point of view, a container for the rubber particles has to be defined that allows the particles to fill the mould cavity without interfering with the laminate. The design of an appropriate blank holder and the amount of force to be applied to it is necessary to improve the quality of the product to be manufactured.

From the designer point of view, in order to have a complete overview of the process, the laminate should be added to the analyses. This is more important when doubly curved products are being produced, since in the case of 3-D forming the deformability of the laminate plays an important role.

About the author

Valeria Antonelli was born in Rome, Italy on 26th of February 1966. In 1985 she enrolled at the faculty of Engineering of the University of Rome "La Sapienza" chosing Aeronautical Engineering as specialisation. In 1994 she obtained an Erasmus scholarship to carry out her Master Thesis at the Faculty of Aerospace Engineering of the TUDelft on the buckling and post buckling behaviour of Glare stiffened panels within the Structure Group of Prof. Johan Arbocz.

She returned to Delft in 1996 as part-time researcher in the Chair of Production Technology (now Design and Production of Composite Structures). Soon after she was offered a position as Project Engineer at the Centre of Lightweight Structures (CLC, in Dutch), a merge between the Dutch Applied Research Centre TNO and the faculty of Aerospace Engineering. At CLC she worked on several projects, from the design of thick composites products for underwater applications, to the impact behaviour of composite guardrails for secondary roads up to design methods for the application of Glare in the A380.

In 2003 she rejoined the Faculty of Aerospace Engineering of the TU Delft to work as a researcher and part-time PhD student for the Chair of Design and Production of Composite Structures, whose results are described in this book.

From May 2009 she works as a researcher at the Faculty of Mechanical Engineering, Institute of Lightweight Structures of the Technische Universität München, in Munich, where she lives with her family.

Acknowledgments

This is for me the last bit left before leaving the Faculty of Aerospace Engineering of Delft University after twenty years; therefore, I would like to take the opportunity to thank all the people that have meant for me here, from both a professional and personal point of view. First, Adriaan Beukers, you involved me from the beginning of my master thesis (although I was part of the structure group back then) in the fun of the composite world. I was in the Netherlands only for a couple of days when you offered me to drive along to pick up some nomex in Belgium. I had the opportunity to see the factory and enjoy some sightseeing (including the highest point in the Netherlands). Two years later, you offered me my very first job, which very quickly turned into an exciting period al CLC after which, you agreed on my come back as a full time university staff member, which allowed me to carry out the research that is described in the present book, something I so much wanted to do.

I had the luck to have always bosses who allowed me to grow at my pace. In-between Adriaan, there has been Jan Olijslager. I will be always grateful for the trust you showed me, letting me do just as much as I dared to do, with the exact amount of challenge. I owe Professor Baier and TUM for allowing me to use TUM facilities to finish my thesis: all calculations in Chapter 8 were carried out at LLB.

I am so glad I was allowed to properly work in a laboratory and be able to do practical work, Hans taught me all the ins and outs of gluing strain gauges, including how to make "the perfect drop". Berthus was always kind to cut my rubber specimens and always curious about everything wild happening around. Peter Nederveen, I so much enjoyed working with you! Never in panic about anything, always inventing tricks on the spot, precise and at the same time creative. It was great to work with somebody who could actually make what the dull engineer was thinking. Willem Souren I think we have always made a good team in the projects we worked together, but what I mostly liked was your expertise and precision on projects: I have learnt a lot and I am very grateful. Jan Hol, we never really worked together, but you helped me so many times I have lost count. I have enjoyed all the witty answers to my FEM and UNIX doubts and all the discussions about sports that followed. I miss not having a FEM guru around anymore.

Otto Bergsma, I owe you from the time you were the only one of LR to be present at my first public speech, last century in Texas, and for being close, together with Lilian, and yet not taking

sides, in any occasion. I appreciated it, as much as I appreciated the comments on this thesis. I am glad my "Dutch adventure" ends with you in my committee.

I was extremely lucky to have great roommates, from the creative Bert and Edwin, to my alter ego – at least for the work bit - Peter de Haan, to end up with my promoter, Roel Marissen. You have always been very inspiring, combining scientific knowledge with incredible creativity and enthusiasm for new things. Thank you for being my promoter and for your patience, especially in the long period in Munich. My luck did not end in Delft, as in Munich I could share my room with Max Wedekind, with whom I could brainstorm about my thesis when needed (and anything else).

A few students who worked on the subject of my PhD are worth mentioning. First of all, the work of Rob de Bie, which gave me some of the first ideas. From him I also inherited the U-beam, which I modified for the high temperature tests and used for the rubber particles tests. Dieter Decoster was able to put into practice the idea of the mould made with the collection of rubber particles: it was a great deal of practical work. Renato Carbone for initiating the material characterisation of the rubber particles. I also want to thank all the others who helped me with the experimental part, not only the students, but also the technicians of the composite and metal lab who had the patience to deal with my weird requests and (the consequences of my) errors.

It is difficult for me to make a list of all the colleagues at TUD and CLC, therefore I will not, in fear of forgetting someone. With some of you I am still in contact, with others we 'only' meet at conferences and, even after many years, it is always fun to meet the "people from Delft" who are spread all over the world. I hope it will always be like this. For the contribution to this thesis, I want to thank in particular Maarten Labordus for helping me out the moment I asked, François Geuskens, for the mental support and the translation of the Summary into Dutch. Tahira Ahmed to improve my English on it and Lisette Vollmer for everything she has arranged.

Last but not least, I want to thank my "orange girlfriends". In particular, Alessandra, Annapaola, Cinzia and Maria Elena, for keeping me focussed on finishing this when I was loosing it. You often made me mad with your comments, but you never let it go. I owe you this one.